

# **The Development and Evaluation of a Range of Phototherapeutic Dyes Towards Infection Control**

**By**

**Charlotte May Taylor**

**A thesis submitted in partial fulfilment for the requirements for the degree of MSc (by Research) at the University of Central Lancashire**

**June 2018**

# STUDENT DECLARATION FORM

## Concurrent registration for two or more academic awards

I declare that while registered as a candidate for the research degree, I have not been a registered candidate or enrolled student for another award of the University or other academic or professional institution

---

## Material submitted for another award

I declare that no material contained in the thesis has been used in any other submission for an academic award and is solely my own work

---

## Collaboration

Where a candidate's research programme is part of a collaborative project, the thesis must indicate in addition clearly the candidate's individual contribution and the extent of the collaboration. Please state below:

---

Signature of Candidate \_\_\_\_\_



Type of Award \_\_\_\_\_ MSc (by research) \_\_\_\_\_

School \_\_\_\_\_ Physical sciences and computing \_\_\_\_\_

## Abstract

The rise in antimicrobial resistance is threatening modern healthcare treatments, such as organ transplants and chemotherapy, due to the immunosuppressive nature of these procedures and the resulting dependency on antimicrobials. The discovery of new antimicrobial agents is happening at a too slow rate to deal with the rapidly emerging resistant microbes.

Photodynamic therapy is an up and coming treatment for topical infections, involving the use of a dye in combination with a light source. Patients who suffer burn wounds are at a higher risk of acquiring an antimicrobial infection due to the immunosuppressive nature of the burn wound site, making infections one of the main causes of deaths in burn patients. The potential use of photodynamic therapy as a treatment for topical infections could potentially help to reduce the amount of deaths caused by infections in burns patients.

During this study a variety of photoactive dyes, belonging to either the flavin, porphyrin or anthraquinone family were synthesised. These dyes were tested to determine the singlet oxygen yield and how the change in the structure affected the singlet oxygen production. The growth inhibition of these compounds were also tested to see how the changing the derivative affected the growth inhibition of each family of compounds. The singlet oxygen and growth inhibition testing was carried out to see if there was a particular derivative or family of compounds which performed better than the other families.

During this study there was a total of 35 dye compounds synthesised which belonged to either the flavin, porphyrin or anthraquinone families. The singlet oxygen production was tested by monitoring the decolourisation of TPCPD. When comparing the half-lives of the compounds the porphyrin derivatives and

hydroxy anthraquinone derivatives had the lowest half-life. The growth inhibition data was obtained by testing the compounds *in vitro* against *C.albicans*, with only four compounds showed antimicrobial activity. The 5,10,15,20-Tetrakis-(4-hydroxyphenyl)-21H,23H-porphine was the only porphyrin to show moderate growth inhibition when illuminated with blue light for 20 minutes. All the hydroxy anthraquinone derivatives showed antimicrobial activity with the hydroxy anthraquinone and hydroxy bianthrone derivatives having a lower minimum inhibitory concentration when compared with fluconazole when illuminated with blue light. The hydroxy anthrone also showed the same minimum inhibitory concentration has fluconazole when illuminated with blue light.

## Contents

Abstract.....	iii
List of Tables.....	vii
List of Figures .....	viii
List of Abbreviations.....	xi
1.0 Introduction .....	1
1.1 Fungal infections.....	1
1.2 Antimicrobial Resistance.....	6
1.3 Photodynamic Therapy Infection Control.....	10
1.3 Wound management.....	14
1.4 Rationale .....	15
References .....	16
2.0 Flavin .....	22
2.1 Background .....	22
2.2 Synthesis .....	26
2.3 Singlet Oxygen .....	33
2.4 Assay for Growth .....	35
2.5 Discussion .....	38
2.6 Experimental.....	39
References .....	57
3.0 Porphyrin.....	59
3.1 Background .....	59

3.2 Synthesis .....	62
3.3 Singlet oxygen studies.....	68
3.4 Microbiology .....	70
3.5 Discussion .....	72
3.6 Experimental.....	73
References .....	81
4.0 Anthraquinone.....	83
4.1 Background .....	83
4.2 Synthesis .....	86
4.3 Singlet Oxygen .....	95
4.4 Assay for Growth .....	97
4.5 Discussion .....	99
4.6 Experimental.....	101
References .....	108
5.0 Conclusion and future work.....	109
5.1 Conclusion.....	109
5.2 Future work.....	110

## List of Tables

Table 2.1 Photophysical and growth inhibition properties of the flavins .....	34
Table 3.1 Photophysical and growth inhibition properties of the porphyrins.....	69
Table 4.1 Photophysical and growth inhibition properties of the anthraquinones.....	96

## List of Figures

Figure 1.1 Antifungal targets .....	2
Figure 1.2 Structure of cholesterol and ergosterol.....	2
Figure 1.3 Timeline of antifungal discovery.....	3
Figure 1.4 Structure of Nystatin.....	4
Figure 1.5 Structure of Amphotericin B.....	4
Figure 1.6 Structure of fluconazole and ketoconazole.....	5
Figure 1.7 Structure of caspofungin.....	6
Figure 1.8 Jablonski Diagram.....	11
Figure 1.9 Photosensitisation pathways.....	12
Figure 2.1 7,8-dimethylisoalloxazine structure.....	22
Figure 2.2 Structure of riboflavin.....	23
Figure 2.3 <sup>1</sup> H NMR of intermediate <b>2a</b> .....	29
Figure 2.4 Mass spectrum of <b>2a</b> .....	29
Figure 2.5 <sup>1</sup> H NMR of <b>2</b> .....	30
Figure 2.6 overlaid <sup>1</sup> H NMR of <b>2</b> and <b>14</b> .....	32
Figure 2.7 Graph showing comparison between compounds 1-8 with fluconazole.....	37
Figure 2.8 Graph showing comparison between compounds 9-14 with fluconazole .....	37



Figure 3.1 skeletal structure of porphyrin.....	59
Figure 3.2 Different reactive positions on a porphine.....	59
Figure 3.3 Structure of heme.....	60
Figure 3.4 <sup>1</sup> H NMR of <b>15</b> .....	64
Figure 3.5 <sup>1</sup> H NMR of <b>18</b> .....	65
Figure 3.6 <sup>1</sup> H NMR of <b>19</b> .....	66
Figure 3.7 Graph showing comparison between compounds 16-21 with fluconazole.....	71
Figure 4.1 structure of anthraquinone.....	83
Figure 4.2 Structure of quinoid moiety.....	83
Figure 4.3 structure od aloe emodin and emodin.....	84
Figure 4.4 structure of phallacinol.....	84
Figure 4.5 <sup>1</sup> H NMR of <b>26</b> .....	89
Figure 4.6 mass spectrum of <b>26</b> .....	90
Figure 4.7 <sup>1</sup> H NMR of <b>32</b> .....	91
Figure 4.8 <sup>1</sup> H NMR of <b>27</b> .....	93
Figure 4.8 <sup>1</sup> H NMR of <b>28</b> .....	94
Figure 4.10 Graph showing comparison between compounds 23-35 with fluconazole.....	98

## List of Schemes

Scheme 2.1 synthetic route of <b>2</b> .....	26
Scheme 2.2 synthetic route of <b>14</b> .....	31
Scheme 2.3 synthetic route of <b>13</b> .....	31
Scheme 2.4 decolourisation of 2,3,4,5-tetraphenylcyclopentadienone .....	33
Scheme 3.1 synthetic route of <b>19</b> .....	63
Scheme 3.2 synthetic route of <b>21</b> .....	67
Scheme 4.1 oxidation states of anthraquinones.....	85
Scheme 4.2 possible synthetic routes for anthraquinones.....	86
Scheme 4.3 synthetic route of anthraquinone derivatives.....	87

## List of Abbreviations

$^1\text{H}$ NMR	Proton Nuclear Magnetic Resonance
$^{13}\text{C}$ NMR	Carbon Nuclear Magnetic Resonance
$\text{CDCl}_3$	Deuteriochloroform
$\text{CHCl}_3$	Chloroform
DCM	Dichloromethane
DMSO	Dimethyl sulfoxide
EtOAc	Ethyl Acetate
FDA	Food and Drug Administration
Hz	Hertz
MIC	Minimum Inhibitory Concentration
MP	Melting Point
PDT	Photodynamic Therapy
ppm	Parts per million
THF	Tetrahydrofuran
TPCPD	2,3,4,5-tetraphenylcyclopentadienone

# 1.0 Introduction

## 1.1 Fungal infections

Within a year in Europe more than four million people develop a healthcare-associated infection, of which approximately 37, 000 die as a result of the infection<sup>[1]</sup>. There are two key types of pathogenic microorganisms: bacteria and fungi. These pathogenic organisms belong to one of two cellular systems: prokaryotic or eukaryotic<sup>[2]</sup>. Eukaryotic cells have a more complex structure than prokaryotic cells, this is because eukaryotic cells have highly developed internal membrane and microtubular structures<sup>[3]</sup>. Fungal and human cells are eukaryotic<sup>[4]</sup> and bacterial cells are prokaryotic<sup>[2]</sup>. Bacteria differ from our cells structurally and metabolically, meaning that their growth can be inhibited and they can be killed with minimal affect to our cells<sup>[5]</sup>.

### Fungal Infections

Fungal and animal cells are eukaryotic<sup>[4]</sup>. Because of this, some protein components are interchangeable, such as proteins involved in stress responses, cell division cycle and gene regulation<sup>[6]</sup>. A consequence of this is the decrease in unique targets for antifungal therapy and an increase in the difficulty to identify targets, which could prove useful<sup>[6]</sup>.

However, the cell wall is where a difference occurs<sup>[4]</sup>, fungal cells have cell walls, unlike animal cells<sup>[7]</sup>. Therefore, the cell wall synthesis of fungi is a major target for the development of new antifungal drugs (see figure 1.1)<sup>[6]</sup>. The main sterol for fungi is ergosterol, whilst the main sterol in animals is cholesterol. Figure 1.2 shows the structural differences between these two sterols, with ergosterol having an extra methyl group on the side chain and two additional double bonds<sup>[8]</sup>. Since only the fungal cell wall and the main sterol is

different to mammalian cells research and development of antifungal drugs is challenging<sup>[9]</sup>.

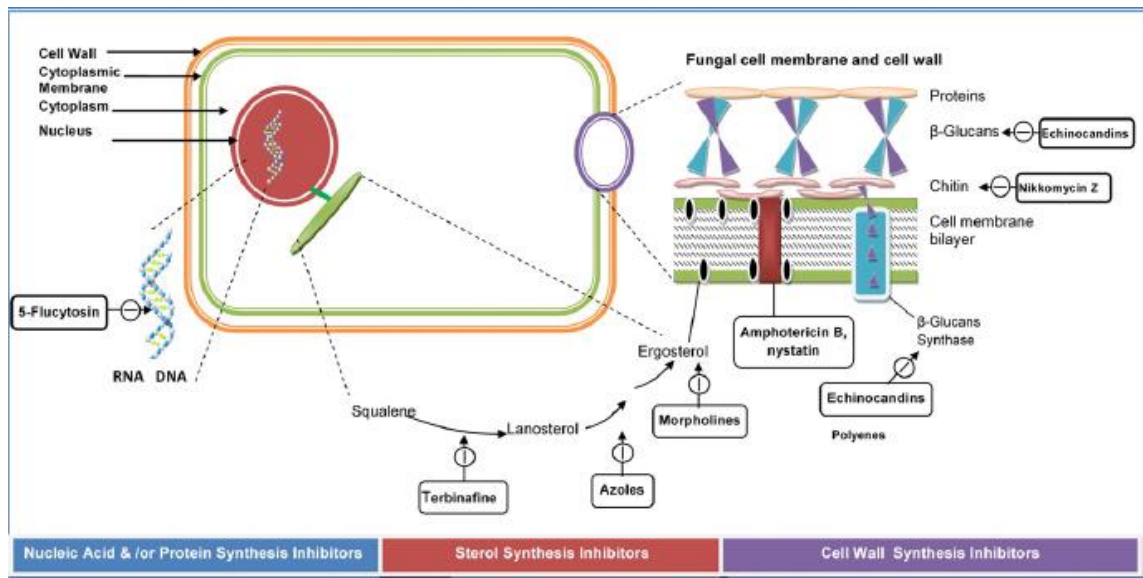


Figure 1.1: Diagram showing the antifungal targets<sup>[10]</sup>

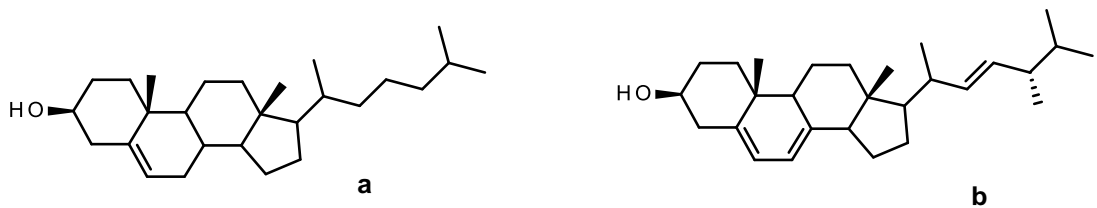


Figure 1.2: Structures of cholesterol (a) and ergosterol (b)<sup>[8]</sup>

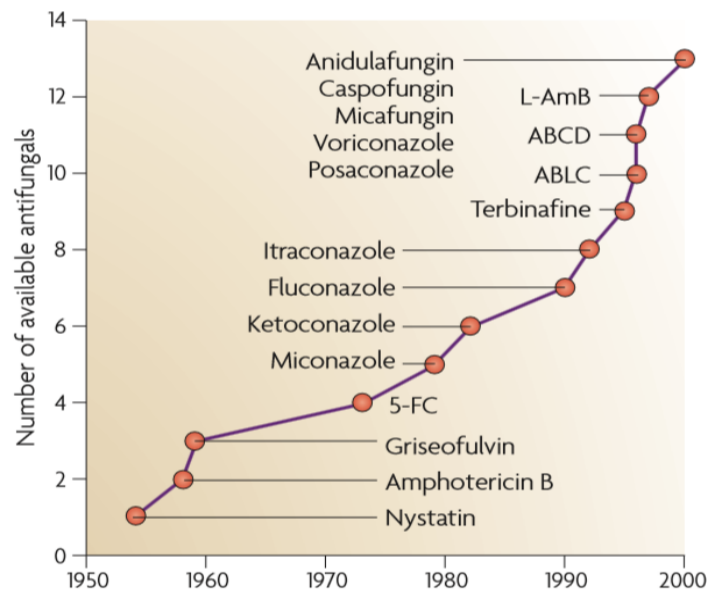


Figure 1.3: Timeline of antifungal discovery<sup>[9]</sup>

An example of medically important fungi is *Candida albicans* which are opportunistic pathogens, causing invasive fungal infections in hospitalized patients<sup>[6, 11]</sup>. Invasive candidiasis is the most found cause of invasive fungal infections, being responsible for high mortality rate<sup>[11]</sup>.

The emergence of fungal infections, associated with the increase of immunosuppressive medical therapies, since 1970s, research has been directed towards the discovery of novel antifungal agents<sup>[12]</sup>. It can be seen from figure 1.3 that there is a lack of new novel antifungals belonging to new classes being developed. This is because of a decline in the discovery of new drugs due to an increase in regulations and economic limitations. The early 1950s saw a set of antifungals, the polyenes, which were limited in their effectiveness due to toxicity by compounds such as nystatin and amphotericin B<sup>[9]</sup>. In the 1980s a new class of antifungals were developed, the azoles which were available both orally and intravenously<sup>[9]</sup>. However, since then, until the 2000s, no new class of antifungals was developed; any new antifungal drugs were just modifications on a previous drug from one of the classes. The new millennia however saw the arrival of a new class of antifungal, the echinocandins<sup>[9]</sup>.

## Polyenes

The first antifungal agent developed was a polyene, produced by *Streptomyces noursei* called nystatin (see figure 1.4)<sup>[9, 13]</sup>.

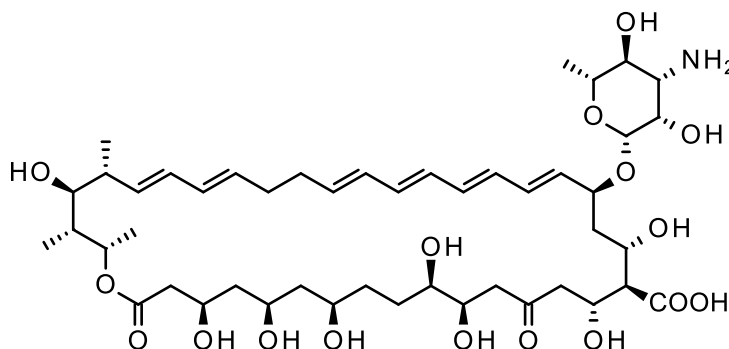


Figure 1.4: Structure of Nystatin<sup>[12]</sup>

Another polyene antifungal is Amphotericin B (see figure 1.5), which has been the gold standard for the treatment of systematic mycoses for the past 6 decades<sup>[14]</sup>.

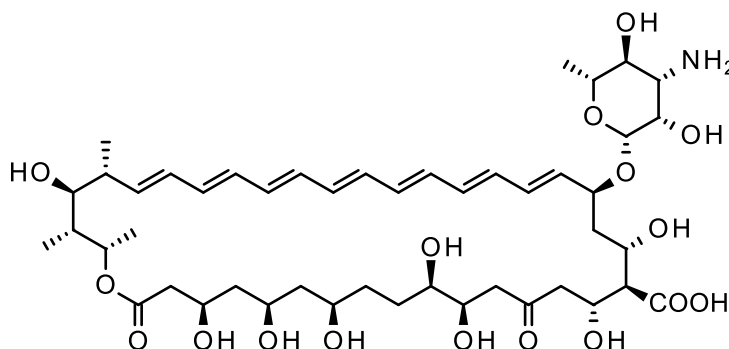


Figure 1.5: Structure of Amphotericin B<sup>[12]</sup>

Polyene antifungals bind to ergosterol, which is the main component in fungal cells, forming a complex<sup>[10]</sup>. These complexes form membrane pores resulting in leakage of intracellular components<sup>[9]</sup>. Ergosterol in most fungi replace the cholesterol component of the cell membranes<sup>[4]</sup>

Mutations to the ERG3 gene, which is involved in the ergosterol biosynthesis, lead to an accumulation of other sterols in the fungal

membrane<sup>[15]</sup>. Some *Candida* strains, for example *Candida lusitanae*, have developed resistance to amphotericin B<sup>[16]</sup>.

### Azoles

There are two broad classes of azoles; imidazoles and triazoles (see figure 1.6)<sup>[13]</sup>. This is the largest class of antifungals used in clinical cases<sup>[12]</sup>.

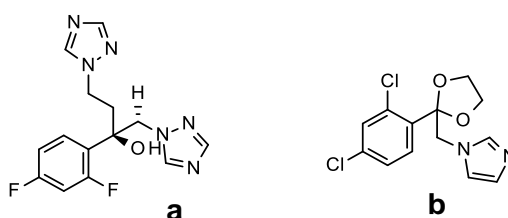


Figure 1.6: Structure of fluconazole, a triazole (a) and ketoconazole, a imidazole (b)<sup>[10]</sup>

Azoles also affect the cell membrane of the fungal cells; however, unlike the polyenes they inhibit the ergosterol synthesis by binding to lanosterol  $\alpha$  demethylase<sup>[14]</sup>. They do this by inhibiting the 14 $\alpha$ -demethylation of lanosterol in the ergosterol biosynthetic pathway<sup>[12]</sup>.

Resistance to azoles can be developed by the alteration to the target site, up-regulation of the target enzyme and by the development of efflux pumps and pathways which bypass the formation of 14 $\alpha$ -methylfecosterol<sup>[15]</sup>.

### Echinocandins

The echinocandins are a new class of antifungal agents, with caspofungin (see figure 1.7) being the first approved drug for this class<sup>[14]</sup>.



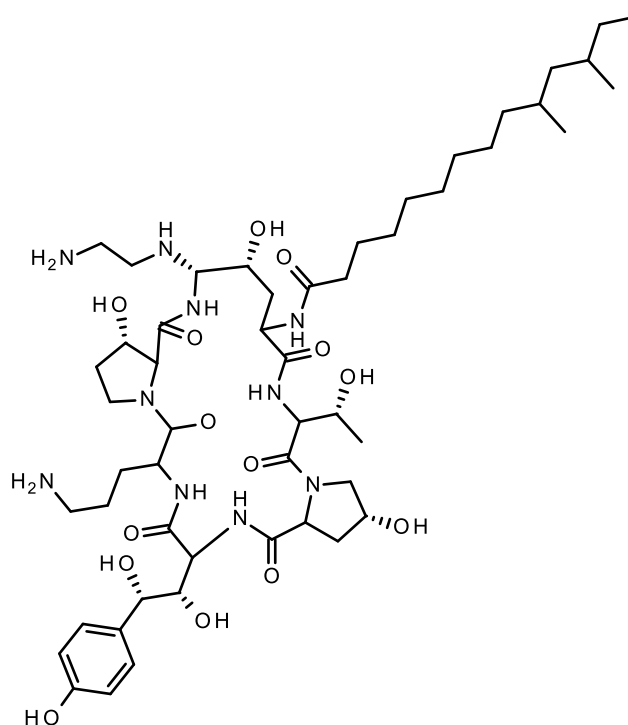


Figure 1.7: Structure of caspofungin<sup>[12]</sup>

The mechanism for echinocandins involves the inhibition of (1,3)- $\beta$ -D-glucan synthase, which is an important component in the cell wall of many pathogenic fungi<sup>[15]</sup>, as seen in figure 1.1. This inhibition destabilises the cell wall resulting in osmotic instability and cell death<sup>[13]</sup>.

Mechanisms of resistance are still being investigated<sup>[15]</sup>. It is believed however, that resistance is associated with point mutations in the *Fks1* gene of the  $\beta$ -1,3-D-glucan synthase complex, which is a large polytopic membrane protein<sup>[17]</sup>.

## 1.2 Antimicrobial Resistance

The discovery of penicillin and other antibiotics in the 20<sup>th</sup> century meant common yet deadly diseases, such as tuberculosis and pneumonia, could be treated effectively<sup>[18]</sup>. The discovery of these effective and safe antimicrobial agents could be said to be the greatest healthcare advance in history, rapidly decreasing the mortality and morbidity associated with these diseases<sup>[19]</sup>.

Bacteria and other organisms have developed resistance to antibiotics that are

naturally occurring and so resistance has always been around<sup>[20]</sup>. The increasing use of antimicrobials only serves to promote resistance in microbes<sup>[21]</sup>, due to selection pressure caused by their use over the past eight decades<sup>[22]</sup>.

Since the era of penicillin's, antimicrobials were seen as wonder drugs and prescribed without fear of harm despite the early warnings of resistance<sup>[22]</sup>. Arguably, it could be said that antimicrobials have done more to improve public health in the last 50 years, however within this success lies the major problem, overuse<sup>[23]</sup>. Within the UK, during 2011, there was 18,219 patients, who were taking at least one type of antimicrobial, with a prevalence of 34.7 % for the use of antimicrobials<sup>[1]</sup>. Due to this overuse of antimicrobials, resistance to the present agents has been developing and spreading at an increased rate, that the development of new antibiotics cannot match<sup>[24]</sup>.

Antimicrobials have become the backbone of modern medicine for the past eight decades<sup>[25]</sup>, being used as prophylactic drugs for surgery or chemotherapy<sup>[26]</sup>. The increase in resistance will reduce the efficacy of treatment of the infectious disease and could affect surgical and cancer treatments<sup>[27]</sup>; this is because patients who have undergone cancer chemotherapy or a transplant will have a compromised immune system<sup>[28]</sup>. This results in an increase in the amount of patients relying on antifungals to stay alive<sup>[29]</sup>.

Antimicrobials are used in livestock to prevent, treat and control diseases<sup>[29]</sup>; they are also used to promote growth<sup>[30]</sup>. Of the antibiotics deemed medically important for humans by the FDA, over 50% were used in agriculture in most countries<sup>[29]</sup>. In 2011, the FDA reported that there was 93% use of medically important antibiotics in feed or water in agriculture<sup>[31]</sup>. Majority of

antimicrobials administered to food animals are either related to or identical to those used in human medicine, including penicillins, cephalosporins, fluoroquinolones and tetracyclines<sup>[32]</sup>. In 1989 there was an EU-wide ban placed on four of the main growth promoters, spiramycin, tylosin, bacteriacin zinc, virginiamycin<sup>[33]</sup>.

The Swann report in 1969 reported that the administration of antibiotics at sub-therapeutic levels, presents hazards to human health. It was therefore recommended that only the use of antibiotics which have little or no therapeutic effect in humans and will not affect the effectiveness of prescribed therapeutic agents through the development of resistance, will be used as growth promoters in agriculture<sup>[34]</sup>. Following consultations, The World Health Organization, in 1997 and 1999, recommended that the use of antimicrobial growth promoters that belong to an antimicrobial class used in humans should be discontinued<sup>[35]</sup>. Over 50% of the antimicrobials produced in several countries are being used in food-producing animals<sup>[36]</sup>. Multi-resistant bacteria from farm animals can be passed along to humans through either direct contact or the food chain<sup>[37]</sup>. Antimicrobials are not only being used in livestock but are also involved Agriculture. Unlike in agriculture only one medically important class of antifungals are being used as a fungicide, the azoles<sup>[29]</sup>. In 2008 the three most used fungicides in the UK were prothioconazole, epoxiconazole and tebuconazole, all belonging to the azole class of antifungals<sup>[38]</sup>. It has been shown that there is a strong link between the countries that use azole fungicides and the incidence of resistance to this antifungal in humans. For example in the Netherlands where a lot of azole fungicides are used, close to 7% of *Aspergillus fumigatus* strains are reported to have become resistant<sup>[29]</sup>.

A misconception developed after the success of antimicrobial drugs in the late 1960's and early 1970's that infectious diseases had been conquered<sup>[39]</sup>. However, this is not true as infectious diseases are the second leading cause of death worldwide despite the availability of antimicrobials<sup>[30]</sup>. It is estimated that 2500 people in Europe alone die each year due to antibiotic resistant bacteria<sup>[40]</sup>, whilst fungal infections contribute to the deaths of 750,000 people each year<sup>[29]</sup>. There is an increase in the amount of patients relying on antifungals to stay alive<sup>[29]</sup>. Antimicrobial resistance has become one of the biggest healthcare challenges to the healthcare systems<sup>[41]</sup>, with resistance to first-line drugs in pathogens causing these diseases ranging from 0-100%<sup>[42]</sup>. During the past two decades there has been a steady increase in the amount of antibiotic-resistant organisms which are now posing a threat to disease management<sup>[43]</sup>. The development of multi-drug resistance is gathering pace and adding to the threat facing the management of diseases<sup>[43]</sup>.

The increase in ease of movement around the globe, for both transport and trade, has allowed the rapid spread of infectious diseases<sup>[42]</sup>, making antimicrobial resistance a global problem<sup>[21]</sup>. Although it is said that resistance presents a risk that we will fall back into a pre-antibiotic era this could be an underestimation because the use of antimicrobials has become crucial in ensuring the overall health of human societies from birth until death<sup>[27]</sup>.

Antimicrobial resistance occurs when pathogens are exposed to a medicine that would normally kill them or stop their growth but fails to do so<sup>[24]</sup>. Resistance is a consequence of a mutation within the microbe<sup>[22]</sup>. These mutations, which are spontaneous changes to the genome<sup>[44]</sup>, are a natural phenomenon<sup>[42]</sup>. The failure in inhibiting or killing the pathogen will allow resistant strains to grow and spread due to a lack of competition<sup>[24]</sup>. An effective

way for the microbe to develop resistance is to expose the microbe to sub-therapeutic level of the antimicrobial<sup>[45]</sup>. Exposure can happen in several ways; the patient not completing the course of antibiotics, or the dose could have been inaccurately calculated<sup>[45]</sup>. The selection pressure caused from the use of the antimicrobial provides a competitive advantage for the mutant strains, sub-therapeutic antimicrobial doses help towards this stepwise selection of resistance<sup>[22]</sup>.

### **1.3 Photodynamic Therapy Infection Control**

There is a desire to replace the present antimicrobial agents, which have one mode of action with those that have multiple modes of action.

Microorganisms can develop resistance quickly, which is the problem associated with the present agents<sup>[46]</sup>. The use of dyes in medicine is based upon the work done by Koch and Ehrlich in the late 19<sup>th</sup> century<sup>[47]</sup>. Dyes, in the form of biological stains, are used in hospitals every day<sup>[48]</sup> for example, in the identification of bacterial strains and tracing the local extent of malignant disease<sup>[49]</sup>.

Given the rise in resistance, active dyes for the use of local therapeutics seem to be the answer to preserving the essential systematic agents<sup>[48]</sup>. A method has been developed that uses a dye in combination with light to have a microbicidal effect<sup>[47]</sup>. These dyes are referred to as photosensitisers and are called photoantimicrobials<sup>[47]</sup>.

Although, the photoantimicrobial effect has only been explored realistically since the 1990s, the photoantimicrobial effect has been known since the turn of last century<sup>[47]</sup>. Photodynamic therapy (PDT) involves the use of dyes

as a photosensitizer in addition with visible light of an appropriate wavelength to excite the photosensitizer<sup>[50]</sup>.

Once the photosensitizer is illuminated with a light of an appropriate wavelength<sup>[51]</sup>, it converts from a ground state to a excited singlet state<sup>[52]</sup>. From its excited state the photosensitizer may emit fluorescence and return to its ground state<sup>[53]</sup> or it can undergo a transition to the excited triplet state via intersystem crossing (figure 1.8)<sup>[52]</sup>. The excited photosensitizer can then interact with endogenous oxygen within the target cell or surrounding tissue to provide cytotoxic effects<sup>[54]</sup>. There are two ways in which this can occur: type I and type II photosensitisation (figure 1.9)<sup>[55]</sup>.

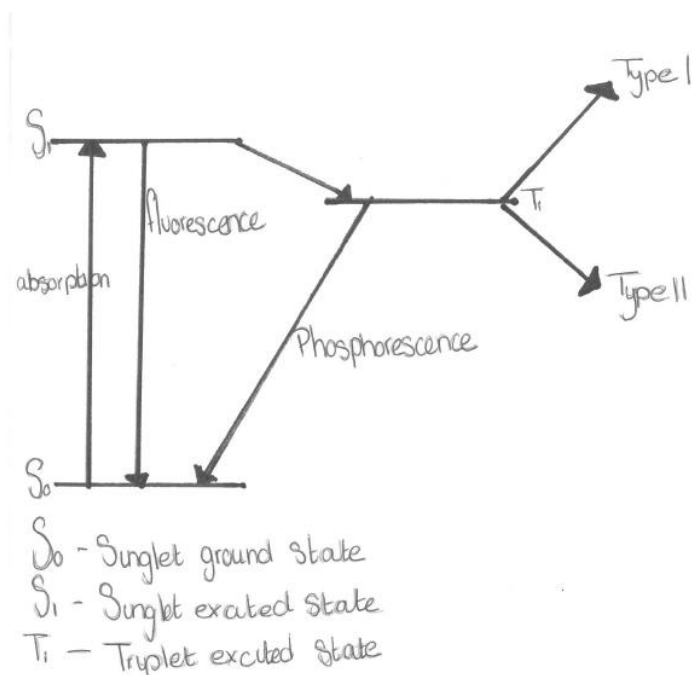


Figure 1.8: Jablonski diagram

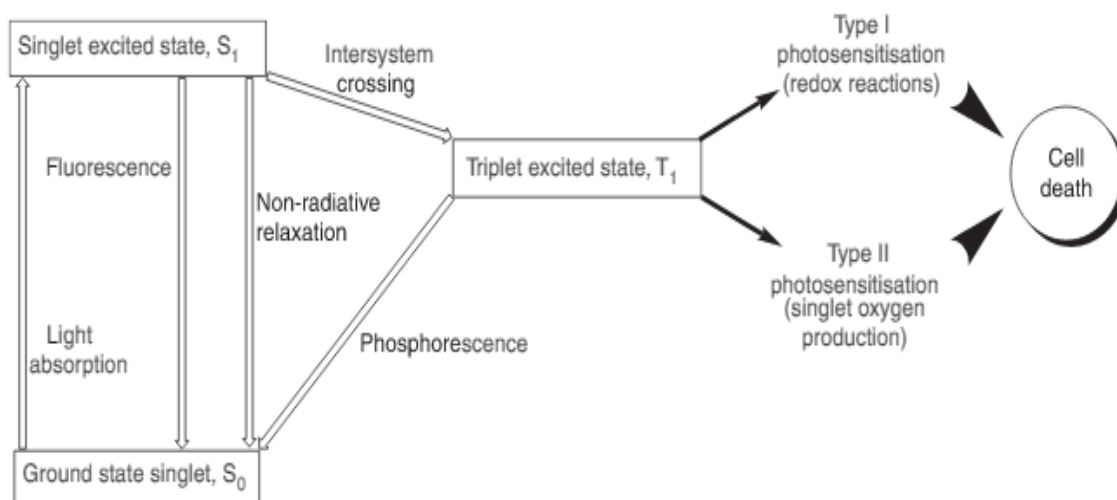


Figure 1.9: Photosensitization pathways<sup>[56]</sup>.

Type I photosensitisation occurs when a hydrogen-atom removal or electron transfer between the excited photosensitiser and a substrate takes place<sup>[57]</sup>, forming either superoxide radical anions or hydroxyl radicals<sup>[58]</sup>. In biological systems, superoxide radicals are notably not reactive and do not cause much oxidative damage. They can however, react with themselves to produce hydrogen peroxide and oxygen. Superoxide radicals are a crucial part in the production of the highly reactive hydrogen peroxide radicals. These radicals can add to an organic substrate forming a hydroxylated adduct that is itself a radical. The hydroxyl radical could also oxidize the substrate, causing the substrate itself to become a radical. This substrate can then react with other molecules causing a chain reaction<sup>[55]</sup>.

Type II photosensitization occurs when there is an energy transfer from the photosensitiser triplet state to ground state molecular oxygen to form excited singlet oxygen<sup>[54]</sup>. This photosensitisation pathway is the most significant method due to most photosensitizers being efficient singlet oxygen producers<sup>[59]</sup>. The singlet oxygen produced is able to react with unsaturated lipids, amino acids and the nucleic acid guanine<sup>[60]</sup>. Both type I and type II

photosensitisation pathways can occur together, the amount of each type however depends upon the type of photosensitiser used, the concentration of oxygen and substrate present<sup>[55]</sup>.

One of the advantages for the use of antimicrobial PDT is their ability to kill microbes even if they have developed resistance to the present antimicrobial agents<sup>[61]</sup>. The radicals and reactive singlet oxygen produced via the photosensitisation can inactivate enzymes and other proteins, and cause the peroxidation of lipids subsequently causing the lysis of cell membranes<sup>[7]</sup>. The multiplicity and non-specific nature of possible targets for PDT makes it highly unlikely that resistance would result<sup>[61, 62]</sup>. In addition, it does not matter if the dye is not taken into the cell, further preventing the outbreak of resistance, this is because the mode of action of the dye is still able to proceed out of the cell due to it being light activated.

In regards to efflux pumps the major classes of antimicrobial photosensitisers have been tested and it has been found that only phenothiaziniums are efflux substrates<sup>[63]</sup>. Resistance to the oxidative burst from the illumination of the dye, might include enzymes such as superoxide dismutase and catalase, however these enzymes will be ineffective against singlet oxygen as it can inactivate the enzymes<sup>[63]</sup>. Photosensitisers with their non-specific microbicidal effect and lack of reported resistance means that the research of new photosensitisers can be carried out without the imminent threat of resistance, unlike current antimicrobial agents.

The use of PDT for the treatment of infections requires enough intensity from the light source to reach the pathogens containing the photosensitiser<sup>[51]</sup>. The further the light travels through the skin the less likely the light will reach its target with the intensity of light required to excite the photosensitiser<sup>[51]</sup>, this is



due to the skin having natural chromophores such as melanin<sup>[56]</sup>. It is clear to see that the light required for the activation of the photosensitiser cannot be applied to the whole body, meaning that for systematic infections, such as candidemia, this method of treatment cannot be used<sup>[47]</sup>. However the use of PDT for topical infections, suggests a simple, non-invasive approach where the photosensitiser is applied topically before using superficial illumination<sup>[47]</sup>. This method shows potential for the treatment of pressure sores, skin wounds and burns<sup>[47]</sup>.

### **1.3 Wound management**

Burns are a worldwide public health problem, with burns caused by fire are responsible for over 300,000 deaths a year<sup>[64]</sup>, with 50 – 75% of these due to microbial infections<sup>[64]</sup>. This is because burn patients are susceptible to infections<sup>[65]</sup>, due to the burn wound destroying the skin, causing the immune system to become compromised<sup>[50]</sup>. The wound which consists of moist necrotic tissue<sup>[66]</sup>, presents an optimal environment for opportunistic pathogens to colonise<sup>[67]</sup>. Gram-positive bacteria are the among the first organisms to colonise on the wound site, with gram-negative bacteria quickly replacing the gram-positive bacteria<sup>[68]</sup>. Fungi may also colonize on the wound<sup>[69]</sup>, with *Candida* spp being the most commonly isolated species<sup>[70]</sup>.

Due to infections in burns patients being frequent and fatal, antimicrobials are often given as prophylactic treatment<sup>[71]</sup> to limit the growth of the bacterial organisms on the site of the wound<sup>[72]</sup>. However the use of antimicrobials in this way has become a controversial topic, about whether any benefit of this treatment will outweigh the risks associated with drug toxicity and the development of multi-drug resistance<sup>[71]</sup>.

A standard treatment worldwide for burns, is the removal of the necrotic tissue before covering the wound with a dressing<sup>[65]</sup>. Wound dressings are used during the healing process because they predominately protect the wound against microorganisms<sup>[73]</sup>. For wounds, such as burns, where the risk of infection is high antimicrobial dressings are used<sup>[65]</sup>. The antimicrobial agent is incorporated within the wound dressing, which can either be used prophylactically or in the treatment of an established infection<sup>[65]</sup>. One example of a wound dressing is Xeroform<sup>®</sup> which has been used in burn care for decades<sup>[74]</sup>. However a recent study carried out by Barillo et al showed that Xeroform<sup>®</sup> as a composite dressing showed no antimicrobial effect even though the bismuth tribromophenate which is present in the dressing did show some antimicrobial activity<sup>[74]</sup>. Another study carried out by Halstead et al it was concluded that there is a significant variation in the ability of the commercial antimicrobial dressings to prevent the biofilm formation by two key burn wound pathogens. Biofilm is an important contributor to the colonisation of the wound and the resulting infection<sup>[65]</sup>.

## **1.4 Rationale**

The lack of evidence reporting the development of resistance to treatment with PDT, along with the potential for burn care, forms the basis of the project. The rationale for this was to investigate the singlet oxygen production and microbicidal effect of three families of dyes. The families of dyes have maximum wavelengths over the wavelength spectrum. The three classes that were chosen were: flavins, porphyrins and anthraquinones. It was hypothesised that the anthraquinones would be the best singlet oxygen producer due to the

conjugated ring system with the two carbonyl groups attached at the 9 and 10 positions. The microicidal effect will be tested against *C.albicans*.

## References

1. England, P.H., *Point prevalence survey of healthcare-associated infections, antimicrobial use and antimicrobial stewardship in England*. ecdc, 2016.
2. Gross, T., et al., *Introductory Microbiology*. 1995: Chapman & Hall.
3. Heritage, J., E.G.V. Evans, and R.A. Killington, *Introductory Microbiology*. Studies in biology. 1996: Cambridge University Press.
4. Madigan, M.T.M., J.M. Parker, J., *Brock biology of microorganisms*. 10 ed. 2003: Prentice Hall.
5. Id, O., *Blackwell Handbooks of Behavioral Neuroscience : Antibiotics and Antibiotic Resistance (1)*. 2011, Hoboken, US: Wiley.
6. Brown, A.J.P., *Fungal pathogens - the devil is in the detail*. Microbiology today, 2002. **29**: p. 120-122.
7. Calzavara-Pinton, P.G., M. Venturini, and R. Sala, *A comprehensive overview of photodynamic therapy in the treatment of superficial fungal infections of the skin*. Journal of Photochemistry and Photobiology B: Biology, 2005. **78**(1): p. 1-6.
8. Baginski, M., A. Tempczyk, and E. Borowski, *Comparative conformational analysis of cholesterol and ergosterol by molecular mechanics*. European Biophysics Journal, 1989. **17**: p. 159-166.
9. Ostrosky-Zeichner, L.C., A. Galgiani, J.N. Odds, F.C. Rex, J.H., *An insight into the antifungal pipeline: selected new molecules and beyond*. Nature reviews, 2010. **9**: p. 719-727.
10. Kathiravan, M.K.S., A. B. Chothe, A. S. Dudhe, P. B. Watode, R. P. Mukta, M. S. Gadhwe, S., *The biology and chemistry of antifungal agents: A review (vol 20, pg 5678, 2012)*. Bioorganic & Medicinal Chemistry, 2013. **21**(5): p. 1367-1367.
11. Castanheira, M.W., L.N. Diekema, D.J. Messer, S.A. Jones, R.N. Pfaller, M.A., *Low Prevalence of fks1 Hot Spot 1 Mutations in a Worldwide Collection of Candida Strains*. Antimicrobial agents and chemotherapy, 2010. **54**: p. 2655-2659.

12. Odds, F.C.b., A.J.P, Gow, A.R, *Antifungal agents: mechanisms of action*. Trends in Microbiology, 2003. **11**: p. 272-279.
13. Brunton, L.L., *Goodman and Gilman's manual of pharmacology and therapeutics*. 2nd edition / Laurence L. Brunton.. ed. Manual of pharmacology and therapeutics, ed. R. Hilal-Dandan, et al. 2014, New York: New York : McGraw-Hill.
14. Wong-Beringer, A.K., J., *Systemic antifungal therapy: New option, New challenges*. Pharmacotherapy, 2003. **23**: p. 1441-1462.
15. Kanafani, Z.A. and J.R. Perfect, *Resistance to Antifungal Agents: Mechanisms and Clinical Impact*. Clinical Infectious Diseases, 2008. **46**(1): p. 120-128.
16. Brunton, L.L., *Goodman and Gilman's manual of pharmacology and therapeutics*. 2nd edition / Laurence L. Brunton.. ed. Manual of pharmacology and therapeutics, ed. R. Hilal-Dandan, et al. 2014, New York: New York : McGraw-Hill.
17. Balashov, S.V., S. Park, and D.S. Perlin, *Assessing Resistance to the Echinocandin Antifungal Drug Caspofungin in Candida albicans by Profiling Mutations in FKS1*. Antimicrobial Agents and Chemotherapy, 2006. **50**(6): p. 2058-2063.
18. O'Neill, J., *Tackling a crisis for the health and wealth of nations*. Review on antimicrobial resistance, 2014.
19. Rice, L.B., *Federal Funding for the Study of Antimicrobial Resistance in Nosocomial Pathogens: No ESKAPE*. Journal of Infectious Diseases, 2008. **197**(8): p. 1079-1081.
20. Phillips, I., et al., *Does the use of antibiotics in food animals pose a risk to human health? A critical review of published data*. Journal of Antimicrobial Chemotherapy, 2004. **53**(1): p. 28-52.
21. O'Neill, J., *Rapid Diagnostics: Stopping unnecessary use of antibiotics*. Review on Antimicrobial Resistance, 2015.
22. Laxminarayan, R., et al., *Antibiotic resistance—the need for global solutions*. The Lancet Infectious Diseases, 2013. **13**(12): p. 1057-1098.
23. Wise, R., *Antimicrobial resistance: priorities for action*. Journal of Antimicrobial Chemotherapy, 2002. **49**(4): p. 585-586.
24. O'Neill, J., *Tackling Drug-Resistant Infections - Final Report and recommendations*. Review on Antimicrobial Resistance, 2016.

25. Laxminarayan, R., et al., *Access to effective antimicrobials: a worldwide challenge*. The Lancet. **387**(10014): p. 168-175.
26. Gould, I.M., *Antibiotic stewardship: prescribing social norms*. The lancet, 2016. **387**: p. 1699-1701.
27. Smith, R. and J. Coast, *The true cost of antimicrobial resistance*. BMJ, 2013. **346**.
28. Wainwright, M., et al., *Photobactericidal activity of methylene blue derivatives against vancomycin-resistant Enterococcus spp.* Journal of Antimicrobial Chemotherapy, 1999. **44**(6): p. 823-825.
29. O'Neill, J., *Antimicrobials in agriculture and the environment - Reducing unnecessary waste and use*. Review on Antimicrobial Resistance, 2015.
30. Spellberg, B.G., Robert. Gilbert, David. Bradley, John. Boucher, Helen W. Scheld, W. Michael. Bartlett, John G. Edwards, John and the Infectious Diseases Society of, America, *The Epidemic of Antibiotic-Resistant Infections: A Call to Action for the Medical Community from the Infectious Diseases Society of America*. Clinical Infectious Diseases, 2008. **46**(2): p. 155-164.
31. Administration, F.a.D., *2011 SUMMARY REPORT On Antimicrobials Sold or Distributed for Use in Food-Producing Animals*. Department of Health and Human Services, FDA, 2014.
32. Tollefson, L. and B.E. Karp, *Human health impact from antimicrobial use in food animals*. Médecine et Maladies Infectieuses, 2004. **34**(11): p. 514-521.
33. Soulsby, L., *Antimicrobials and animal health: a fascinating nexus*. Journal of Antimicrobial Chemotherapy, 2007. **60**(suppl\_1): p. i77-i78.
34. House, o.L.S.C.o.S.a.T. House, and o.L.S.C.o.S.a. Technology, *Resistance to Antibiotics and other Antimicrobial agents*. London: Her Majesty's Stationary Office, 1998. **1997-1998 (seventh report)**.
35. Angulo, F.J., et al., *Antimicrobial use in agriculture: controlling the transfer of antimicrobial resistance to humans<sup>1</sup>*. Seminars in Pediatric Infectious Diseases, 2004. **15**(2): p. 78-85.
36. Gyles, C., *The growing problem of antimicrobial resistance*. The Canadian Veterinary Journal, 2011. **52**(8): p. 817-820.

37. Nordberg, P.M., D.L. Cars, O, *Antibacterial Drug Resistance*. Priority Medicines for Europe and the World. A Public Health Approach to Innovation.
38. Parker, J.E., et al., *Resistance to antifungals that target CYP51*. Journal of Chemical Biology, 2014. **7**(4): p. 143-161.
39. Spellberg, B.P., John H. Brass, Eric P. Miller, Loren G. Edwards, John E., *Trends in Antimicrobial Drug Development: Implications for the Future*. Clinical Infectious Diseases, 2004. **38**(9): p. 1279-1286.
40. Leonard, C.T., D. Ward, and C. Longson, *Antimicrobial resistance: a light at the end of the tunnel?* The Lancet, 2017. **389**(10071): p. 803.
41. Syed, S.N., M.J. Ducrotoy, and T.T. Bachmann, *Antimicrobial resistance diagnostics: time to call in the young?* The Lancet Infectious Diseases, 2016. **16**(5): p. 519-521.
42. Organization, W.H., *WHO Global Strategy for Containment of Antimicrobial Resistance*. 2001.
43. Norrby, S.R., C.E. Nord, and R. Finch, *Lack of development of new antimicrobial drugs: a potential serious threat to public health*. The Lancet Infectious Diseases, 2005. **5**(2): p. 115-119.
44. Standing Medical Advisory, s.-g.o.A.R., *The Path of Least Resistance*. 1998.
45. O'Neill, J., *Safe, Secure and Controlled - Managing supply chain of antimicrobials*. Review on Antimicrobial Resistance, 2015.
46. Wainwright, M., et al., *Photoantimicrobials&#x2014;are we afraid of the light?* The Lancet Infectious Diseases. **17**(2): p. e49-e55.
47. Wainwright, M., *In defence of 'dye therapy'*. International Journal of Antimicrobial Agents, 2014. **44**(1): p. 26-29.
48. Wainwright, M., *Safe' photoantimicrobials for skin and soft-tissue infections*. International Journal of Antimicrobial Agents. **36**(1): p. 14-18.
49. M, W., *Therapeutic applications of near infre-red dyes*. Coloration Technology, 2010. **126**(3): p. 115-126.
50. Dai, T., Y.-Y. Huang, and M.R. Hamblin, *Photodynamic therapy for localized infections—State of the art*. Photodiagnosis and Photodynamic Therapy, 2009. **6**(3): p. 170-188.
51. Maisch, T., *Anti-microbial photodynamic therapy: useful in the future?* Lasers Med Sci, 2007. **22**: p. 83-91.

52. Buytaert, E., M. Dewaele, and P. Agostinis, *Molecular effectors of multiple cell death pathways initiated by photodynamic therapy*. *Biochimica et Biophysica Acta (BBA) - Reviews on Cancer*, 2007. **1776**(1): p. 86-107.
53. Wainwright, M., *Photosensitisers in Biomedicine*. 2009: Wiley-Blackwell.
54. O'Riordan, K., O.E. Akilov, and T. Hasan, *The potential for photodynamic therapy in the treatment of localized infections*. *Photodiagnosis and Photodynamic Therapy*, 2005. **2**(4): p. 247-262.
55. Castano, A.P., T.N. Demidova, and M.R. Hamblin, *Mechanisms in photodynamic therapy: part one—photosensitizers, photochemistry and cellular localization*. *Photodiagnosis and Photodynamic Therapy*, 2004. **1**(4): p. 279-293.
56. Wainwright, M., *Therapeutic applications of near-infrared dyes*. *Coloration Technology*, 2010. **126**: p. 115-126.
57. DeRosa, M.C. and R.J. Crutchley, *Photosensitized singlet oxygen and its applications*. *Coordination Chemistry Reviews*, 2002. **233**(Supplement C): p. 351-371.
58. Baldea, I., et al., *Efficiency of photodynamic therapy on WM35 melanoma with synthetic porphyrins: Role of chemical structure, intracellular targeting and antioxidant defense*. *Journal of Photochemistry and Photobiology B: Biology*, 2015. **151**(Supplement C): p. 142-152.
59. Mehraban, N.F., H.S, *Developments in PDT Sensitizers for increased selectivity and singlet oxygen production*. *Materials*, 2015. **8**: p. 4421-4456.
60. Baptista, M.S., Cadet, J., Di Mascio, P., Ghogare, A. A., Greer, A., Hamblin, M. R., Lorente, C., Nunez, S. C., Ribeiro, M. S., Thomas, A. H., Vignoni, M. and Yoshimura, T. M., *Type I and Type II Photosensitized Oxidation Reactions: Guidelines and Mechanistic Pathways* . *Photochemistry and Photobiology*, 2017. **93**: p. 912-919.
61. Yin, R., et al., *Light based anti-infectives: ultraviolet C irradiation, photodynamic therapy, blue light, and beyond*. *Current Opinion in Pharmacology*, 2013. **13**(5): p. 731-762.
62. Wainwright, M., *Photoantimicrobials—So what's stopping us?* *Photodiagnosis and Photodynamic Therapy*, 2009. **6**(3): p. 167-169.

63. Wainwright, M., et al., *Photoantimicrobials*; are we afraid of the light? *The Lancet Infectious Diseases*. **17**(2): p. e49-e55.
64. Ramirez-Blanco, C.E., et al., *Infection in burn patients in a referral center in Colombia*. *Burns*, 2017. **43**(3): p. 642-653.
65. Halstead, F.D., et al., *Antimicrobial dressings: Comparison of the ability of a panel of dressings to prevent biofilm formation by key burn wound pathogens*. *Burns*, 2015. **41**(8): p. 1683-1694.
66. Fadeyibi, I.O., et al., *Bacteriology of infected burn wounds in the burn wards of a teaching hospital in Southwest Nigeria*. *Burns*, 2013. **39**(1): p. 168-173.
67. Alharbi, S.A. and M.E. Zayed, *Antibacterial susceptibility of bacteria isolated from burns and wounds of cancer patients*. *Journal of Saudi Chemical Society*, 2014. **18**(1): p. 3-11.
68. Rafla, K. and E.E. Tredget, *Infection control in the burn unit*. *Burns*, 2011. **37**(1): p. 5-15.
69. Serio, S., B. Burgess, and D. Voigt, *Fungal periapical abscess and the burn patient: A report of two cases of an unreported source for systemic infection*. *Burns*, 2017.
70. Rosanova, M.T., et al., *Fusarium spp infections in a pediatric burn unit: nine years of experience*. *The Brazilian Journal of Infectious Diseases*, 2016. **20**(4): p. 389-392.
71. Ramos, G., et al., *Systemic antimicrobial prophylaxis in burn patients: systematic review*. *Journal of Hospital Infection*, 2017. **97**(2): p. 105-114.
72. Park, H.-S., et al., *Early pathogenic colonisers of acute burn wounds: A retrospective review*. *Burns*, 2017.
73. Mogoşanu, G.D. and A.M. Grumezescu, *Natural and synthetic polymers for wounds and burns dressing*. *International Journal of Pharmaceutics*, 2014. **463**(2): p. 127-136.
74. Barillo, D.J., et al., *The antimicrobial spectrum of Xeroform®*. *Burns*, 2017. **43**(6): p. 1189-1194.



## 2.0 Flavin

### 2.1 Background

#### 2.1.1 What are flavins?

Flavins are yellow compounds based upon the nitrogen heterocycle 7,8-dimethylisoalloxazine (Figure 2.1)<sup>[1]</sup>, which are involved in many biochemical reactions as coenzymes and photoreceptors<sup>[2]</sup>. When illuminated with UV light, flavins produce a yellow-green fluorescence<sup>[3]</sup>.

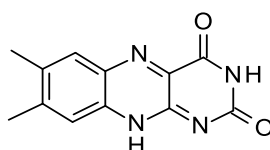


Figure 2.1: 7,8- Dimethylisoalloxazine structure

Flavins are a vital nutrients for all prokaryotic and eukaryotic cells<sup>[3]</sup>, with most microorganisms being able to synthesise riboflavin whereas mammals cannot<sup>[4]</sup>. Vitamins mainly occur in cofactor forms within the body<sup>[5]</sup> with B vitamins being crucial cofactors for numerous aspects of human metabolism, including fat and carbohydrate metabolism and DNA synthesis<sup>[6]</sup>. One B vitamin, riboflavin (Figure 2.2), is an essential component in human and animal diets<sup>[3]</sup> and must be present in the body for good health<sup>[7]</sup>. Riboflavin is a precursor for all biologically important flavins<sup>[2]</sup>, due to this riboflavin is an obligatory component of cellular metabolism and is responsible for normal development, growth, reproduction, lactation, physical performance of well-being<sup>[8]</sup>.

The importance of their biological role is in most cases related to the coenzymes flavin mononucleotide (FMN) and flavin adenine dinucleotide (FAD), which bind to proteins to make flavoproteins<sup>[3]</sup>. Non-complex flavoproteins carry out similar reactions to cytochrome P450 in the liver microsomes<sup>[9]</sup>. FMN and

FAD are involved in numerous enzyme catalysed reactions as non-covalently or covalently bound redox cofactors<sup>[10]</sup>.

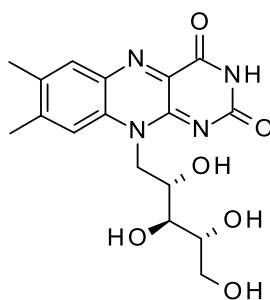


Figure 2.2: Structure of riboflavin

### 2.1.2 Chemistry of Flavins

The chemical entity responsible for the variety of biological activity of the flavin is the isoalloxazine moiety<sup>[3]</sup>. Since the discovery and chemical characterisation of flavins, it has been known that they can undergo both one and two electron transfer processes<sup>[9]</sup>. Flavin is an amphoteric molecule existing as neutral, anionic and cationic species in all three of the redox states<sup>[3]</sup> listed below:

1. Quinone (Oxidized state),
2. Semiquinone (One-electron reduced state)
3. Hydroquinone (Two-electron reduced state)<sup>[10]</sup>.

Flavins are also known for their ability to act as both electrophiles and nucleophiles<sup>[9]</sup>, making flavoenzymes very versatile in terms of substrate reactions, which is a major reason for the ubiquity of flavin-dependent enzymes in biological systems<sup>[2]</sup>. The isoalloxazine chromophore is involved in redox reactions not the side chains<sup>[3]</sup>.

Riboflavin is essential for flavoenzymes, which are the most adaptable cofactors in redox reactions<sup>[4]</sup>. Flavoproteins are involved in a variety of redox

reactions, catalyse dehydrogenations, oxidation, one – or two – electron transfer and hydroxylation<sup>[4]</sup>. Due to this they often form part of multi-redox centre enzymes<sup>[9]</sup>.

### **2.1.3 Photochemistry of Flavins**

The photochemistry of flavins was of particular interest in the 1940's<sup>[1]</sup>. This is because of the suggested involvement of flavin excited states in several important photochemical and photobiological processes such as photodynamic action, phototaxis, phototropism and photodegradation of pesticide residues used to treat waste water<sup>[11]</sup>.

Riboflavin, FMN and FAD are photosensitisers<sup>[12]</sup>. Photosensitisers are dyes which can induce photomodification of compounds that do not directly absorb or are not modified by visible light, either by direct interaction with a substrate to generate radical intermediates or by energy transfer to oxygen generating singlet oxygen<sup>[13]</sup>. FMN, FAD and riboflavin are degraded easily by UV and visible light within the range 420-560 nm<sup>[14]</sup>.

After being illuminated riboflavin is converted into an excited triplet state. There are two pathways in which riboflavin can be reduced; type I and type II as seen in figure 1.8<sup>[15]</sup>. The ability to produce both singlet oxygen and radical intermediates means that riboflavin has the ability of both type I and type II photosensitisation upon illumination<sup>[15]</sup>.

### **2.1.4 Flavins as treatment for bacterial/fungal infections**

*Mycobacterium* and many other deadly pathogens depend strictly on the endogenous biosynthesis of riboflavin because they lack a riboflavin transporter<sup>[4]</sup>. Due to the importance of flavoproteins for versatile and fundamental biochemical reactions, the prospect for use as targets in

pharmacological treatments is immense. Pharmacological treatments could include FAD and FMN dependent enzymes such as, thymidylate synthase, lipoamide dehydrogenase which are being studied<sup>[16]</sup>. The biosynthesis pathway of riboflavin may be rife in highly selective therapeutic targets for mammals<sup>[4]</sup>.

Studies carried out in the 1960's and 70's showed that upon exposure to UV/visible light riboflavin is successful in inactivating viruses and bacteria <sup>[7]</sup>. Further, it can be used as a topical dermatological therapy or as antiviral and antibacterial applications to blood safety<sup>[13]</sup>. Light activated riboflavin oxidizes guanine in nucleic acids, preventing replication of the pathogen's genome<sup>[7]</sup>. Recently, riboflavin has been shown to increase the efficiency of conventional therapies in different diseases for example *Staphylococcus aureus* infection<sup>[8]</sup>.

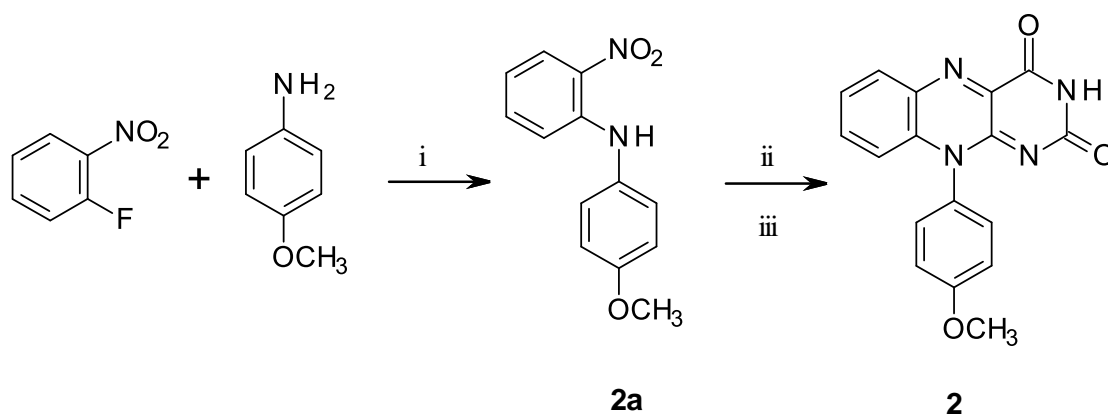
### **2.1.5 Rational**

Riboflavin (Vitamin B1) is a natural photosensitiser and well known to undergo Type I and II photosensitisation upon illumination with blue light ( $\lambda = 475\text{nm}$ )<sup>[15]</sup>. The reported photoantimicrobial activity of Riboflavin is remarkable showing activity across a broad spectrum of gram positive and gram-negative bacteria. Inspired by this, we decided to make a variety of synthetic flavin photosensitisers, based on the core alloxazine structure as shown in Table 2.1 (page 34). The rational for this was to investigate how singlet oxygen production and the subsequent microbicidal effects of these compounds would change, if the ribose sugar unit was replaced with a p-substituted phenyl derivative. This is because the removal of the sugar unit could change the ability of the microbe to uptake the flavin compounds. Indeed, it was hypothesised that when the substituted atom was a Cl, Br or I, the singlet oxygen yield would increase due to the heavy atom effect. This should in turn should increase antimicrobial activity due to the higher singlet oxygen

production causing there to be more singlet oxygen to attack more targets within the cell. The singlet oxygen production was obtained via spectrophotometric technique decolourisation 2,3,4,5-tetraphenylcyclopentadienone (TPCPD) in dichloromethane. In order to determine the antifungal activity of the novel compounds they were tested against the yeast like fungi, *Candida albicans*, using the EUCAST microdilution method (EUCAST E.DEF 7.3 December 2015).

## 2.2 Synthesis

All but two of the fourteen flavin derivatives were synthesised via a two-step procedure as shown in scheme 2.1 using 10-(4-methoxyphenyl)isoalloxazine (**2**) as an example.



i. K<sub>2</sub>CO<sub>3</sub>, 3h, 150°C, 78%; ii. Zn, AcOH, 2h, r.t.; iii. Alloxan.H<sub>2</sub>O, B(OH)<sub>3</sub>, AcOH, 3h, r.t., 93%.  
Scheme 2.1: Synthetic route for the synthesis of 4-methoxy-2-nitrodiphenylamine (**2a**) and 10-(4-methoxyphenyl)isoalloxazine (**2**)

The synthesis was accomplished with modifications to previous method<sup>[17]</sup>. An aromatic amine was reacted with 2-fluoro-1-nitrobenzene in the presence of potassium carbonate as base, to yield the p-substituted 2-nitrodiphenylamines which were isolated at the pump as red solids and carried forward without purification. The yields of the p-substituted 2-

nitrodiphenylamines were good to poor and no issues in the synthesis were noted.

The  $^1\text{H}$  analysis of 4-methoxy-2-nitrodiphenylamine is shown below in figure 2.3 and clearly confirms the structure of the target intermediate (**2a**). The spectrum clearly shows 12H in the expected regions, with the correct splitting and integrations. The 3H singlet can be attributed to the OMe group, which are visible at 3.85 ppm and the aromatic  $2^\circ$  amine is seen at 9.42 ppm again as a singlet, with an integration just below 1H, which can possibly be attributed to exchange. The aromatic region clearly shows 8 aromatic protons between 8.21 ppm – 6.69 ppm respectively. The mass spectrum of the intermediate **2a**, also shows the formation of the compound with a signal at 245  $[\text{M}^+]$  which can be seen in Figure 2.4.

The crude material (**2a**) was reduced using zinc dust under acidic conditions, and subsequently treated with alloxan monohydrate in the presence of boric acid to yield 10-(4-methoxyphenyl)isoalloxazine (**2**) in 93 % yield. Once again the spectroscopic analysis ( $^1\text{H}$  NMR) confirms the correct amount of signals this time with the amide ( $\text{C}(\text{O})\underline{\text{N}}\text{HC}(\text{O})$ ) of the flavin being seen at 11.43 ppm with an integration of 1H, confirming the attachment of the extra ring system. Also, the aromatic protons are clearly defined along with the OMe protons seen as a 3H singlet at 3.88 ppm.

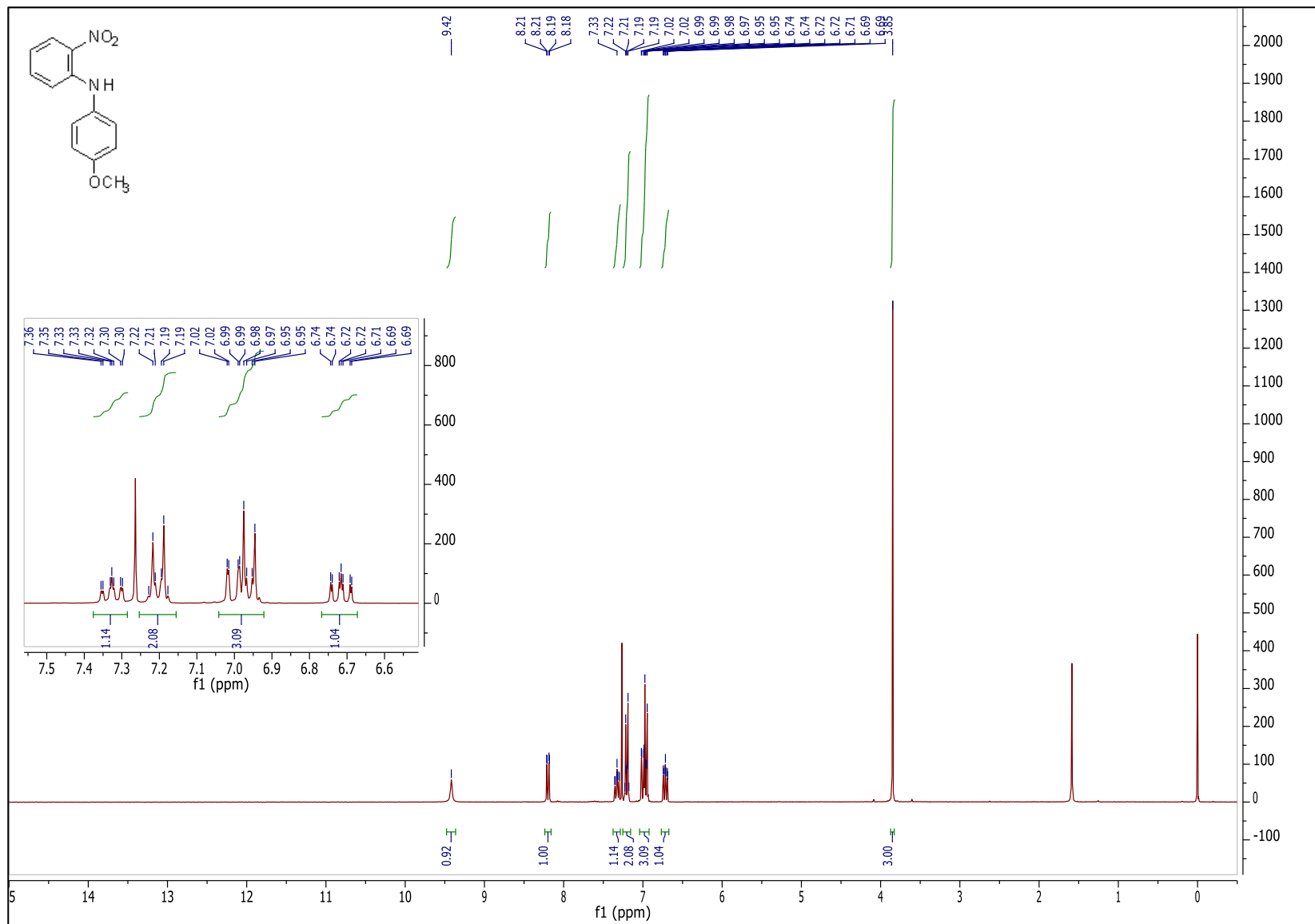


Figure 2.3 - <sup>1</sup>H NMR of Intermediate 2a

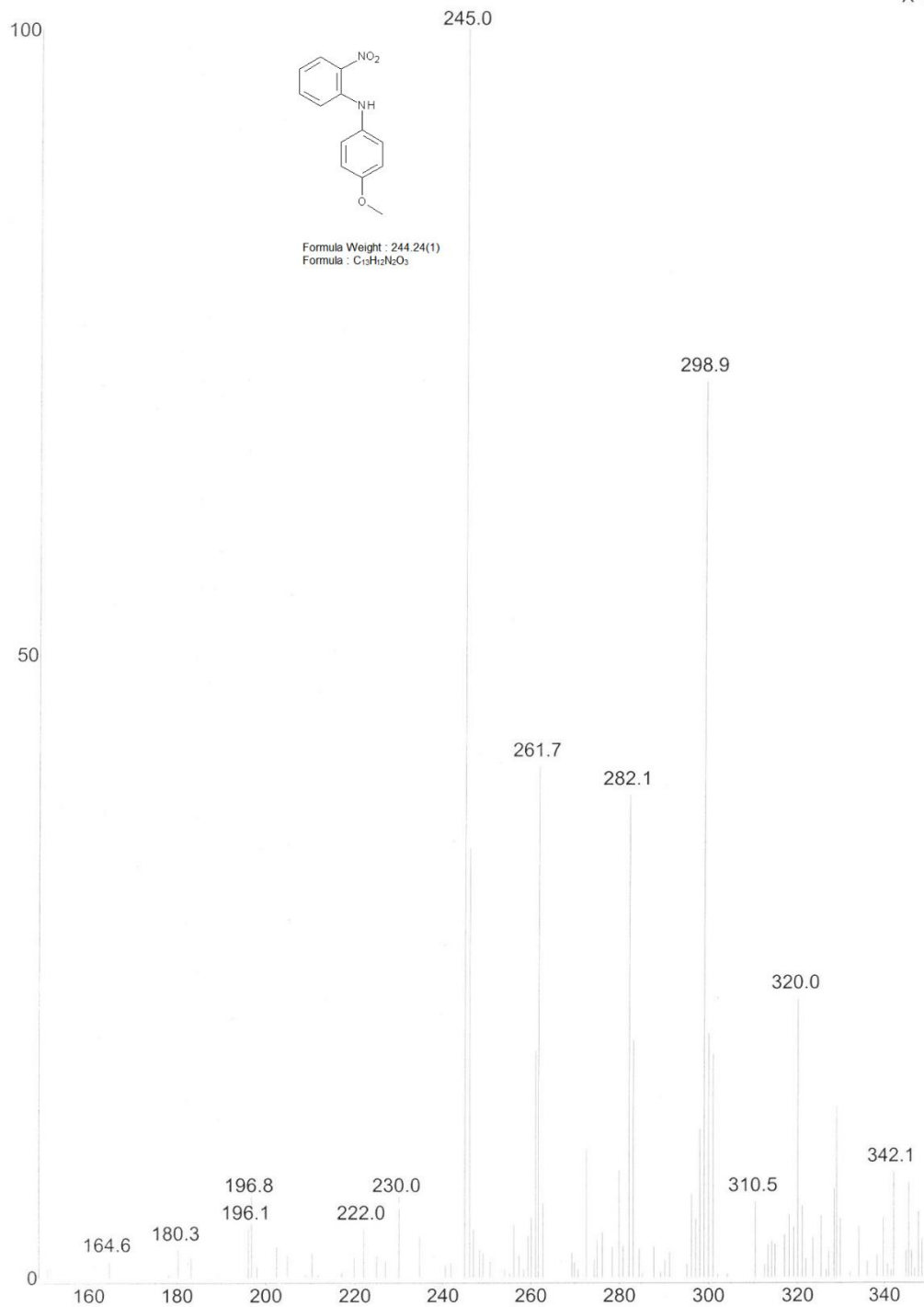


Figure 2.4 mass spectrum of the intermediate 2a



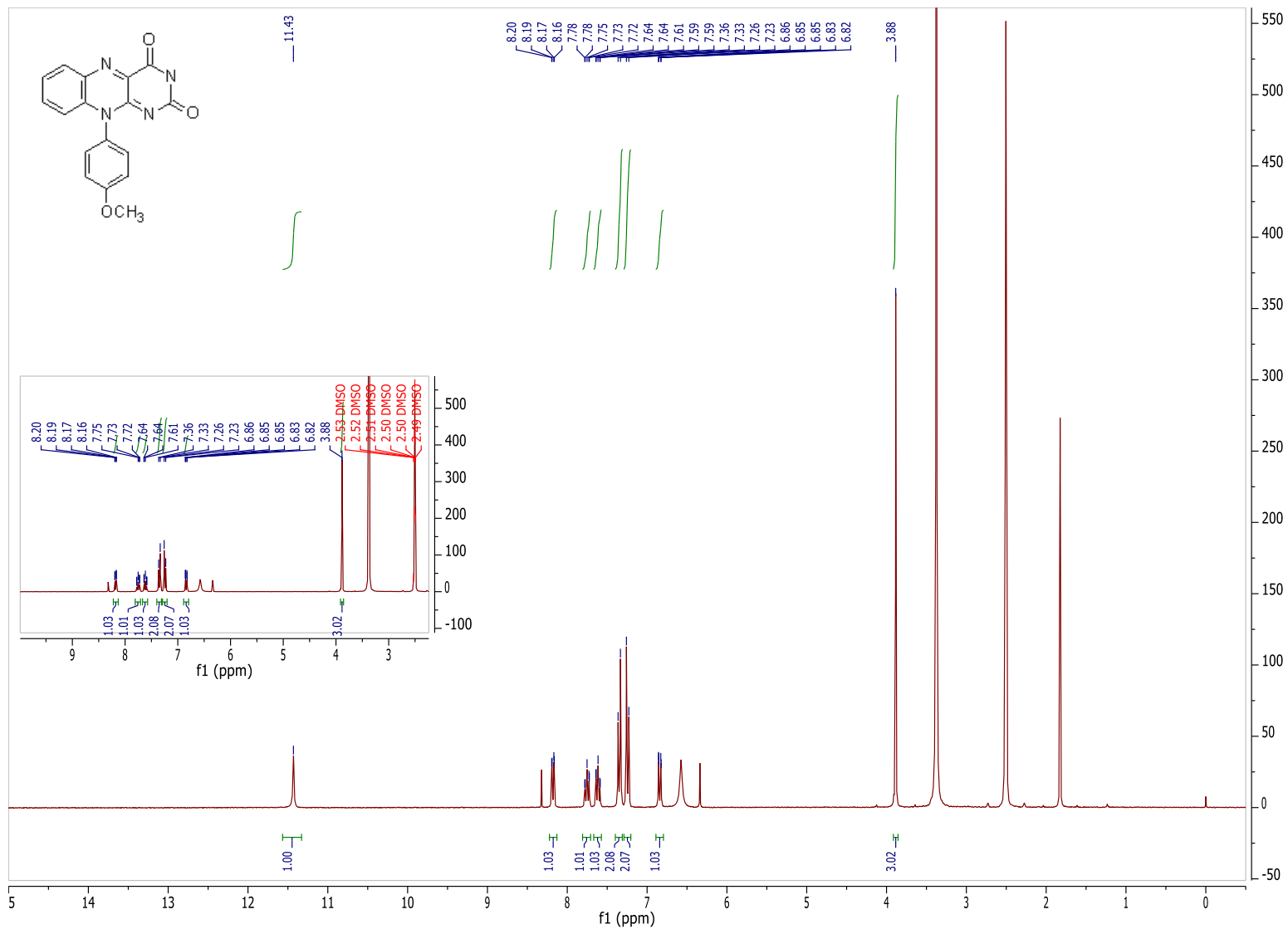
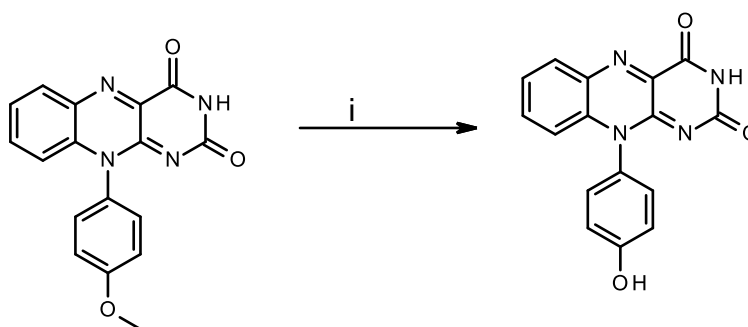


Figure 2.5 - <sup>1</sup>H NMR of 2

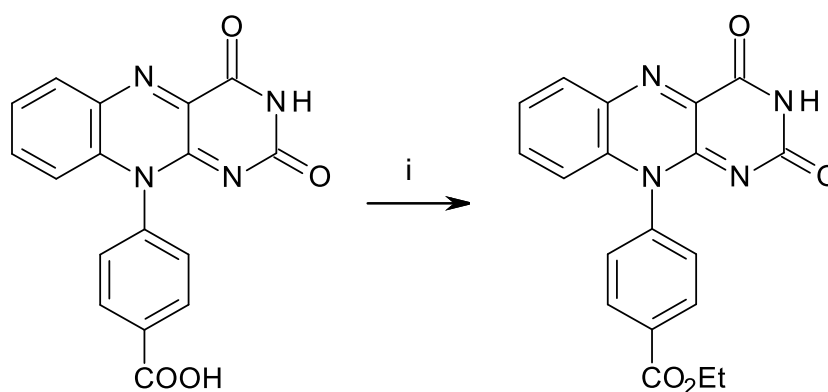
Finally, as shown in scheme 2.2, compound **13** was prepared in 98 % yield via the demethylation of **2** using hydrobromic acid. It is clear to see this has been successful due to the disappearance of the OMe at 3.88 ppm and the appearance of the phenolic OH at 10.09 ppm. An overlay of both spectrums can be seen in Figure 2.6 clearly highlighting the aforementioned observations.



i) HBr, CH<sub>3</sub>COOH, reflux 6hr, 98%

Scheme 2.2: Synthetic route of 10-(4-hydroxyphenyl)isoalloxazine (**13**)

The other flavin which was not prepared by this route, **13** was prepared by standard methods and shown in Scheme 2.3<sup>[18]</sup>.



i. EtOH, H<sub>2</sub>SO<sub>4</sub>, Reflux, 6h, 65%

Scheme 2.3: Synthetic route of 10-(4-ethylbenzoatephenyl)isoalloxazine (**13**)

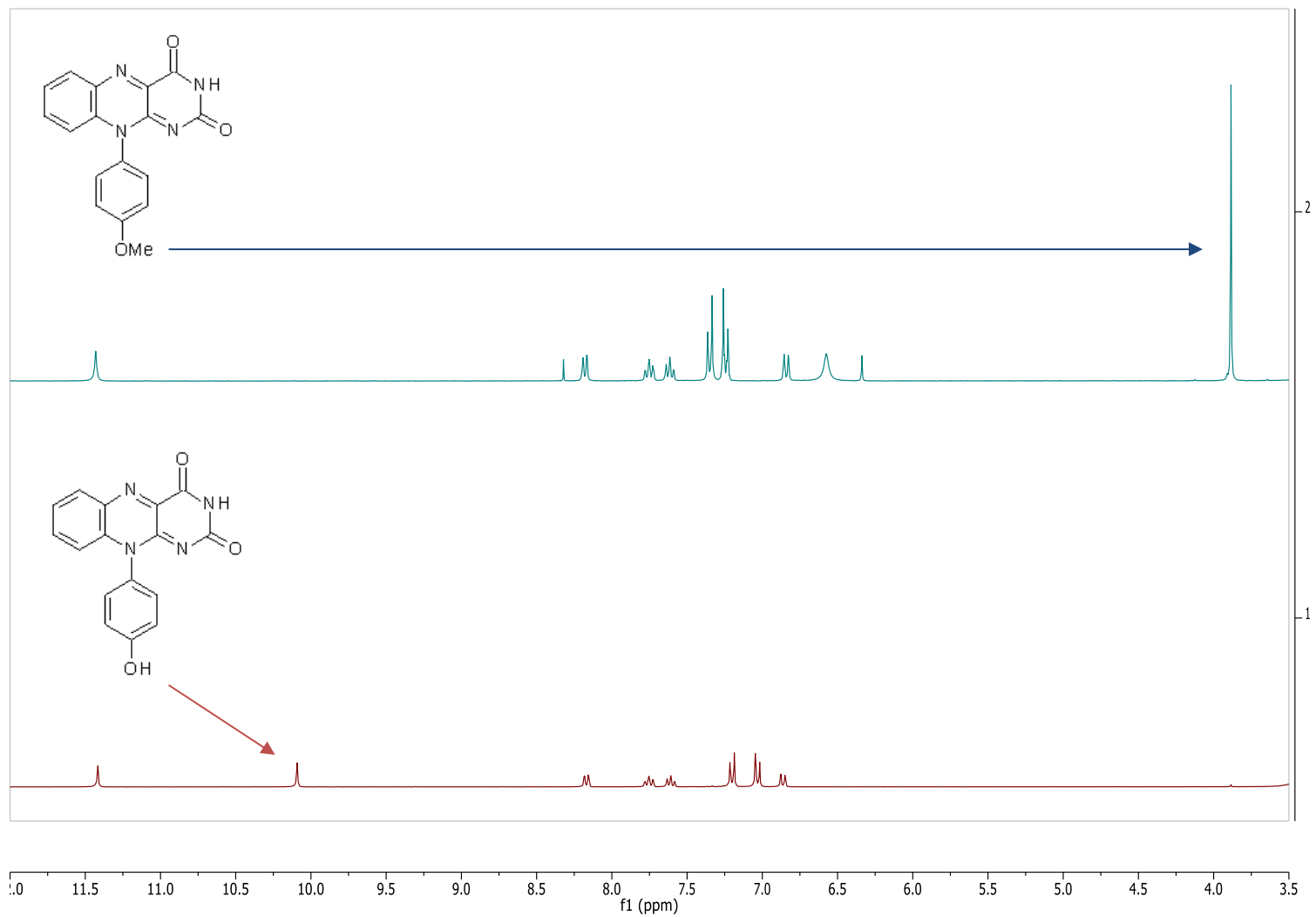
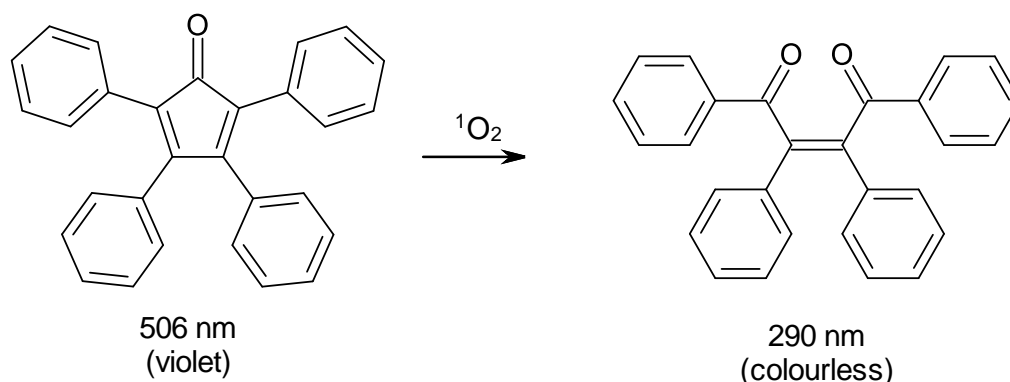


Figure 2.6 HNMR of 10-(4-methoxyphenyl)isoalloxazine (**2**) (top) and 10-(4-hydroxyphenyl)isoalloxazine (**14**) (bottom)

## 2.3 Singlet Oxygen

The singlet oxygen production for the prepared flavins was assayed using the decolourisation 2,3,4,5-tetraphenylcyclopentadienone (TPCPD) in dichloromethane which occurs through the chemical reaction shown in Scheme 2.4.



Scheme 2.4: Chemical reaction showing the decolourisation of TPCPD

The decrease in absorbance of TPCPD was monitored at 506 nm spectrophotometrically with time over a 60-minute period, using 10-phenylisoalloxazine as a standard. By assuming that the decrease in TPCPD absorption at 506 nm is directly proportional to the reaction with singlet oxygen, the time for a 50 % decrease in absorption caused by the flavin derivatives under identical conditions ( $t_{1/2FD}$ ) therefore gives a measure of its photosensitising efficiency. Thus, if the time for TPCPD absorption to decrease by 50 % due to flavin photosensitisation is  $t_{1/2F}$ , relative singlet oxygen yields for the derivatives are calculated using the formulae in Equation 2.1.

$$\text{Relative } ^1\text{O}_2 \text{ yield} = \frac{t_{1/2F}}{t_{1/2FD}}$$

Equation 2.1

Flavins give off their own absorbance value. Therefore, a blank needs to be taken that contains the flavin so that the flavin absorbance can be removed allowing the decolourisation of the TPCPD to be monitored accurately.

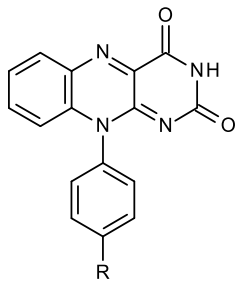
Compound		cLog P	Absorption (nm)	Relative $^1\text{O}_2$ Yield	Minimum inhibitory concentration (mg/mL)
	<b>R</b>				
1	H	2.06	268	1	*
2	OMe	2.12	269	1	*
3	CH <sub>3</sub>	2.51	269	1	*
4	Cl	2.74	268	2	*
5	I	3.15	267	2	*
6	CF <sub>3</sub>	2.96	267	1	*
7	COOH	1.97	264	0.285	*
8	Phenyl	3.86	266	1	*
9	Br	2.87	253	2	*
10	N(CH <sub>3</sub> ) <sub>2</sub>	2.17	266	0.0278	*
11	CN	1.82	263	0.285	*
12	NHCOCH <sub>3</sub>	1.28	269	0.333	*
13	COOEt	2.61	268	0.666	*
14	OH	1.58	269	0.365	*
Fluconazole	-	-	-	-	0.156

Table 2.1: Photophysical and growth inhibition data for the flavin derivatives. Minimum inhibition concentration is shown for 20 minutes exposure to blue light. \* indicates growth was observed at the maximum concentration tested, 10 mg/mL. cLog P is a partition coefficient of compound between aqueous and lipophilic phases and was calculated using molinspiration.

As it can be seen from the table above there were 3 flavin compounds that had a higher singlet oxygen yield than 10-phenylisoalloxazine (**1**). This is due to a heavy atom effect with the halogen flavins (compounds 4, 5, 9).

## **2.4 Assay for Growth**

In order to test the antifungal activity of the novel compounds they were tested against the yeast like fungi, *Candida albicans*, using the EUCAST microdilution method (EUCAST E.DEF 7.3 December 2015). Exponentially growing *C. albicans* was incubated at 30°C in YPD (2 % glucose, 1 % yeast extract, 1 % peptone) with shaking at 180 rpm, before being diluted to a concentration of approximately  $0.5 - 2.5 \times 10^5$  cells/ml. Varying concentrations (0.048 – 25mg/L) of the test compounds were prepared in DMSO and RPMI 1640 culture media (2 % RPMI 1640, 6.9 % MOPS, 3.6 % glucose), before being added to wells of a 96 well plate. A standard inoculum of the previously prepared *C. albicans* cells were then added to each of the wells. The 96 well plates were then exposed to blue light for either 0 mins, 10 mins or 20 mins. The antifungal drug, fluconazole, was used as a control compound for growth inhibition. Plates were incubated for 24 hrs at 34°C, before growth was determined by visual inspection. The minimum inhibitory concentration (MIC) was determined to be the well before growth was first seen. The experiments were repeated at least twice in duplicate.

### **Results:**

#### **The blue light has no effect on growth of *C. albicans*.**

In order to determine if exposure to blue light alone had an effect on growth of *C. albicans*, RPMI 1640 culture media was added to wells of a 96 well plate with a standard inoculum of previously prepared *C. albicans* cells. The plates were then exposed to blue light for 0 mins, 10 mins or 20 mins. Plate

were incubated for 24 hours at 34 °C, before growth was determined by visual inspection. The results showed that there was growth on all three plates, therefore it is determined that the blue light has no effect on the growth of the *C. albicans*.

**Flavins have no effect on the growth of *C. albicans*.**

In order to see if the flavin derivatives had an effect on growth of *C. albicans*, cells were exposed to a range of concentrations, 0.0195 mg/mL to 10 mg/mL, in the absence and presence of blue light. Visual inspection of the plates after 24 hr incubation at 34°C, table 2.1 and figures 2.7 and 2.8, showed compounds 1-14 have no effect on the growth of *C. albicans*, when compared to the control, at the concentrations tested. However, in the presence of the antifungal agent fluconazole, an effect was observed with an MIC determined to be 0.156 mg/mL.

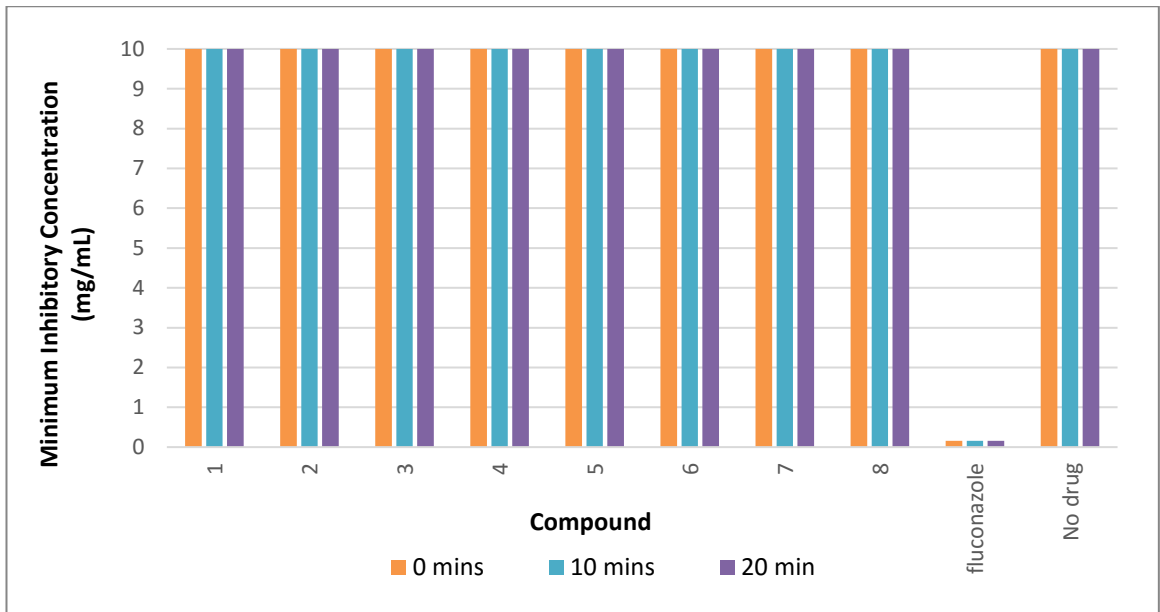


**Figure 2.7:** Comparison of compounds 1-8 with fluconazole on *C.albicans*. The MIC was obtained according to the EUCAST method in the absence and presence of blue light. The maximum concentration tested was 10 mg/mL

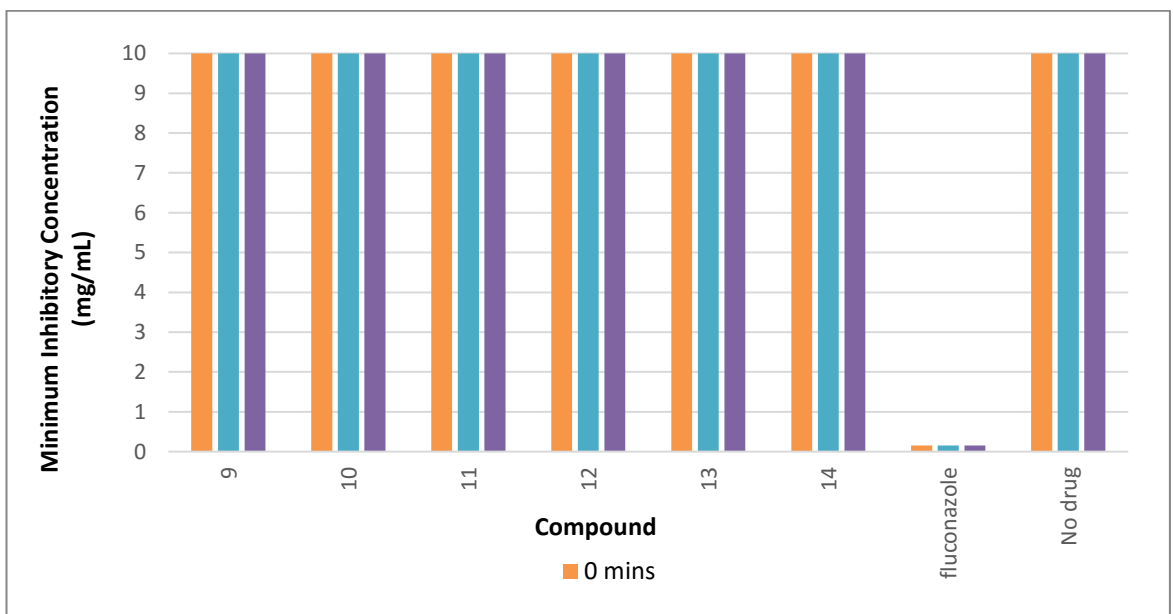


**Figure 2.8:** Comparison of compounds 9-14 with fluconazole on *C.albicans*. The MIC was obtained according to the EUCAST method in the absence and presence of blue light. The maximum concentration tested was 10 mg/mL



## 2.5 Discussion

The synthesis of the flavins required no harsh or unusual methodologies as shown in scheme 2.1. The intermediate compounds were synthesised by reacting an aromatic amine with 2-fluoro-1-nitrobenzene in the presence of potassium carbonate, to yield p-substituted-2-nitrodiphenylamines which were isolated at the pump. The resulting p-substituted-2-nitrodiphenylamines were then reduced in the presence of zinc in acidic conditions, and subsequently treated with alloxan monohydrate in the presence of boric acid to yield the p-substituted-phenylisoalloxazine in good yields.

The photophysical properties of compounds **1-14** are shown in table 2.1. It is clear to see that the absorption spectra maxima all absorb in the UV region between 253- 269 nm.

The incorporation of halogens onto the isoalloxazine moiety was shown to exhibit a 2-fold increase in the singlet oxygen yield. This result indicates that the heavy atom effect increases the possibility of the transition into the excited triplet state, causing an increase in the amount of singlet oxygen produced. Compound **10** showed a 35-fold decrease in the singlet oxygen yield, causing it to be the flavin compound with the lowest yield of singlet oxygen.

The growth inhibition data can also be seen in table 2.1 and shows that although the singlet oxygen yield looked promising with compounds **4,5,9** no microbicidal effect on *C.albicans* was observed at the maximum concentration tested (10 mg/mL). This was surprising because it was thought that because of the similarity in the flavin derivatives to riboflavin, there would be some effect on the yeast. The Log P data for all of these compounds is below 5 which according to Lipinski's rule of 5 is less likely to cause poor membrane permeation. The lack of antimicrobial activity of these flavin derivatives may be due to poor permeability into the cell, as seen by the cLog P of these

compounds being between 1 and 3 (see table 2.1). In contrast, Riboflavin has a lower cLog P of -0.76 and hence a higher permeability into the cell. This property increases the likelihood of causing damage upon illumination, due to the proximity of intercellular targets.

It has been known that blue light, especially of wavelengths between 400 and 470nm, is effective against pathogens even when not used in combination with a photosensitiser<sup>[19]</sup>. Since it has been shown that *C.albicans* are susceptible to blue light<sup>[20]</sup>, we carried out a growth assay to determine if the blue light was causing any effect. The assay showed that no effect on the growth of *C.albicans*. A time-lapse study carried out by Trzaska et al showed that initial growth inhibition occurred with *C.albicans* however the fungi recovered full growth capability<sup>[20]</sup>.

## **2.6 Experimental**

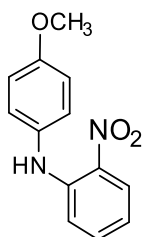
### Experimental

<sup>1</sup>H and <sup>13</sup>C NMR spectra were measured on Bruker Avance-III 300 MHz spectrometer at ambient temperature with tetramethylsilane (TMS) as internal standard for <sup>1</sup>H NMR and deuteriochloroform (CDCl<sub>3</sub>,  $\delta$ C 77.23 ppm) and deuteriodimethylsulfoxide (d<sub>6</sub>-DMSO,  $\delta$ C 39.51 ppm) for <sup>13</sup>C NMR unless otherwise stated. All chemical shifts are quoted in  $\delta$  (ppm) and coupling constants in Hertz (Hz) using the high frequency positive convention. Coupling constants were rounded up into whole numbers. Low and high resolution mass spectra were obtained using electrospray ionization (ESI) mass spectrometry on a hybrid linear ion trap-fourier transform mass spectrometer. Infrared spectra were recorded on a Specac ATR with a He Ne -633 nm laser. Thin Layer Chromatography (TLC) was carried out on Machery-Nagel polygramSil/G/UV254 pre-coated plates. Melting point (m.p) analysis was

carried out using a Griffin melting point apparatus. All chemicals were purchased from commercial sources and used without further purification.

The intermediate 2-nitrodiphenylamine was purchased from Sigma Aldrich and used without any purification.

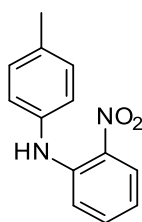
### 2.6.1 4-Methoxy-2'-nitrodiphenylamine (**2a**)



A round bottom flask was charged p-anisidine (2.46 g, 20 mmol), 1-fluoro-2-nitrobenzene (2.82 g, 20 mmol) and potassium carbonate (4.15 g, 30 mmol) and with constant stirring, the reaction mixture was heated at 150 °C for 3 hours. Upon cooling to room temperature, the reaction was quenched with acidic water until neutral, upon which a red solid precipitated from the reaction mixture. The crude red solid was isolated at the pump and dried under reduced pressure to yield **2a** as a dark red solid with a yield 3.82 g, 78 %.

$^1\text{H}$  NMR ( $\text{CDCl}_3$ , 300 MHz):  $\delta$  9.42 (s, 1H, N-H), 8.20 (d,  $J = 9$  Hz, 1H, Ar-H), 7.33 (t,  $J = 9$  Hz, 1H, Ar-H), 7.20 (d,  $J = 9$  Hz, 2H, Ar-H), 7.02 – 6.93 (m, 3H, Ar-H), 6.74 – 6.67 (m, 1H, Ar-H), 3.85 (s, 3H,  $\text{OCH}_3$ ).  $^{13}\text{C}$  NMR (75 MHz,  $\text{CDCl}_3$ )  $\delta$  157.92, 144.51, 135.75, 132.43, 131.17, 127.14, 126.61, 116.77, 115.75, 114.96, 55.55. MS (ESI)  $m/z$ : 291.11 [ $\text{M}^+$ ].

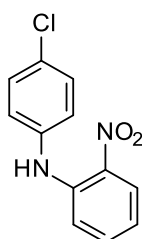
### 2.6.2 4-Methyl-2'-nitrodiphenylamine (3a)



Compound **3a** was synthesised using the same methodology and reaction stoichiometry as **2a** to yield **3a** as a red solid Yielding 2.41 g, 52 %.

$^1\text{H}$  NMR ( $\text{CDCl}_3$ , 300 MHz):  $\delta$  9.46 (s, 1H, N-H), 8.20 (d,  $J = 9$  Hz, 1H, Ar-H), 7.34 (t,  $J = 6$  Hz, 1H, Ar-H), 7.22 (d,  $J = 9$  Hz, 2H, Ar-H), 7.24 – 7.12 (m, 3H, Ar-H), 6.74 (t, 1H, Ar-H), 2.38 (s, 3H,  $\text{CH}_3$ ).  $^{13}\text{C}$  NMR (75 MHz,  $\text{CDCl}_3$ ):  $\delta$  143.72, 135.88, 135.75, 135.70, 132.78, 130.32, 126.64, 124.83, 117.09, 115.94, 21.04. MS (ESI)  $m/z$ : 228 [ $\text{M}^+$ ].

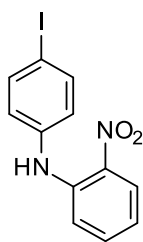
### 2.6.3 4-Chloro-2'-nitrodiphenylamine (4a)



Compound **4a** was synthesised using the same methodology and reaction stoichiometry as **2a** to yield **4a** as a red solid. Yielding 10.07 g, 21 %

$^1\text{H}$  NMR ( $\text{d}_6$ -DMSO, 300 MHz):  $\delta$  9.32 (s, 1H, N-H), 8.13 (t,  $J = 9$  Hz, 1H, Ar-H), 7.44 (d,  $J = 9$  Hz, 2H, Ar-H), 7.33 (d,  $J = 9$  Hz, 2H, Ar-H), 7.22 (d,  $J = 6$  Hz, 2H, Ar-H), 6.93 (t,  $J = 9$  Hz, 2H, Ar-H).  $^{13}\text{C}$  NMR (75 MHz, DMSO):  $\delta$  141.64, 139.11, 136.39, 134.73, 129.8, 128.67, 126.70, 125.29, 119.14, 117.69. MS (ESI)  $m/z$ : 248 [ $\text{M}^+$ ]. Yield: 1.07 g, 21%

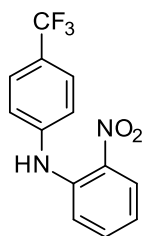
#### 2.6.4 4-Iodo-2'-nitrodiphenylamine (5a)



Compound **5a** was synthesised using the same methodology and reaction stoichiometry as **2a** to yield **5a** as a red solid. Yielding 0.5 g, 7 %.

$^1\text{H}$  NMR ( $d_6$ -DMSO, 300 MHz):  $\delta$  9.27 (s, 1H, NH), 8.10 (d,  $J = 9$  Hz, 1H, Ar-H), 7.72 (d,  $J = 9$  Hz, 2H, Ar-H), 7.53 (t,  $J = 6$  Hz, 1H, Ar-H), 7.25 (d,  $J = 9$  Hz, 1H, Ar-H), 7.13 (d,  $J = 9$  Hz, 2H, Ar-H), 6.94 (t,  $J = 9$  Hz, 1H, Ar-H).  $^{13}\text{C}$  NMR (75 MHz, DMSO):  $\delta$  148.96, 137.53, 137.15, 137.03, 126.72, 126.68, 125.91, 125.85, 125.30, 116.94. MS (ESI)  $m/z$ : 339 [ $\text{M}^+$ ].

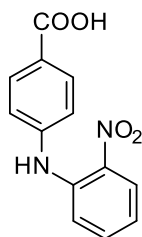
#### 2.6.5 4-Trifluoromethyl-2'-nitrodiphenylamine (6a)



To a round bottom flask was charged 4-(Trifluoromethyl) aniline (2.76 g, 20 mmol), 1-fluoro-2-nitrobenzene (2.82 g, 20 mmol) and potassium carbonate (4.15 g, 30 mmol) and with constant stirring the reaction mixture was heated at 150°C for 3 hours. Upon cooling to room temperature, the reaction was quenched with acidic water until neutral. The reaction mixture was subsequently extracted with dichloromethane, dried over anhydrous sodium sulphate, and then evaporated to dryness. The crude compound was purified via column chromatography on silica 1:1 Toluene: Petroleum ether. Yielding 1.05 g, 19 %.

$^1\text{H}$  NMR ( $d_6$ -DMSO, 300 MHz): 9.33 (s, 1H,  $\text{NH}$ ), 8.18 (t,  $J=6$  Hz, 2H, Ar-H), 7.47 (t,  $J=6$  Hz, 2H, Ar-H), 7.26 (t,  $J=6$  Hz, 2H, Ar-H), 7.17 (t,  $J=6$  Hz, 2H, Ar-H).  $^{13}\text{C}$  NMR (75 MHz, DMSO):  $\delta$  156.79, 153.33, 137.80, 137.13, 137.01, 129.35, 128.65, 126.67, 125.84, 119.05, 118.78. MS (ESI)  $m/z$ : 282 [ $\text{M}^+$ ].

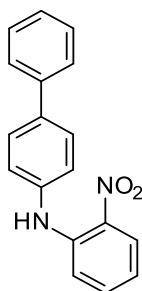
#### 2.6.6 4-Carboxy-2'-nitrodiphenylamine (7a)



A round bottom flask was charged with 4-aminobenzoic acid (10 g, 72.9 mmol) and amyl alcohol. Potassium carbonate (12.88 g, 92.69 mmol), 1-Bromo-2-nitrobenzene (9.01 g, 44.6 mmol) and copper bronze (0.4 g, 6 mmol) were added to the round bottom flask. The mixture was refluxed at 180 °C for 4 hours and cooled to room temperature. Once cooled solid precipitated and diethyl ether was added to the round bottom flask to help filter the solid at the pump. The solid was transferred to a conical flask and heated with water. The mixture was hot filtered through celite to remove the copper. Hydrochloric acid was added to the liquid until became pH 5. An orange precipitate was produced which was isolated at the pump and dried under reduced pressure. Yielding 3.1 g, 26 %

$^1\text{H}$  NMR ( $d_6$ -DMSO, 300 MHz):  $\delta$  9.32 (s, 1H,  $\text{NH}$ ), 8.12 (t,  $J=9$  Hz, 1H, Ar-H), 7.89 (d,  $J=9$  Hz, 2H, Ar-H), 7.61 (t,  $J=9$  Hz, 1H, Ar-H), 7.50 (d,  $J=6$  Hz, 1H, Ar-H), 7.30 (d,  $J=9$  Hz, 2H, Ar-H), 7.08 (t,  $J=9$  Hz, 1H, Ar-H).  $^{13}\text{C}$  NMR (75 MHz, DMSO):  $\delta$  167.35, 145.40, 139.03, 137.41, 136.00, 131.96, 126.69, 124.88, 121.18, 120.29, 119.70. MS (ESI)  $m/z$ : 258 [ $\text{M}^+$ ].

### 2.6.7 2-Nitro-*N*-(4-diphenyl)aniline (**8a**)

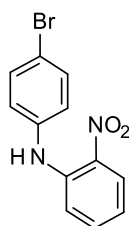


Compound **8a** was synthesised using the same methodology and reaction stoichiometry as **2a** to yield **8a** as a red solid. The solid was washed in acetone, filtered at the pump and the acetone was evaporated off to leave the product.

Yielding 1.47 g, 25 %

$^1\text{H}$  NMR ( $\text{CDCl}_3$ , 300 MHz):  $\delta$  9.55 (s, 1H, NH), 8.22 (d,  $J = 6$  Hz, 1H, Ar-H), 8.07 (t,  $J = 9$  Hz, 1H, Ar-H), 7.66-7.59 (m, 5H, Ar-H), 7.46 (t,  $J = 9$  Hz, 2H, Ar-H), 7.32 (d,  $J = 9$  Hz, 4H, Ar-H).  $^{13}\text{C}$  NMR (75 MHz,  $\text{CDCl}_3$ ): 140.22, 138.43, 137.96, 135.76, 135.67, 135.55, 128.91, 128.34, 127.42, 126.91, 126.73, 124.38, 117.71, 116.23. MS (ESI)  $m/z$ : 285 [ $\text{M}^+$ ].

### 2.6.8 4-Bromo-2'-Nitrodiphenylamine (**9a**)

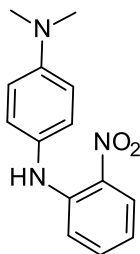


Compound **9a** was synthesised using the same methodology and reaction stoichiometry as **2a** to yield **9a** as a red solid. Yielding 1.25 g, 24 %.

$^1\text{H}$  NMR ( $d_6$ -DMSO, 300 MHz):  $\delta$  9.29 (s, 1H, NH), 8.20 (d,  $J = 12$  Hz, 1H, Ar-H), 7.94 (d,  $J = 9$  Hz, 2H, Ar-H), 7.75 (t,  $J = 9$  Hz, 1H, Ar-H), 7.63 (t,  $J = 9$  Hz, 1H, Ar-H), 7.41 (d,  $J = 12$  Hz, 2H, Ar-H), 6.82 (d,  $J = 9$  Hz, 1H, Ar-H).  $^{13}\text{C}$  NMR (75

MHz, DMSO):  $\delta$  141.44, 139.68, 139.63, 136.36, 132.70, 126.72, 125.45, 119.26, 117.88, 116.58. MS (ESI)  $m/z$ : 293 [ $M^+$ ].

### 2.6.9 *N,N*-Dimethyl-2'-nitro-1,4-phenyldiamine (10a)

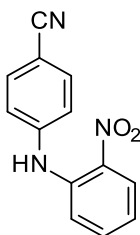


A round bottom flask was charged with *N,N*-Dimethyl-*p*-phenylenediamine (2.72 g, 20 mmol), 1-fluoro-2-nitrobenzene (2.82 g, 20 mmol) and potassium carbonate (4.15 g, 30 mmol) and with constant stirring the reaction mixture was heated at 150°C for 3 hours. During the heating, a heat gun was used to melt the sublimed solid. Upon cooling to room temperature, the reaction was quenched with acidic water until neutral. The solid was isolated at the pump and dried.

Yielding 2.06 g, 40 %.

$^1\text{H}$  NMR ( $d_6$ -DMSO, 300 MHz):  $\delta$  9.36 (s, 1H,  $\text{NH}$ ), 8.08 (d,  $J = 9$  Hz, 1H, Ar- $\text{H}$ ), 7.43 (t,  $J = 9$ Hz, 1H, Ar- $\text{H}$ ), 7.16 (d,  $J = 6$ Hz, 2H, Ar- $\text{H}$ ), 6.93 (d,  $J = 6$  Hz, 1H, Ar- $\text{H}$ ), 6.83 (d,  $J = 9$ Hz, 2H, Ar- $\text{H}$ ), 6.76 (t,  $J = 6$ Hz, 1H, Ar- $\text{H}$ ), 2.93(s, 6H,  $\text{CH}_3$ ). MS (ESI)  $m/z$ : 260 [ $M^+$ ].

### 2.6.10 4-Nitrile-2'-nitrodiphenylamine (11a)

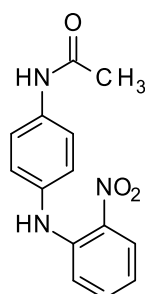




Compound **11a** was synthesised using the same methodology and reaction stoichiometry as **2a** to yield **11a** as a red solid. Purified via silica column with a solvent system of 9:1 petroleum ether: ethyl acetate. Yielding 0.34 g, 7 %.

$^1\text{H}$  NMR ( $\text{CDCl}_3$ , 300 MHz):  $\delta$  9.44 (s, 1H,  $\text{NH}$ ), 7.67 (d,  $J = 9$  Hz, 2H, Ar-H), 7.49 (t,  $J = 9$  Hz, 2H, Ar-H), 7.33 (d,  $J = 9$  Hz, 3H, Ar-H), 6.99 (t,  $J = 6$  Hz, 1H, Ar-H).  $^{13}\text{C}$  NMR (75 MHz, DMSO):  $\delta$  153.47, 148.59, 136.01, 135.57, 134.06, 133.91, 125.80, 121.83, 119.05, 113.88, 95.90. MS (ESI)  $m/z$ : 239 [ $\text{M}^+$ ].

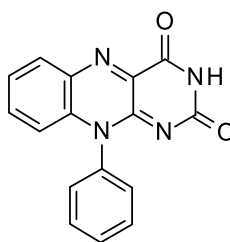
### 2.6.11 4-Acetamido-2'-nitrodiphenylamine (**12a**)



Compound **16a** was synthesised using the same methodology and reaction stoichiometry as **2a** to yield **16a** as a red solid. The solid was washed in acetone, filtered at the pump and the acetone was evaporated off. Purified via impregnated silica column with a solvent system of ethyl acetate. Yielding 2.71 g, 50 %.

$^1\text{H}$  NMR ( $\text{d}_6$ -DMSO, 300 MHz):  $\delta$  10.06 (s, 1H,  $\text{NH}$ ), 9.38 (s, 1H,  $\text{NH}$ ), 8.11 (d,  $J = 6$  Hz, 1H, Ar-H), 7.63 (d,  $J = 9$  Hz, 2H, Ar-H), 7.48 (t,  $J = 9$  Hz, 1H, Ar-H), 7.26 (d,  $J = 6$  Hz, 2H, Ar-H), 7.08 (d,  $J = 6$  Hz, 1H, Ar-H), 6.83 (t,  $J = 9$  Hz, 1H, Ar-H), 2.06 (s, 3H,  $\text{CH}_3$ ).  $^{13}\text{C}$  NMR (75 MHz,  $\text{d}_6$ -DMSO): 168.74, 143.34, 137.20, 136.59, 134.17, 133.08, 126.60, 125.55, 120.43, 117.90, 116.74, 24.41. MS (ESI)  $m/z$ : 271 [ $\text{M}^+$ ].

### 2.6.12 10-Phenylisoalloxazine (1)

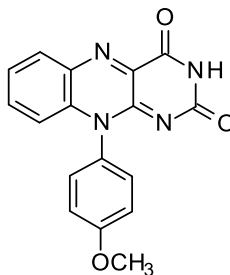


To a stirred solution of 2-nitrodiphenylamine (2.15 g, 10 mmol) in glacial acetic acid (30 mL) was gradually added zinc dust (13 g, 200 mmol) whilst maintaining reaction temperature below 40°C. Upon total addition of the zinc dust, the reaction was stirred at room temperature for 2 hours. The reaction mixture was filtered at the pump through a pad of celite and washed with glacial acetic acid (10 mL).

The acidic mixture was isolated and to it was added alloxan monohydrate (1.59 g, 10 mmol) and boric acid (0.92 g, 15 mmol) was added and the mixture was stirred for 3 hours to produce a crude yellow precipitate. The yellow precipitate was isolated at the pump and washed with diethyl ether to yield compound **1** which was dried *in vacuo*. Yielding 2.71 g, 93 %.

<sup>1</sup>H NMR (d<sub>6</sub>-DMSO, 300 MHz): δ 11.45 (s, 1H, N-H), 8.20 (d, *J*=9.0 Hz, 1H, Ar-H), 7.77-7.60 (m, 5H, Ar-H), 7.44 (d, *J*=6Hz, 2H, Ar-H), 6.76 (d, *J*=6Hz, 1H, Ar-H). <sup>13</sup>C NMR (75 MHz, DMSO) δ 160.02, 156.02, 152.19, 139.95, 136.53, 135.23, 135.17, 134.49, 131.83, 130.79, 130.27, 128.26, 126.47, 117.22. IR (ATR, cm<sup>-1</sup>): 3023.74, 1716.17, 1688.44, 1607.66, 1507.66, 806.81, 768.89. MS (ESI) *m/z*: 291.11 [M<sup>+</sup>]. Melting point = >300°C.

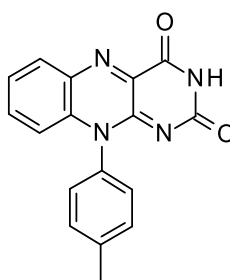
### 2.6.13 10-(4-Methoxyphenyl)isoalloxazine (2)



Compound **2** was synthesised using the same methodology and reaction stoichiometry as **1** to yield **2** as a yellow solid Yielding 3.01 g, 93 %

$^1\text{H}$  NMR ( $d_6$ -DMSO, 300 MHz,)  $\delta$  11.43 (s, 1H, N-H), 8.18 (d,  $J = 6.9$  Hz, 1H, Ar-H), 7.75 (t,  $J = 7.2$  Hz, 1H, Ar-H), 7.61 (t,  $J = 7.1$  Hz, 1H, Ar-H), 7.35 (d,  $J = 8.9$  Hz, 2H, Ar-H), 7.24 (d,  $J = 9.0$  Hz, 2H, Ar-H), 6.84 (d,  $J = 8.1$  Hz, 1H, Ar-H), 2.88 (s, 3H, OCH<sub>3</sub>).  $^{13}\text{C}$  NMR (75 MHz, DMSO)  $\delta$  160.33, 160.08, 156.06, 139.89, 135.21, 134.95, 131.81, 129.41, 128.94, 126.40, 117.40, 115.87, 99.99, 78.58, 56.02. IR (ATR, cm<sup>-1</sup>): 3050.621708.99, 1655.56, 1612.10, 1502.34, 1273.01, 764.39 MS (ESI)  $m/z$ : 321.12 [M<sup>+</sup>]. Melting point = >300°C.

### 2.6.14 10-(4-Methylphenyl)isoalloxazine (3)

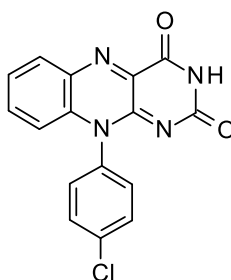


Compound **3** was synthesised using the same methodology and reaction stoichiometry as **1** to yield **3** as a yellow solid. Yielding 3.03 g, 99 %

$^1\text{H}$  NMR ( $d_6$ -DMSO, 300 MHz,)  $\delta$  11.43 (s, 1H, N-H), 8.18 (d,  $J = 6$  Hz, 1H, Ar-H), 7.7 (t,  $J = 9$  Hz, 1H, Ar-H), 7.61 (t,  $J = 6$  Hz, 1H, Ar-H), 7.50 (d,  $J = 9$  Hz, 2H, Ar-H), 7.30 (d,  $J = 6$  Hz, 2H, Ar-H), 6.79 (d,  $J = 9$  Hz, 1H, Ar-H), 1.88 (s, 3H,

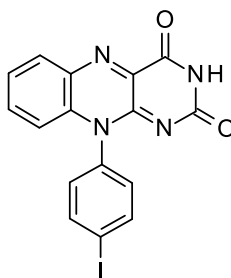
CH<sub>3</sub>). <sup>13</sup>C NMR (75 MHz, DMSO) δ 188.18, 185.01, 163.87, 160.05, 156.04, 139.94, 139.89, 135.19, 134.64, 133.94, 131.86, 131.80, 131.21, 127.97, 117.32, 111.17, 99.01, 77.36. IR (ATR, cm<sup>-1</sup>): 3038.19, 1744.58, 1707.48, 1637.95, 1613.42, 1541.76, 1502.83, 838.08, 725.04. MS (ESI) m/z: 305.19 [M<sup>+</sup>]. Melting point = >300°C.

#### 2.6.15 10-(4-Chlorophenyl)isoalloxazine (4)



Compound **4** was synthesised using the same methodology and reaction stoichiometry as **1** to yield **4** as a yellow solid. Yielding 1.46 g, 76 %  
<sup>1</sup>H NMR (*d*<sub>6</sub>-DMSO, 300 MHz): δ 11.48 (s, 1H, N-H), 8.2 (d, *J* = 6 Hz, 1H, Ar-H), 7.80 (d, *J* = 9 Hz, 1H, Ar-H), 7.75 (t, *J* = 9 Hz, 1H, Ar-H), 7.63 (t, *J* = 6 Hz, 2H, Ar-H), 7.48 (d, *J* = 9 Hz, 2H, Ar-H), 6.83 (d, *J* = 9 Hz, 1H, Ar-H). <sup>13</sup>C NMR (75 MHz, DMSO) δ 159.95, 159.92, 152.22, 135.32, 135.16, 134.96, 131.88, 130.95, 130.35, 117.27, 117.21. IR (ATR, cm<sup>-1</sup>): 3066.94, 1690.23, 1643.68, 1613.32, 1513.60, 844.56, 770.30, 606.80. MS (ESI) m/z: 321.12 [M<sup>+</sup>]. Melting point = >300 °C.

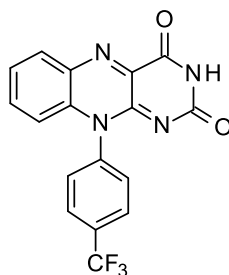
### 2.6.16 10-(4-Iodophenyl)isoalloxazine (5)



Compound **5** was synthesised using the same methodology and reaction stoichiometry as **1** to yield **5** as a yellow solid. Yielding 0.56 g, 90 %

$^1\text{H}$  NMR ( $d_6$ -DMSO, 300 MHz,)  $\delta$  11.47 (s, 1H, N-H), 8.19 (d,  $J = 6$  Hz, 1H, Ar-H), 8.09 (d,  $J = 9$  Hz, 2H, Ar-H), 7.75 (t,  $J = 9$  Hz, 1H, Ar-H), 7.63 (t,  $J = 6$  Hz, 1H, Ar-H), 7.24 (d,  $J = 9.0$  Hz, 2H, Ar-H), 6.83 (d,  $J = 9$  Hz, 1H, Ar-H). IR (ATR,  $\text{cm}^{-1}$ ): 3008.07, 1713.05, 1638.26, 1612.68, 1538.05, 1484.19, 840.21, 753.06. MS (ESI)  $m/z$ : 417.1 [ $\text{M}^+$ ]. Melting point =  $>300$  °C.

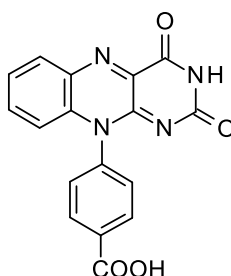
### 2.6.17 10-(4-Trifluoromethylphenyl)isoalloxazine (6)



Compound **6** was synthesised using the same methodology and reaction stoichiometry as **1** to yield **6** as a yellow solid. The Solid was washed with Dichloromethane and the liquid was transferred into a round bottom flask and evaporated to dryness. Purified via an impregnated silica column with a solvent system of ethyl acetate. Yielding 0.97 g, 90 %.

$^1\text{H}$  NMR ( $d_6$ -DMSO, 300 MHz):  $\delta$  11.50 (s, 1H, N-H), 8.21 (d,  $J = 9$  Hz, 1H, Ar-H), 8.13 (d,  $J = 9$  Hz, 1H, Ar-H), 7.76-7.62 (m, 4H, Ar-H), 7.30 (d,  $J = 9$  Hz, 1H, Ar-H), 6.80 (d,  $J = 9$  Hz, 1H, Ar-H). IR (ATR,  $\text{cm}^{-1}$ ): 3058.98, 1708.74, 1682.02, 1617.50, 1543.86, 1543.86, 1459.62, 855.58, 753.41. MS (ESI)  $m/z$ : 359.1 [ $\text{M}^+$ ].  
Melting point =  $>300$  °C.

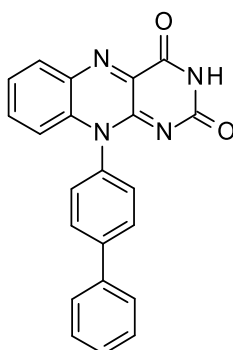
### 2.6.18 10-(4-Carboxyphenyl)isoalloxazine (7)



Compound **7** was synthesised using the same methodology and reaction stoichiometry as **1** to yield **7** as an orange solid. The product was purified by recrystallization with sodium hydroxide pellets and hydrochloric acid. Yielding 2.55 g, 85 %.

$^1\text{H}$  NMR ( $d_6$ -DMSO, 300 MHz,)  $\delta$  11.47 (s, 1H, N-H), 8.26 (d,  $J = 6$  Hz, 1H, Ar-H), 8.20 (d,  $J = 6$  Hz, 1H, Ar-H), 7.74 (t,  $J = 9$  Hz, 1H, Ar-H), 7.64 (t,  $J = 6$  Hz, 2H, Ar-H), 7.58 (d,  $J = 9$  Hz, 2H, Ar-H), 6.78 (d,  $J = 9$  Hz, 1H, Ar-H).  $^{13}\text{C}$  NMR (75 MHz, DMSO)  $\delta$  167.05, 159.96, 155.92, 152.11, 140.20, 139.96, 139.96, 135.15, 134.06, 132.67, 132.01, 131.86, 131.83, 131.72, 117.15, 109.90. IR (ATR,  $\text{cm}^{-1}$ ): 2979.34, 1700.18, 1637.17, 1614.34, 1542.37, 1497.33, 1201.07, 865.39, 815.42. MS (ESI)  $m/z$ : 335.2 [ $\text{M}^+$ ]. Melting point =  $> 300$ °C.

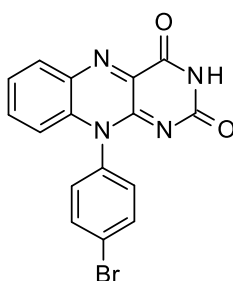
### 2.6.19 10-(4-Biphenyl)isoalloxazine (8)



Compound **8** was synthesised using the same methodology and reaction stoichiometry as **1** to yield **8** as a yellow solid. Yielding 1.61 g, 87 %.

$^1\text{H}$  NMR ( $d_6$ -DMSO, 300 MHz):  $\delta$  11.47 (s, 1H, N-H), 8.21 (d,  $J = 6$  Hz, 1H, Ar-H), 8.00 (d,  $J = 9$  Hz, 2H, Ar-H), 7.82 (d,  $J = 9$  Hz, 2H, Ar-H), 7.76 (d,  $J = 9$  Hz, 1H, Ar-H), 7.64 (t,  $J = 6$  Hz, 1H, Ar-H), 7.43-7.58 (m, 5H, Ar-H), 6.88 (d,  $J = 9$  Hz, 1H, Ar-H).  $^{13}\text{C}$  NMR (75 MHz,)  $\delta$  217.38, 175.77, 160.43, 160.05, 056.05, 152.31, 152.14, 142.03, 139.94, 139.57, 139.36, 135.76, 135.22, 134.54, 134.51, 129.06, 9.99, 76.66. IR (ATR,  $\text{cm}^{-1}$ ): 3069.07, 1720.72, 1668.18, 1610.91, 1537.25, 856.82, 763.45, 726.88. MS (ESI)  $m/z$ : 367.2 [ $\text{M}^+$ ]. Melting point =  $>300$  °C.

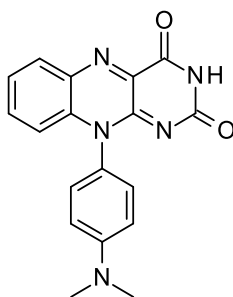
### 2.6.22 10-(4-Bromophenyl)isoalloxazine (9)



Compound **9** was synthesised using the same methodology and reaction stoichiometry as **1** to yield **9** as a brown solid. Yielding 1.43 g, 91 %.

$^1\text{H}$  NMR ( $d_6$ -DMSO, 300 MHz,)  $\delta$  11.47 (s, 1H, N-H), 8.20 (d,  $J = 9$  Hz, 1H, Ar-H), 7.93 (d,  $J = 9$  Hz, 1H, Ar-H), 7.75 (t,  $J = ?$  1 Hz, 1H, Ar-H), 7.63 (t,  $J = ?$  Hz, 2H, Ar-H), 7.41 (d,  $J = 9$  Hz, 2H, Ar-H), 6.83 (d,  $J = 9$  Hz, 1H, Ar-H).  $^{13}\text{C}$  NMR (75 MHz,)  $\delta$  172.57, 159.95, 152.17, 139.86, 135.75, 135.15, 134.21, 131.91, 131.41, 129.83, 123.60, 118.14, 116.30. IR (ATR,  $\text{cm}^{-1}$ ): 3081.23, 1688.02, 1640.52, 1613.11, 1538.52, 1484.38, 840.73, 709.08, 680.82. MS (ESI)  $m/z$ : 369.0 [ $\text{M}^+$ ]. Melting point =  $>300$   $^\circ\text{C}$ .

### 2.6.23 10-(4-Dimethylaminophenyl)isoalloxazine (10)

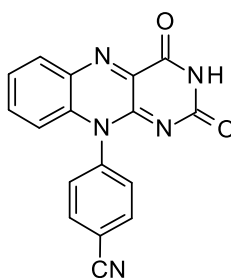


Compound **10** was synthesised using the same methodology and reaction stoichiometry as **1** to yield **10** as a brown solid. Yielding 2.39 g, 93 %

$^1\text{H}$  NMR ( $d_6$ -DMSO, 300 MHz,)  $\delta$  11.39 (s, 1H, N-H), 8.16 (d,  $J = 9$  Hz, 1H, Ar-H), 7.75 (t,  $J = 6$  Hz, 1H, Ar-H), 7.60 (t,  $J = 6$  Hz, 1H, Ar-H), 7.15 (d,  $J = 9$  Hz, 2H, Ar-H), 6.94 (d,  $J = 9$  Hz, 2H, Ar-H), 6.90 (d,  $J = 9$  Hz, 1H, Ar-H).  $^{13}\text{C}$  NMR (75 MHz,)  $\delta$ . IR (ATR,  $\text{cm}^{-1}$ ): 3034.96, 1744.41, 1709.23, 1639.34, 1543.13, 1507.25, 878.73, 828.12, 725.92. MS (ESI)  $m/z$ : 334 [ $\text{M}^+$ ]. Melting point =  $>300$   $^\circ\text{C}$ .



### 2.6.24 10-(4-Nitrilephenyl)isoalloxazine (11)

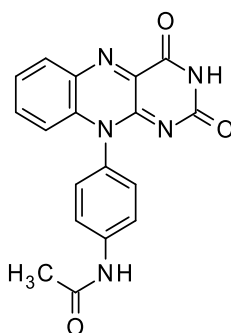


Compound **11** was synthesised using the same methodology and reaction stoichiometry as **1** to yield **11** as a yellow solid. Yielding 0.4 g, 90 %.

$^1\text{H}$  NMR ( $d_6$ -DMSO, 300 MHz):  $\delta$  11.53 (s, 1H, N-H), 8.22 (,  $J = 9$  Hz, 3H, Ar-H), 7.77-7.63

(m, 4H, Ar-H), 6.80 (d,  $J = 9$  Hz, 1H, Ar-H), IR (ATR,  $\text{cm}^{-1}$ ): 3069.53, 1686.96, 1503.62, 879.23, 852.75. MS (ESI)  $m/z$ : 316.4 [ $\text{M}^+$ ]. Melting point =  $>300^\circ\text{C}$ .

### 2.6.25 10-(4-Acetamidophenyl)isoalloxazine (12)

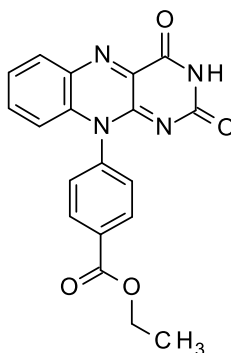


Compound **12** was synthesised using the same methodology and reaction stoichiometry as **1** to yield **12** as a yellow solid. Yielding 2.80 g, 92 %

$^1\text{H}$  NMR ( $d_6$ -DMSO, 300 MHz):  $\delta$  11.43 (s, 1H, N-H), 10.32 (s, 1H, N-H), 8.18 (d,  $J = 6$  Hz, 1H, Ar-H), 7.87 (d,  $J = 9$  Hz, 2H, Ar-H), 7.75 (t,  $J = 9$  Hz, 1H, Ar-H), 7.62 (t,  $J = 6$  Hz, 1H, Ar-H), 6.83 (d,  $J = 9$  Hz, 2H, Ar-H).  $^{13}\text{C}$  NMR (75 MHz,)  $\delta$  151.64, 144.55, 143.21, 142.71, 140.88, 139.95, 138.99, 138.64, 136.89, 135.18, 134.74, 128.63,

120.60, 120.51, 99.99, 21.78. IR (ATR,  $\text{cm}^{-1}$ ): 3053.99, 1674.86, 1611.46, 1502.50, 878.20, 848.25, 727.41. MS (ESI)  $m/z$ : 305.19 [ $\text{M}^+$ ]. Melting point =  $>300^\circ\text{C}$ .

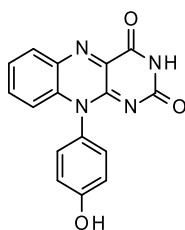
### 2.6.26 10-(4-Ethylbenzoatephenyl)isoalloxazine (13)



A two-necked round bottom flask was charged with compound **7** (1 g, 3 mmol) and ethanol (30mL) and heated to reflux. Once the solution was clear sulphuric acid (1.6mL) was added dropwise. Refluxed for 6 hours. Once cooled to room temperature saturated sodium carbonate water was added until the solution became neutral and solid precipitated out. The solid was isolated at the pump and washed with water until the aqueous layer turned neutral. Yielding 0.70 g, 65 %

$^1\text{H}$  NMR ( $\text{d}_6$ -DMSO, 300 MHz):  $\delta$  11.48 (s, 1H, N-H), 8.29 (d,  $J = 9$  Hz, 2H, Ar-H), 8.20 (d,  $J = 9$  Hz, 1H, Ar-H), 7.74 (d,  $J = 9$  Hz, 1H, Ar-H), 7.62 (d,  $J = 9$  Hz, 3H, Ar-H), 6.78 (d,  $J = 9$  Hz, 1H, Ar-H).  $\delta$   $^{13}\text{C}$  NMR (75 MHz,)  $\delta$  167.14, 159.96, 155.93, 152.10, 140.07, 139.93, 135.15, 134.07, 133.0, 133.03, 131.96, 131.84, 131.76, 128.73, 120.15, 117.20, 117.15. IR (ATR,  $\text{cm}^{-1}$ ): 3055.94, 1702.52, 1683.57, 1613.47, 1500.61, 1216.44, 809.97, 757.97, 721.79. MS (ESI)  $m/z$ : 362.32 [ $\text{M}^+$ ]. Melting point  $\Rightarrow 300^\circ\text{C}$ .

### 2.6.27 10-(4-Hydroxyphenyl)isoalloxazine (14)



A round bottom flask was charged with **2** (1.6 g, 5 mmol) Hydrobromic acid (10 mL) and acetic acid (10 mL) were refluxed for 6 hours. Once cooled to room temperature the mixture was poured over ice and diluted with water. Potassium hydroxide pellets were added until precipitation occurred. The solid was isolated at the pump and dried under a vacuum. Yielding 0.15 g, 98 %

$^1\text{H}$  NMR ( $d_6$ -DMSO, 300 MHz,)  $\delta$  11.47 (s, 1H, N-H), 10.09 (s, 1H, OH), 8.17 (d,  $J = 6$  Hz, 1H, Ar-H), 7.75 (t,  $J = 9$  Hz, 1H, Ar-H), 7.61 (t,  $J = 9$  Hz, 1H, Ar-H), 7.20 (d,  $J = 9$  Hz, 2H, Ar-H), 7.03 (d,  $J = 9$  Hz, 2H, Ar-H), 6.86 (d,  $J = 9$  Hz, 1H, Ar-H).  $^{13}\text{C}$  NMR (75 MHz, DMSO)  $\delta$  160.12, 158.78, 158.78, 156.12, 152.53, 139.88, 135.22, 135.15, 135.09, 131.78., 129.28, 127.43, 126.37, 117.05. IR (ATR,  $\text{cm}^{-1}$ ): 3052.32, 3151.73, 1716.20, 1666.31, 1611.52, 1527.94, 1503.20, 1191.86, 875.96, 844.29. MS (ESI)  $m/z$ : 307.1 [ $\text{M}^+$ ]. Melting point =  $>300^\circ\text{C}$ .

## References

1. Heelis, P.F., *The photophysical and photochemical properties of flavins (isoalloxazines)*. Chemical Society Reviews, 1982. **11**(1): p. 15-39.
2. Edwards, A.M., *Chapter 1 General Properties of Flavins*, in *Flavins: Photochemistry and Photobiology*. 2006, The Royal Society of Chemistry. p. 1-11.
3. Abbas, C.A. and A.A. Sibirny, *Genetic Control of Biosynthesis and Transport of Riboflavin and Flavin Nucleotides and Construction of Robust Biotechnological Producers*. Microbiology and Molecular Biology Reviews, 2011. **75**(2): p. 321-360.
4. Long Quanxin , J.L., Wang Honghai, Xi Jianping, *Riboflavin biosynthetic and regulatory factors as potential novel anti-infective drug targets*. Chemical biology and drug design, 2010. **75**(4).
5. Brody, T., *Nutritional biochemistry*. 2 ed. 1994: Elsevier Science.
6. Magnúsdóttir S, R.D., de Crécy-Lagard V , Thiele I, *Systematic genome assessment of B-vitamin biosynthesis suggests co-operation among gut microbes*. Frontiers in Genetics, 2015. **6**.
7. Corbin, F., *Pathogen inactivation of blood components: Current status and introduction of an approach using riboflavin as a photosensitizer*. International Journal of Hematology, 2002. **76**(2): p. 253-257.
8. Thakur, K., S.K. Tomar, and S. De, *Lactic acid bacteria as a cell factory for riboflavin production*. Microbial Biotechnology, 2016. **9**(4): p. 441-451.
9. Massey, V., *The Chemical and Biological Versatility of Riboflavin*. Biochemical Society Transactions, 2000. **28**(4): p. 283-296.
10. Banerjee, R., *Redox Biochemistry*. 1 ed. 2007: John Wiley & sons, Incorporated.
11. Lu, C.-Y., et al., *Generation and photosensitization properties of the oxidized radical of riboflavin: a laser flash photolysis study*. Journal of Photochemistry and Photobiology B: Biology, 1999. **52**(1–3): p. 111-116.
12. Goodrich, R.p.E., Richard A. Li, Junzhi. Seghatchian, Jerard., *The Mirasol PRT system for pathogen reduction of platelets and plasma: An overview of current status and future trends*, in *Transfusion and Apheresis Science*. 2006. p. 5-17.
13. Muñoz, M.A., et al., *Different cell death mechanisms are induced by a hydrophobic flavin in human tumor cells after visible light irradiation*.

- Journal of Photochemistry and Photobiology B: Biology, 2011. **103**(1): p. 57-67.
14. Eitenmiller. Ronald R., L.W.O.J., Ye Lin *Vitamin analysis for the health and food sciences*. 2nd Edition ed. 2008: CRC Press.
  15. Wainwright, M., *Photosensitisers in Biomedicine (1)*. 2009, Hoboken, GB: Wiley.
  16. Jortzik Esther , W.L., Ma Jipeng , Becker Katja, *Flavins and flavoproteins*. Methods in Molecular Biology. Vol. 1146. 2014: Springer.
  17. Bejugam, M., et al., *Trisubstituted Isoalloxazines as a New Class of G-Quadruplex Binding Ligands: Small Molecule Regulation of c-kit Oncogene Expression*. Journal of the American Chemical Society, 2007. **129**(43): p. 12926-12927.
  18. Kathiresan, M., et al., *Viologen-based benzylic dendrimers: selective synthesis of 3,5-bis(hydroxymethyl)benzylbromide and conformational analysis of the corresponding viologen dendrimer subunit*. Tetrahedron Letters, 2010. **51**(16): p. 2188-2192.
  19. Halstead, F.D., et al., *Antibacterial Activity of Blue Light against Nosocomial Wound Pathogens Growing Planktonically and as Mature Biofilms*. Applied and Environmental Microbiology, 2016. **82**(13): p. 4006-4016.
  20. Trzaska, W.J., et al., *Species-specific antifungal activity of blue light*. Scientific Reports, 2017. **7**(1): p. 4605.

## 3.0 Porphyrin

### 3.1 Background

#### 3.1.1 Chemistry of porphyrins

Porphyrins are purple pigments<sup>[1]</sup>, which are naturally occurring organic compounds<sup>[2]</sup>. The basic skeletal structure (see figure 3.1) comprises of four pyrrole rings<sup>[3]</sup> linked together by four carbon atoms in a planar arrangement with an 18  $\pi$  distinct aromatic character<sup>[4]</sup>.

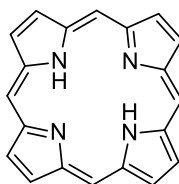


Figure 3.1: Skeletal structure of a porphyrin<sup>[3]</sup>.

Porphyrins are aromatic compounds<sup>[6]</sup>, which are relatively stable due to their extended aromatic structure and their ability to complex with transition metals<sup>[7]</sup>. Porphyrins however differ from benzene due to having two different sites in which electrophilic substitution may take place <sup>[1]</sup>, *meso* and  $\beta$  (see figure 3.2)<sup>[4]</sup>. The shape of the porphyrins bring about unique selectivity issues, one of these being the regioselectivity of porphine, an unsubstituted porphyrin<sup>[4]</sup>. Furthermore, there is only one type of *meso*-position, which in the case of 5, 10, 15-trisubstituted porphyrin are each potentially reactive<sup>[4]</sup>. There are however, four different types of  $\beta$  -positions that, are generally less reactive than the *meso*-positions<sup>[4]</sup>.

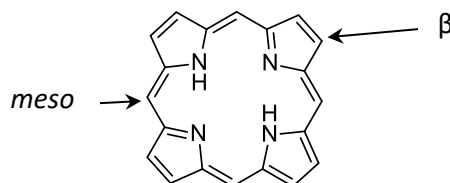


Figure 3.2: Different reactive position on a porphyrin<sup>[4]</sup>

Porphyrins belong to a class of tetrapyrroles, which comprises of a highly conjugated heterocyclic macrocycle<sup>[8]</sup>. They are large macrocyclic compounds<sup>[9]</sup> which, due to their special absorption, emission, charge transfer and complexing properties play important roles in nature<sup>[10]</sup>. These properties are caused by their characteristic ring structure of conjugated double bonds<sup>[10]</sup>.

### 3.1.2 What are porphyrins?

Porphyrins are family of compounds, which differ in their substituents around the same basic skeletal structure<sup>[3]</sup>. Porphyrins can be found in all cells and are possibly the most important class of compounds in biological systems<sup>[3]</sup>. This is because they are involved in numerous biological processes<sup>[2]</sup>, for example they are involved in metabolism<sup>[1]</sup>. Porphyrins are also associated with blood and other redox enzymes involved in metabolism through heme, an iron porphyrin<sup>[1]</sup>. The heme (see figure 3.3) porphyrin is part of a family of proteins called globins<sup>[5]</sup>; within this family are haemoglobin and myoglobin<sup>[5]</sup>, which are responsible for one of the most important aspects of animal metabolism – obtaining and usage of oxygen<sup>[5]</sup>. Myoglobin is responsible for the storage of oxygen within the muscles whilst haemoglobin is responsible for the transport of oxygen<sup>[6]</sup> and removal of carbon dioxide from tissues<sup>[5]</sup>.

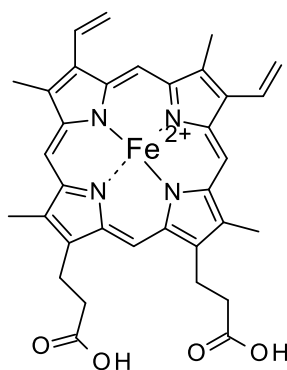


Figure 3.3: Structure of heme<sup>[5]</sup>

### 3.1.3 Photochemistry of porphyrins

Porphyrin sensitizers need both light and oxygen and because of this they are said to be true photo-oxidants [3]. Porphyrins can be good photosensitizers for PDT because they generally possess considerably long-lived triplet states<sup>[10]</sup>. Photosensitizers that produce singlet oxygen have received much attention in connection to photodynamic therapy<sup>[11]</sup>. Porphyrins are interesting photochemically and exhibit characteristics desirable for drug candidates in photodynamic therapy. These characteristics include:

- High quantum yield of singlet oxygen production
- Significant absorption at longer wavelengths
- Minimal dark toxicity
- Stability and ability to dissolve in an injectable solvent system<sup>[12]</sup>.

Porphyrin complexes with high absorptivity in visible-light regions have been widely utilized as chemical and biological functional chromophores<sup>[13]</sup>. Recently bioactive porphyrins have received attention in connection with photo-inactivation and photodynamic therapy<sup>[13]</sup>. Porphyrins and metalloporphyrins are attractive candidates because of their strong absorption band in the visible light region<sup>[11]</sup>.

### 3.1.4 Porphyrins as treatment for bacterial/fungal infections

The production of singlet oxygen by porphyrins makes them useful for antimicrobial use in light accessible areas, such as cutaneous and subcutaneous<sup>[7]</sup>. It has been shown that photosensitization of different tetrapyrrole compounds can be efficient in the killing of bacterial cells<sup>[7]</sup>. These tetrapyrrole compounds are able to kill gram-positive bacteria efficiently<sup>[14]</sup>. However only cationic photosensitizers combined with agents that make the membrane permeable are able to kill gram-negative bacteria<sup>[14]</sup>. Dastgheyb



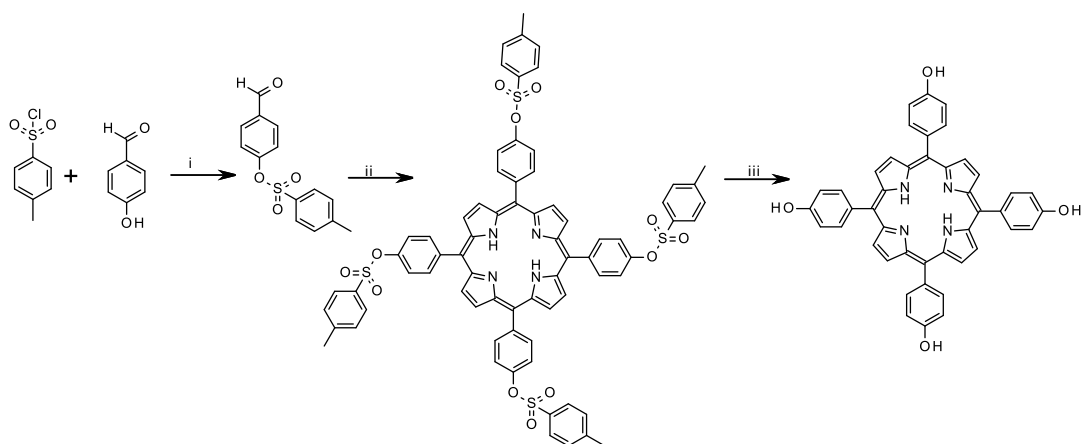
carried out a study which showed that a meso-substituted cationic porphyrin (4-aminophenyl)porphine, had antimicrobial activity against multiple strains of bacteria, for example, *S. aureus*<sup>[7]</sup>. Importantly porphyrins also lack eukaryotic cytotoxicity in the absence of light at antibacterial concentrations<sup>[7]</sup>.

### 3.1.5 Rationale

Porphyrins are natural chromophores and are able to produce singlet oxygen upon photosensitisation. The reported antimicrobial activity of meso-substituted porphyrins against *S. aureus* is the inspiration behind the decision to synthesise different substituted porphyrin compounds based on the tetraphenylporphine structure as shown in table 3.1. The rationale for this was to investigate how singlet oxygen and the subsequent microbicidal effect of these compounds would change with the different substituents. The singlet oxygen production was obtained via spectrophotometric technique decolourisation of TPCPD in DCM (see section 2.3). In order to determine the antifungal activity of the novel compounds they were tested against the yeast like fungi, *Candida albicans*, using the EUCAST microdilution method (EUCAST E.DEF 7.3 December 2015).

## 3.2 Synthesis

There were two methodologies for the synthesis of the porphyrins. For the hydroxy porphyrins, a 4-hydroxybenzaldehyde was protected before being reacted with pyridine under acidic conditions, for the monosubstituted porphyrin a stoichiometric amount of benzaldehyde was also put into the reaction vessel. The protecting group was then cleaved in basic conditions. The synthetic route for 5,10,15,20-tetrakis-(4-hydroxyphenyl)-21H,23H-porphine (**19**) is shown in scheme 3.1.



i) DCM, Triethylamine, r.t, 6 hr; ii) pyrrole, propionic acid, 140°C, 30 mins; iii) EtOH, DMF, 80°C, 2 hr

Scheme 3.1: Synthetic route for 5,10,15,20-tetrakis-(4-hydroxyphenyl)-21H,23H-porphine (**19**)

The HNMR of **15** (figure 3.4) clearly shows the protection of the 4-hydroxybenzaldehyde with the p-tosylchloride. This can be seen by the 8 aromatic protons in the region 7.84 -7.17 ppm. The formation of 5,10,15,20-tetrakis-(4-tosyloxyphenyl)-21H,23H-porphine can be seen in figure 3.5 by the singlet at 8.75 ppm with an integration of 8 and the increase of the integration of the CH peak to 12. It is clear to see from the overlaid HNMR spectra figure 3.6 that the deprotection of the tosyl group with KOH was successful by the disappearance of the CH peak at 2.53 ppm.

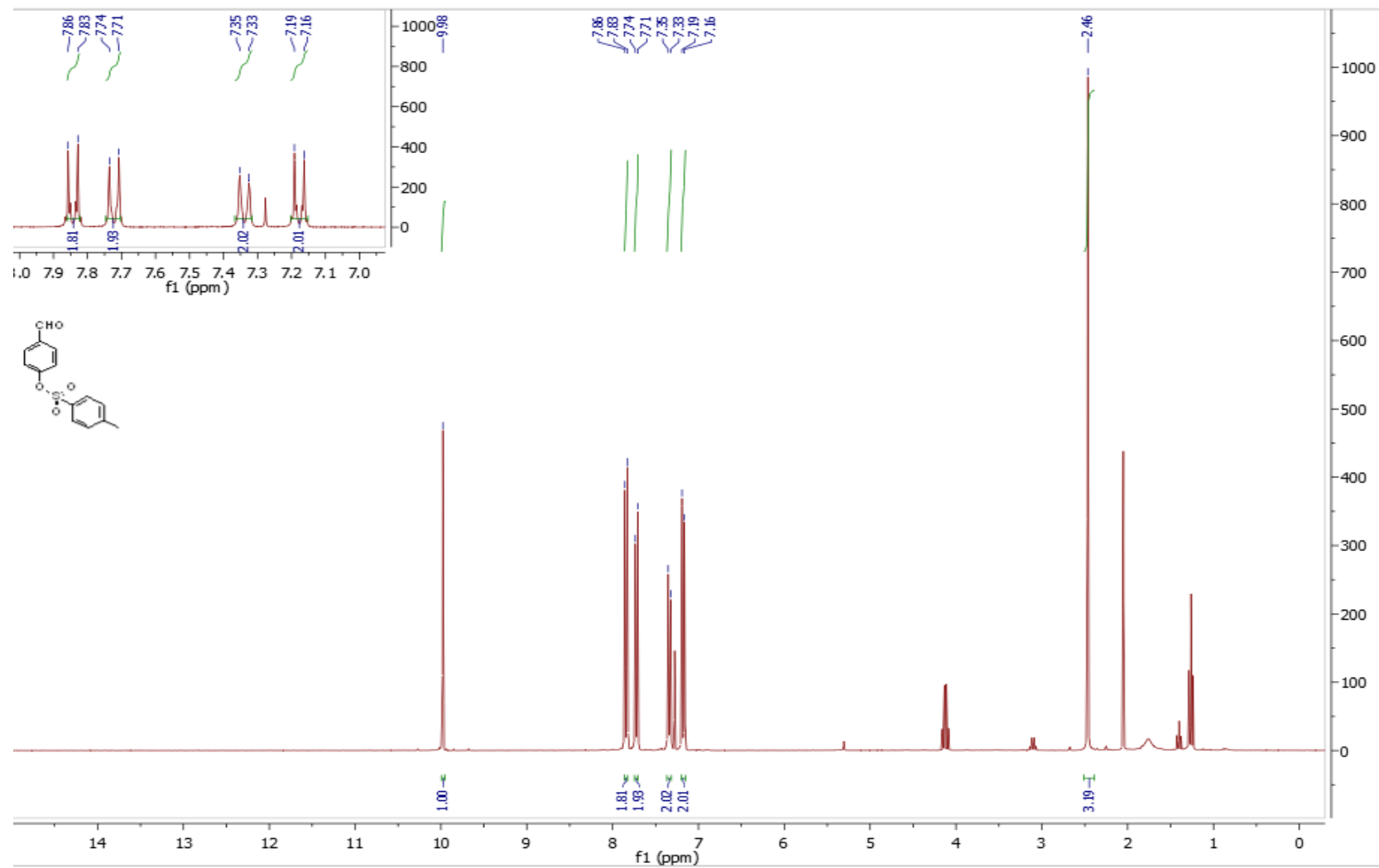


Figure 3.4: <sup>1</sup>H NMR 4-Tosylbenzaldehyde **15**

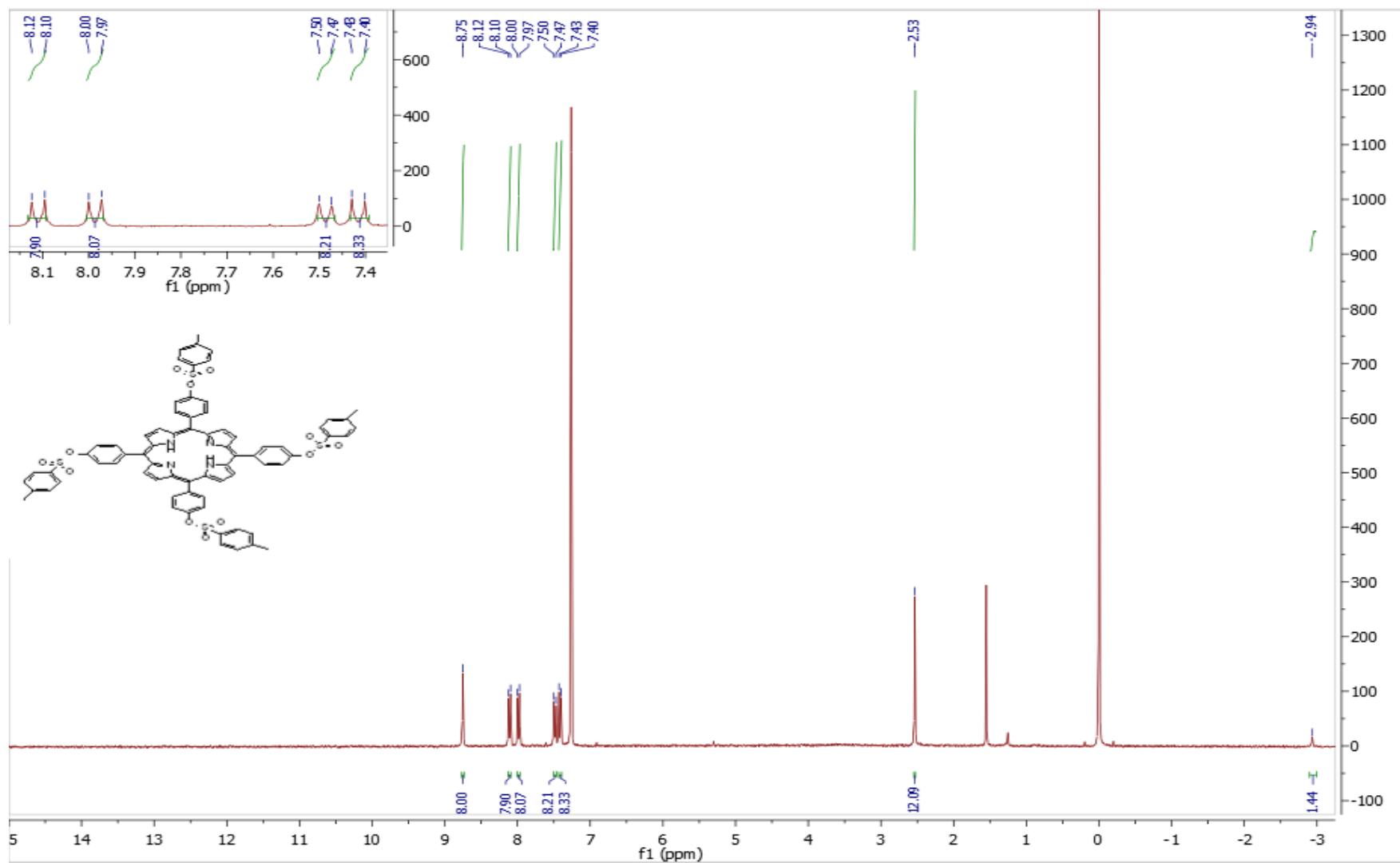


Figure 3.5: <sup>1</sup>H NMR 5,10,15,20-Tetrakis-(4-tosyloxyphenyl)-21H,23H-porphine (**18**)

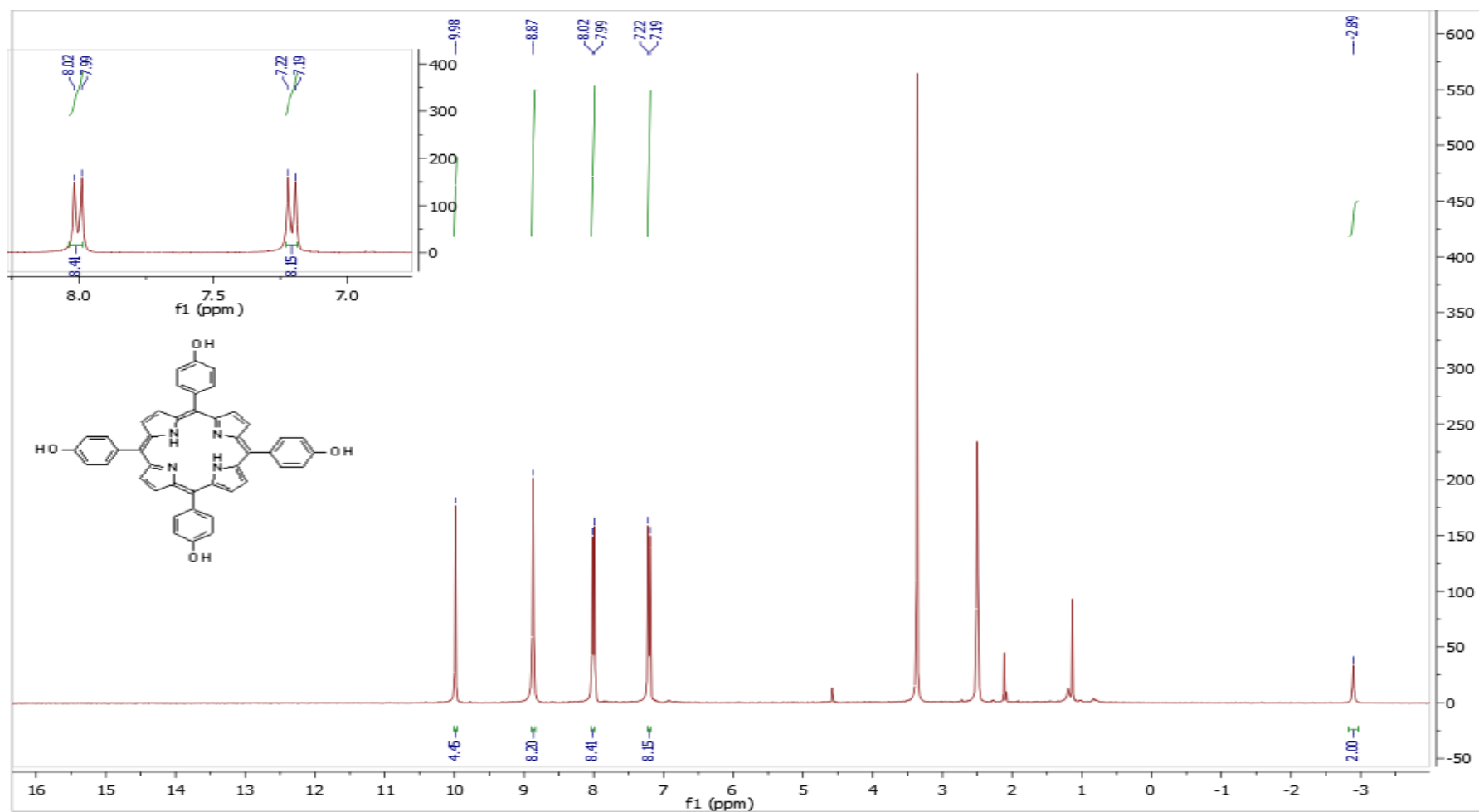
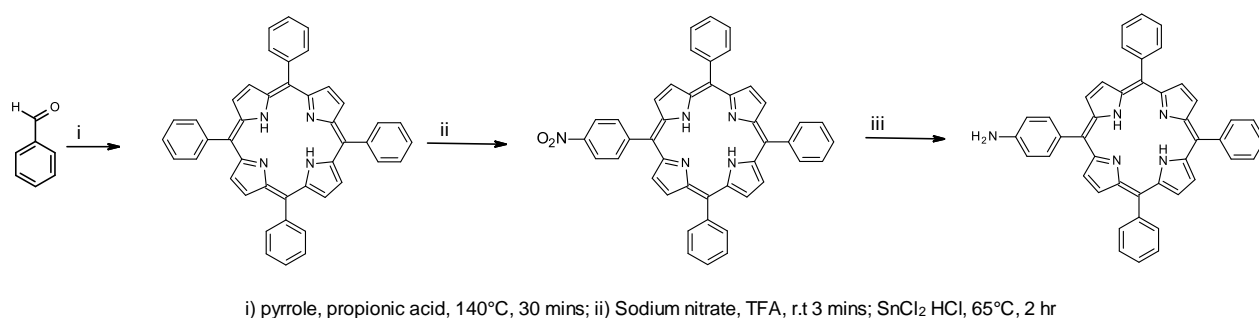


Figure 3.6: <sup>1</sup>H NMR 5,10,15,20-Tetrakis-(4-hydroxyphenyl)-21H,23H-porphine (**19**)

The amino porphyrin was synthesised by first making tetraphenyl porphyrin (**16**) reacting pyrrole and benzaldehyde in the presence of propionic acid. **16** was then nitrated using Trifluoroacetic acid and sodium nitrate, before reducing using tin(II)chloride in an acidic solution. The synthetic scheme for this is shown in scheme 3.2 using 5-(4-aminophenyl)-10,15,20-triphenyl-21H,23H-porphine (**21**).



Scheme 3.2: synthetic route for 5-(4-aminophenyl)-10,15,20-triphenyl-21H,23H-porphine (**21**).

### 3.3 Singlet oxygen studies

The same methodology was used as on page 33. The singlet oxygen of the porphyrins was taken with a blank of 50:50 dye DCM due to the dye masking the half-life. It can be seen from the table above that all the porphyrin derivatives have the same singlet oxygen yield.

It was expected that the derivatives of tetraphenylporphyrin would have a different singlet oxygen yields due to the different R groups affecting the relative yield of singlet oxygen.

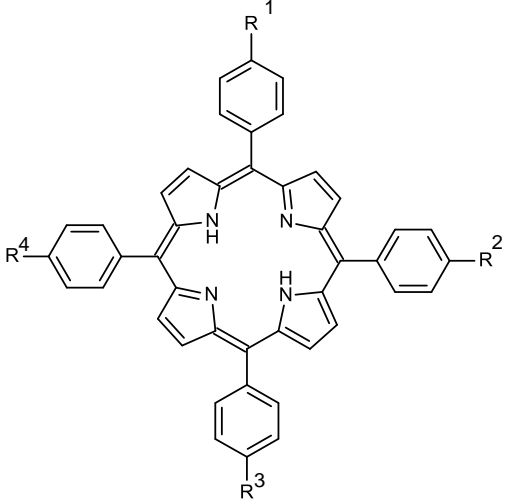
Compound					cLog P	Absorption (nm)	Relative <sup>1</sup> O <sub>2</sub> Yield	Minimum inhibitory concentration (mg/mL)
	R1	R2	R3	R4				
16	H	H	H	H	9.64	416	1	*
17	OH	H	H	H	9.54	417	1	*
18	OTs	OTs	OTs	OTs	10.38	418	1	*
19	OH	OH	OH	OH	9.17	420	1	2.5
20	NO <sub>2</sub>	H	H	H	9.63	420	1	*
21	NH <sub>2</sub>	H	H	H	9.44	420	1	*
Fluconazole	-	-	-	-	-	-	-	0.156

Table 3.1: Photophysical and growth inhibition data for the porphyrin derivatives. Minimum inhibition concentration is shown for 20 minutes exposure to blue light. \* indicates growth was observed at the maximum concentration tested, 10 mg/mL. cLog P is a partition coefficient of compound between aqueous and lipophilic phases and was calculated using molinspiration.



### 3.4 Assay for Growth

The same methodology was used as page 35

#### Results

##### **All but one porphyrin had no effect on *C.albicans***

In order to see if the porphyrin derivatives had an effect on growth of *C.albicans*, cells were exposed to a range of concentrations, 0.0195 mg/mL to 10 mg/mL, in the absence and presence of blue light. Visual inspection of the plates after 24 hr incubation at 34°C, table 3.1 and figure 3.7 showed compounds 17,18,20,21,22 have no effect on the growth of *C. albicans*, when compared to the control, at the concentrations tested. Compound 19 did show an effect against the growth of *C.albicans*. In the presence of the antifungal agent fluconazole, an effect was observed with an MIC determined to be 0.156 mg/mL. Compound 16 was dissolvable in DMSO.

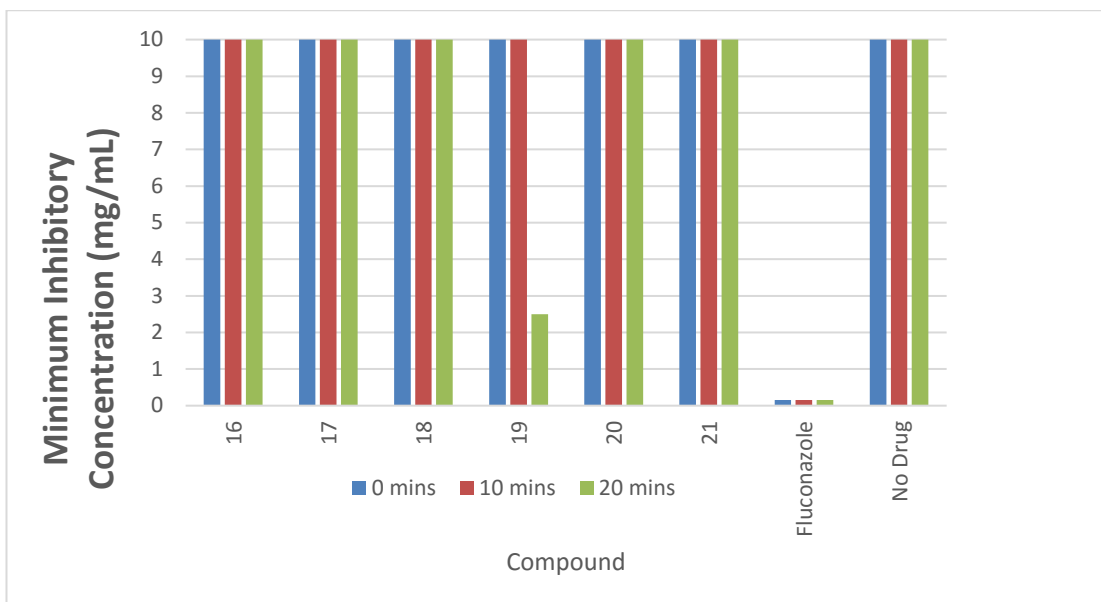


Figure 3.7: Comparison of compounds 16-21 with fluconazole on *C.albicans*. The MIC was obtained according to the EUCAST method in the absence and presence of blue light. The maximum concentration tested was 10 mg/mL.

### 3.5 Discussion

The synthesis of the porphyrins was straightforward and did not require the use of harsh or unusual methodologies as seen in schemes 3.1 and 3.2. The hydroxy porphyrins were produced by first synthesising the appropriate tosyloxyphenylporphines, which were subsequently deprotected using potassium hydroxide, resulting in the hydroxyphenylporphines. The amine porphyrins were produced by first synthesising 5,10,15,20-tetraphenyl-21H,23H-porphine, which were then nitrated to produce 5-(4-nitrophenyl)10,15,20-21H,,23H-porphine before being reduced using tin (II)chloride, yielding 5-(4-aminophenyl)-10,15,20-21H,23H-porphine.

The photophysical and growth inhibition properties of compounds **16-21** are summarised in table 3.1. It is clear to see that all the porphyrin compounds exhibited an absorption spectra maxima within the region of 416 – 420 nm.

When comparing the singlet oxygen data for the porphyrins it is clear to see that all the compounds had the appear to have the same relative yield. This is interesting because although **16** has no added substituents, the rate of singlet oxygen production is the same as **19**, which has an additional four hydroxy groups attached the phenyl ring. Its postulated that if iodine atoms had been substituted onto the phenyl ring, the heavy atom effect from the iodine's would have yielded a larger amount of singlet oxygen upon illumination.

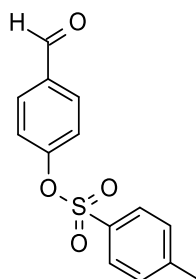
The growth inhibition data also shown in table 3.1, shows that only compound **19** had an effect on the growth of *C.albicans* upon illumination with blue light for 20 minutes. When comparing the Log P data against the MIC values it is clear to see that the compound with the lowest Log P, compound **19**, produced an microbicidal effect. The microbicidal effect could be due to the

increase in the polarity, which is shown by the Log P, of compound **19** due to the addition of four hydroxyl groups which increases the polarity of the compound. When compared to the MIC of fluconazole (0.156 mg/mL) the MIC of compound **19** (2.5 mg/mL) shows a significant difference in the ability of compound **19** to produce antimicrobial activity. This could be due to this size of compound **19** affecting their ability to permeate the membrane of the fungal cell.

## 3.6 Experimental

### Experimental

#### 3.6.1 4-Tosylbenzaldehyde (**15**)

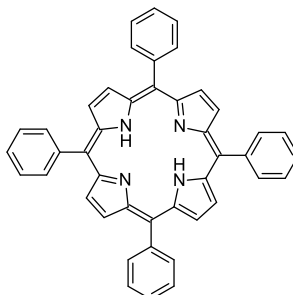


A round bottom flask was charged with 4-hydroxybenzaldehyde (3.0 g, 24.5 mmol), p-toluenesulphonyl chloride (4.68 g, 24.5 mmol) and DCM (50 mL). The round bottom flask was placed in an ice bath and with constant stirring triethylamine (4.1 mL, 29.4 mmol) was added to the reaction mixture. The mixture was left to stir in the ice bath for 5 minutes, and then removed and stirred at room temperature for 6 hours. The reaction mixture was added to a separating funnel with ethyl acetate and washed with water and brine. The organic layer was isolated, dried over sodium sulphate and the solvents were evaporated under reduced pressure. Yielding 2 g, 29.6 %.

$^1\text{H NMR}$  ( $\text{CDCl}_3$ , 300 MHz,):  $\delta$  9.98 (s, 1H,  $\text{CHO}$ ), 7.84 (d,  $J=9$  Hz, 2H, Ar-H), 7.72 (d,  $J=9$  Hz, 2H, Ar-H), 7.34 (d,  $J=6$  Hz, 2H, Ar-H), 7.17 (d,  $J=9$  Hz, 2H, Ar-

H), 2.46 (s, 3H, CH<sub>3</sub>) . <sup>13</sup>C NMR (75 MHz): δ 190.71, 153.85, 145.94, 134.80, 131.94, 131.29, 129.98, 128.47, 123.10, 21.78. MS (ESI) m/z: 277 [M<sup>+</sup>].

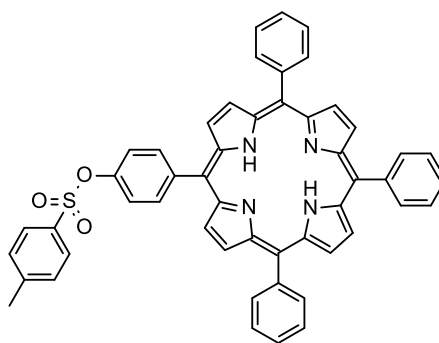
### 3.6.2 5,10,15,20-Tetraphenyl 21H,23H-porphine (16)



A round bottom flask was charged with benzaldehyde (5 g, 18 mmol) and propionic acid (62.5 mL) and heated to reflux with constant stirring. Pyrrole (1.22 g, 18 mmol) was added to the reaction slowly and with continuous stirring heated for 30 minutes. Upon cooling, the reaction mixture was placed into a freezer overnight. Absolute ethanol (20 mL) was added and the reaction mixture was stirred at room temperature for 7 hours. The black reaction mixture was filtered to yield the crude porphyrin and washed with cold methanol until the washing were clear. The crude porphyrin was removed from the filter, placed into a conical flask and hot methanol was added. The hot methanol solution was filtered to leave a clean purple solid which was washed with hot methanol until the washings ran clear. Yielding 2 g, 18 %.

<sup>1</sup>H NMR (CDCl<sub>3</sub>, 300 MHz): δ 8.90 (s, 8H, Pyrrole H), 8.26 (d, J= 9 Hz, 8H, Ar-H), 7.78 (d, J= 6 Hz, 12H, Ar-H), -2.73 (s, 2H, Pyrrole NH). <sup>13</sup>C NMR (75 MHz, δ. IR (ATR, cm<sup>-1</sup>):. MS (ESI) m/z: 615 [M<sup>+</sup>]. Melting point = >300 °C.

### 3.6.3 5-(4-Tosyloxyphenyl)-10,15,20-21H,23H-porphine (17a)



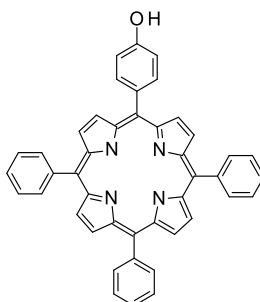
A round bottom flask was charged with benzaldehyde (5.96 g, 54 mmol), 4-tosyloxybenzaldehyde (5 g, 18 mmol) and propionic acid (62.5 mL). Once the mixture was refluxing and the solid dissolved, pyrrole (1.22 g, 18 mmol) was added, the reaction was heated for 30 minutes with constant stirring. Upon cooling, the reaction mixture was placed into a freezer overnight. Absolute ethanol (20 mL) was added and the reaction was stirred at room temperature for 7 hours. The black reaction mixture was filtered, to yield the crude porphyrin and washed with cold methanol until the washing were clear. The crude porphyrin was removed from the filter, placed into a conical flask and hot methanol was added. The hot methanol solution was filtered to leave a clean purple solid which was washed with hot methanol until the washings ran clear. The compound was purified by column chromatography with neutral alumina as adsorbent and toluene as eluent to yield **17a**, 0.08 g, 0.6 %.

$^1\text{H NMR}$  ( $\text{CDCl}_3$ , 300 MHz):  $\delta$  8.86 (s, 8H, pyrrole H), 8.74 (d,  $J=6\text{Hz}$ , 2H, Ar-H), 8.23 (d,  $J=6\text{Hz}$ , 6H, Ar-H), 8.14 (d,  $J=9\text{ Hz}$ , 2H, Ar-H), 7.98 (d,  $J=9\text{ Hz}$ , 2H, Ar-H), 7.83-7.74 (m, 9H, Ar-H), 7.48 (d,  $J=9\text{Hz}$ , 2H, Ar-H), 7.40 (d,  $J=9\text{Hz}$ , 2H, Ar-H), 2.19 (s, 3H,  $\text{CH}_3$ ), -2.82 (s, 2H, Pyrrole NH). MS (ESI)  $m/z$ : 785 [ $\text{M}^+$ ].

Melting point =  $>300\text{ }^\circ\text{C}$ .

### 3.6.4 5-(4-Hydroxyphenyl)-10,15,20-triphenyl-21H,23H-porphine

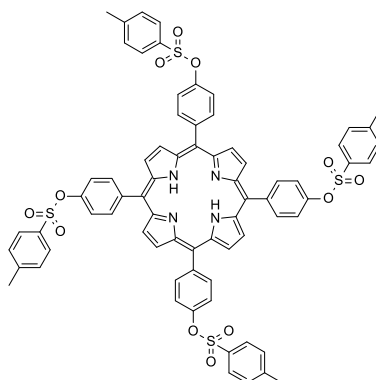
(17)



To a stirred solution of **17a** (0.08 g, 0.10 mmol) in absolute alcohol (12 mL) and dimethylformamide (6 mL) was added potassium hydroxide pellets (0.3 g). The reaction was heated 80 °C with constant stirring for 2 hours. After two hours additional potassium hydroxide (0.3 g) was added to the reaction mixture and the reaction proceeded at 60 °C for a further 2 hours. Upon cooling, the reaction mixture was poured into distilled water (20 mL), treated with 3M HCl (12mL), brine (10 mL) and extracted into chloroform. The organic layer was washed with distilled water (3 x 20 mL), isolated, dried over sodium sulphate and concentrated under reduced pressure. Yielding 0.0095 g, 15 %

$^1\text{H}$  NMR (DMSO, 300 MHz,):  $\delta$  10.00 (s, 1H, OH), 8.82 (s, 8H, Pyrrole H), 8.24-8.21 (m, 6H, Ar-H), 8.02 (d, J= 9 Hz, 2H, Ar-H), 7.85-7.83, (m, 9H, Ar-H), -2.93 (s, 2H, Pyrrole NH) .  $^{13}\text{C}$  NMR (75 MHz,)  $\delta$  148.24, 135.74, 134.57, 132.81, 131.39, 127.70, 127.57, 126.69, 123.94, 115.96, 105.66, 104.71, 99.57, 96.20. IR (ATR,  $\text{cm}^{-1}$ ):3031.41, 2924.36, 1348.39, 1168.81, 846.96, 702.27. MS (ESI) m/z: 631 [ $\text{M}^+$ ]. Melting point = >300 °C.

### 3.6. 5,10,15,20-Tetrakis-(4-tosyloxyphenyl)-21H,23H-porphine (18)



A round bottom flask was charged with **15** (5 g, 18 mmol) and propionic acid (62.5 mL). Once the mixture was refluxing and the solid dissolved, pyrrole (1.22 g, 18 mmol) was added, the reaction was heated for 30 minutes with constant stirring. Upon cooling, the reaction mixture was placed into a freezer overnight. Absolute ethanol (20 mL) was added and the reaction was stirred at room temperature for 7 hours. The black reaction mixture was filtered, to yield the crude porphyrin and washed with cold methanol until the washing were clear. The crude porphyrin was removed from the filter, placed into a conical flask and hot methanol was added. The hot methanol solution was filtered to leave a clean purple solid which was washed with hot methanol until the washings ran clear.

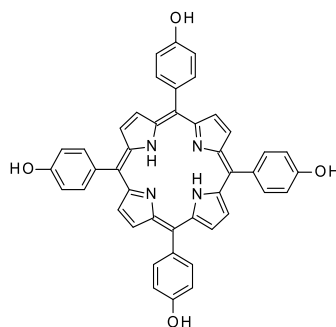
The compound was purified by column chromatography with silica as adsorbent and DCM as eluent to yield **18**, 0.33 g, 1.4 %.

$^1\text{H}$  NMR ( $\text{CDCl}_3$ , 300 MHz,):  $\delta$  8.75 (s, 8H, Pyrrole CH), 8.11 (d,  $J=6$  Hz, 8H, Ar-H), 7.99 (d,  $J=9$  Hz, 8H, Ar-H), 7.49 (d,  $J=9$  Hz, 8H, Ar-H), 7.42 (d,  $J=9$  Hz, 8H, Ar-H), 2.53 (s, 12H,  $\text{CH}_3$ ), -2.94 (s, 2H, Pyrrole NH).  $^{13}\text{C}$  NMR (75 MHz,)  $\delta$  149.64, 132.54, 129.99, 128.73, 120.81, 105.28, 99.99. MS (ESI)  $m/z$ :  $[\text{M}^+]$ .

Melting point  $\Rightarrow$  300 °C.



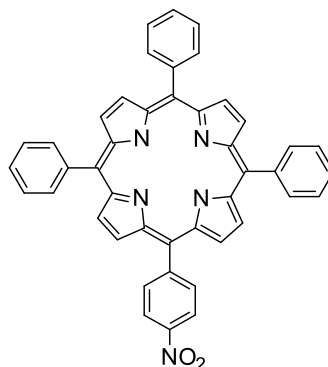
### 3.6.6 5,10,15,20-Tetrakis-(4-hydroxyphenyl)-21H,23H-porphine (19)



To a stirred solution of **18** (0.1 g, 0.077 mmol) in absolute alcohol (12 mL) and dimethylformamide (6 mL) was added potassium hydroxide pellets (0.3 g). The reaction was heated 80 °C with constant stirring for 2 hours. After two hours additional potassium hydroxide (0.3 g) was added to the reaction mixture and the reaction proceeded at 60 °C for a further 2 hours. Upon cooling, the reaction mixture was poured into distilled water (20 mL), treated with 3M HCl (12mL), brine (10 mL) and extracted into chloroform. The organic layer was washed with distilled water (3 x 20 mL), isolated, dried over sodium sulphate and concentrated under reduced pressure. Yielding 0.3 g, 0.57 %.

$^1\text{H}$  NMR (DMSO, 300 MHz,):  $\delta$  8.86 (s, 8H, Pyrrole CH), 8.00 (d,  $J$ = Hz, 8H, Ar-H), 7.20 (d,  $J$ = 9Hz, 8H, Ar-H), -2.91(s, 2H, Pyrrole NH).  $^{13}\text{C}$  NMR (75 MHz,)  $\delta$  158.85, 149.01, 144.68, 142.18, 138.31, 134.59, 131.74, 131.02, 127.74, 126.71, 120.16, 113.27, 113.23, 99.99. IR (ATR,  $\text{cm}^{-1}$ ): 3643.63, 3488.86, 1607.60, 2506.53, 1060.20, 964.40, 798.87. MS (ESI)  $m/z$ : 679 [ $\text{M}^+$ ]. Melting point  $\Rightarrow$ 300 °C.

### 3.6.7 5-(4-Nitrophenyl)-10,15,20-triphenylporphyrin (**20**)

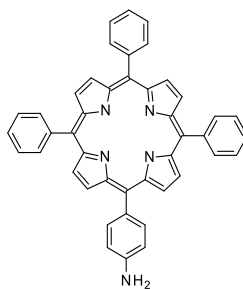


To a solution of **(16)** (0.10g, 0.163 mmol) in trifluoroacetic acid (10 mL) was added sodium nitrite (0.02g, 0.29 mmol). The reaction was stirred at room temperature for 3 minutes, before being poured into water (100 mL). The mixture was extracted dichloromethane (6x 25mL). The organic layer was washed once with saturated sodium bicarbonate and water before being dried over anhydrous sodium sulphate and the solvent evaporated under reduced pressure.

Purified using column chromatography with silica as an adsorbent and DCM as an eluent to yield compound **20**, 0.02 g, 18.62 %.

$^1\text{H}$  NMR ( $\text{CDCl}_3$ , 300 MHz,):  $\delta$  8.87 (s, 8H, Pyrrole CH), 8.77 (d,  $J= 3\text{Hz}$ , 1H, Ar-H), 8.66 (d,  $J= 9\text{Hz}$ , 1H, Ar-H), 8.42 (d,  $J= 9\text{Hz}$ , 2H, Ar-H), 8.26-8.22(m, 6H, Ar-H), 7.80-7.75 (m, 9H, Ar-H), -2.77 (s, 2H, Pyrrole NH).  $^{13}\text{C}$  NMR (75 MHz,)  $\delta$  169.92, 161.98, 158.41, 142.16, 134.57, 127.72, 126.79, 126.70, 123.47, 121.71, 120.15, 99.98. MS (ESI)  $m/z$ : 660 [ $\text{M}^+$ ]. Melting point  $\Rightarrow$ 300 °C.

### 3.6.8 5-(4-Aminophenyl)-10,15,20-triphenyl-21H,23H-porphine (21)



**20** (0.02 g, 0.03 mmol) was added to a solution of tin(II)chloride dihydrate (0.024 g, 0.11 mmol) in 9M HCl (10 mL) and the solution was stirred for 2 hours at 65 °C. The reaction was cooled, poured into distilled water and the pH was adjusted to 8 with concentrated ammonia solution. The resulting suspension was extracted with chloroform (9 x 50 mL) and the residual distilled water was further washed with ethyl acetate (50 mL) and isolated. Both the organic layers were combined, dried with anhydrous sodium sulphate and evaporated under reduced pressure. Purification via column chromatography with silica as adsorbent and DCM as eluent to yield **21**,

$^1\text{H}$  NMR ( $\text{CDCl}_3$ , 300 MHz,):  $\delta$  8.91(s, 2H, NH), 8.86 (s, 8H, Pyrrole CH), 8.77 (t,  $J= 6$  Hz, 1H, Ar-H), 8.66 (d,  $J= 9$  Hz, 2H, Ar-H), 8.23 (d,  $J= 9$  Hz, 6H, Ar-H), 7.80-7.76 (m, 9H, Ar-H), -2.78 (s, 2H, Pyrrole NH). IR (ATR,  $\text{cm}^{-1}$ ): 3312.26, 1555.96, 1471.08, 794.68. MS (ESI)  $m/z$ : 630 [ $\text{M}^+$ ]. Melting point  $\Rightarrow$ 300 °C.

## References

1. Milgram, L.R., *The colours of life - An introductory to the chemistry of porphyrins and related compounds*. 1997: Oxford University Press.
2. Kempa, M.K., Patrycja. Kimbal, Joesph. Rojkiewicz, Marcin. Kus, Piotr. Gryczynski, Zugmunt. Ratuszna, Alicja., *Physicochemical properties of potential porphyrin photosensitizers for photodynamic therapy*. *Spectrochimica Acta Part A: Molecular and Biomolecular Spectroscopy*, 2015. **146**: p. 249-254.
3. Coyle, H., Roberts, *Light, Chemical change and life*. 1988: Open university.
4. Shinokubo, H.O., Atsuhiko, *Marriage of porphyrin chemistry with metal-catalysed reactions*. *Chemical communications*, 2009: p. 1011-1021.
5. Mathews, C.K.A., Kevin G and K.E. Van Holde, *Biochemistry*. 2000: Addison Wesley Longman.
6. Garrett, R.G., Charles M and M. Sabat, *Biochemistry*. 2013, Brooks/Cole Cengage Learning.
7. Dastgheyb, S.S.E., David. M. Composto, Russel. J. Hickok, Noreen. J, *Photo-activated porphyrin in combination with antibiotics: therapies against Staphylococci*. *Journal of photochemistry and photobiology B: Biology*, 2013. **129**: p. 27-35.
8. Ibrahim, H.K., Athena. You, Changjiang. Millard, Philippe. Rosilio, Vweibique. Pansu, Robert. Prognon, Patrice, *Meso-tetraphenyl porphyrin derivative: The effect of structural modification on binding to DMPC liposomes and albumin*. *Journal of Photochemistry and Photobiology A: Chemistry*, 2011. **217**: p. 10-21.
9. Johnson, B.J.T., Chris.R. Gleaves, A. North, Stella.H. malanoski, Anthony.P. Leska. Iwon.A. Archibong, Edikan. Monk, Stormie. M, *Poprhyrin-modified antimicrobial peptide indicators for detection of bacteria*. *Sensing and Bio-sensing*, 2016. **8**: p. 1-7
10. Horvath, O.H., Robert. Valicsek, Zsolt. Lendvay, Gyorgy, *Photophysics and photochemistry of kinetically liable, water-soluble porphyrin complexes*. *Coordination Chemistry Reviews*, 2006. **250**: p. 1792-1803.

11. Matsumoto, J.K., Haruhiko. Okazaki, Shigetoshi. Yasuda, Masahide, *Assistance of human serum albumin to photo-sensitized inactivation of Saccharomyces cerevisiae with axially pyridino-bonded P-porphyrins.* Journal of photochemistry and photobiology B: Biology, 2016. **161**: p. 279-283.
12. Rinco, O.B., J. Douglas, A. Maxwell, A. Henderson, M, Indrelie, K. Wessels, J. Widin, J., *The effect of porphyrin structure in binding to human serum albumin by fluorescence spectroscopy.* Journal of photochemistry and photobiology A: Chemistry, 2009. **208**: p. 91-96.
13. Matsumoto, J.S., T. Hirakawa, K. Yasuda, M., *Water-solubilization of P(V) and Sb(V) Porphyrins and their photobiological applications.* International journal of photoenergy, 2015.
14. Dosselli, R.T., C. Ruiz-Gonzalez, R, De Munari, S. Ragas, X. Sanchez-Garcia, D. Agut, M. Nonell, S. Reddi, E. Gobbo, M., *Synthesis, characterization and photoinduced antibacterial activity of porphyrin-type photosensitizer conjugated to the antibacterial peptide Apidaecin 1b.* Journal of medicinal chemistry, 2013. **56**: p. 4185-1063.

## 4.0 Anthraquinone

### 4.1 Background

Anthraquinones (Figure 4.1) have a polycyclic structure, which contain 14 carbons, including two benzene rings, with two carbonyl groups<sup>[1,2]</sup>.

Anthraquinones are natural ubiquitous compounds<sup>[3]</sup> being one of the largest group of natural pigments of quinoid (Figure 4.2) nature<sup>[4]</sup>, which can be found in plants, fungi, insects and lichens<sup>[4,5]</sup>.

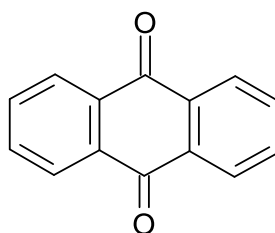


Figure 4.1: Structure of anthraquinone<sup>[2]</sup>

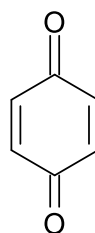


Figure 4.2: Structure of quinoid moiety.

There is a wide range of applications<sup>[6]</sup> for anthraquinones in industry, biology and pharmaceutical chemistry<sup>[7]</sup>. Anthraquinone-containing plants, for example rhubarb and aloe, have been used for more than 4000 years in folk medicine<sup>[6]</sup>. Anthraquinones such as aloe-emodin and emodin (Figure 4.3) are two examples of the bioactive components in rhubarb<sup>[8]</sup>. Aloe-emodin has been shown to have favoured toxicity towards carcinoma cells, whilst it has been reported that emodin is toxic to leukaemia cells after exposure to blue light<sup>[9]</sup>. Emodin is a strong uncoupling agent, the hydroxyl groups at the  $\beta$  position have been shown to be required for the uncoupling of mitochondrial respiration<sup>[4]</sup>.

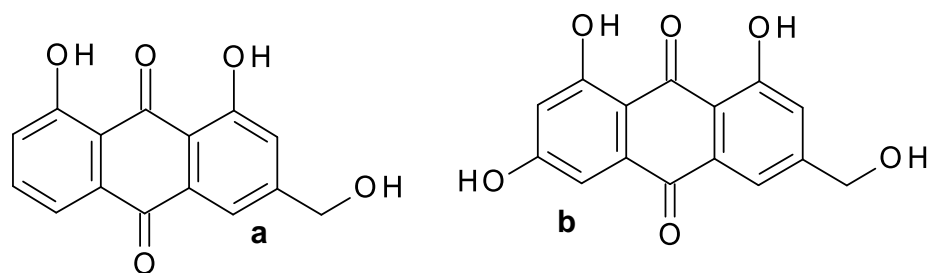


Figure 4.3: Structure of aloemodin (a) and emodin (b)

Anthraquinone derivatives show a wide range of pharmacological activities including laxative, anticancer, antifungal, antibacterial [6]. Phallacinol (Figure 4.4) exhibits antibacterial and antifungal properties, and was first found in *Dermocybe* sp.<sup>[4]</sup>. Singh et al isolated one novel and known anthraquinone from *Saprosma fragrans* and found that these anthraquinones showed prominent antifungal activity<sup>[10]</sup>.

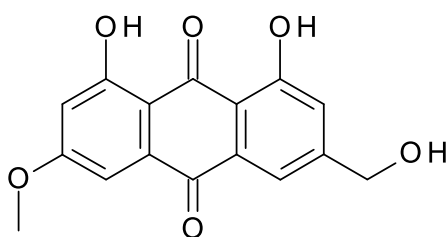
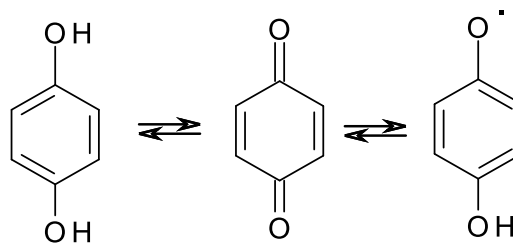


Figure 4.4: Structure of phallacinol<sup>[4]</sup>

Biologically active anthraquinones can be involved in many chemical reactions and biogeochemical processes<sup>[6]</sup>. These chemical and biogeochemical processes, such as reductive degradation of contaminants, are based on the redox potential of the anthraquinones<sup>[6]</sup>. The anthraquinones can either be fully reduced, fully oxidized, or in an intermediate state (see scheme 4.1)<sup>[11]</sup>. Biogeochemical processes such as iron respiration by microorganisms and the nutrient uptake involve naturally occurring quinones<sup>[11]</sup>. Due to the planar structure of anthraquinones, it has been hypothesized that they were able to intercalate to DNA<sup>[8]</sup>. Anthraquinone derivatives are frequently found in motif DNA targeting drugs<sup>[12]</sup>.



Scheme 4.1: Scheme showing the oxidation states possible for anthraquinones<sup>[11]</sup>.

Quinones are known to be involved in reversible electron transfer reactions, these characteristics arise from the resonance-stabilisation of the semiquinone radical intermediates<sup>[11]</sup>. Many anthraquinone derivatives are able to mediate one electron transfer to molecular oxygen to form superoxide radicals and are able to generate reactive oxygen species upon visible light illumination<sup>[13]</sup>. Photoexcited anthraquinones can produce reactive singlet oxygen via two pathways; type I and type II<sup>[13]</sup>. Naturally occurring anthraquinones have been associated with singlet oxygen yields of up to 70 % efficiency dependent on conditions, via a type I pathway<sup>[3]</sup>. The notable chemical characteristic of anthraquinones is their ability to undergo redox cycling to generate reactive oxygen species<sup>[14]</sup>.

#### 4.1.5 Rationale

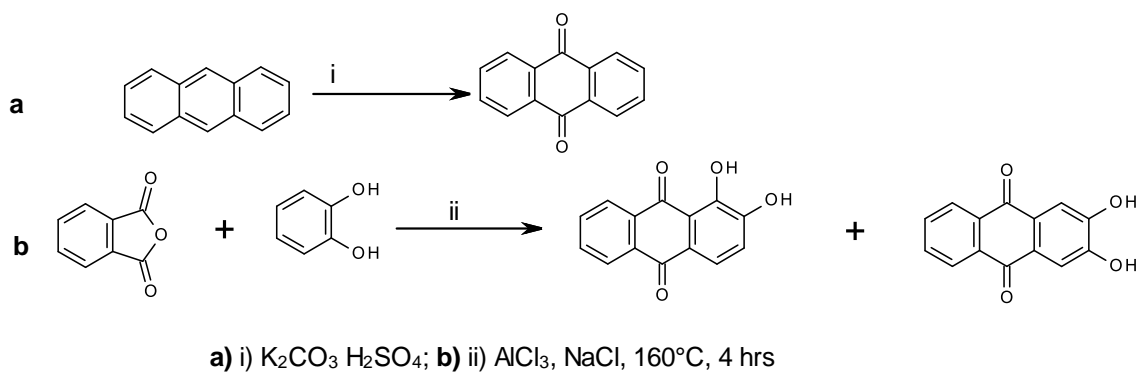
Anthraquinones have been reported to show activity against bacteria and fungi, as well as being able to undergo type I and type II photosensitisation upon illumination. Inspired by this, I decided to make a range of anthraquinone derivatives based upon the anthraquinone moiety shown in table 4.1. The rationale for this was to investigate how the singlet oxygen and microbicidal effects changed with the different derivatives. The singlet oxygen production was collected via spectrophotometric technique decolourisation TPCPD in DCM. In order to determine the antifungal activity of the novel compounds they



were tested against the yeast like fungi, *Candida albicans*, using the EUCAST microdilution method (EUCAST E.DEF 7.3 December 2015).

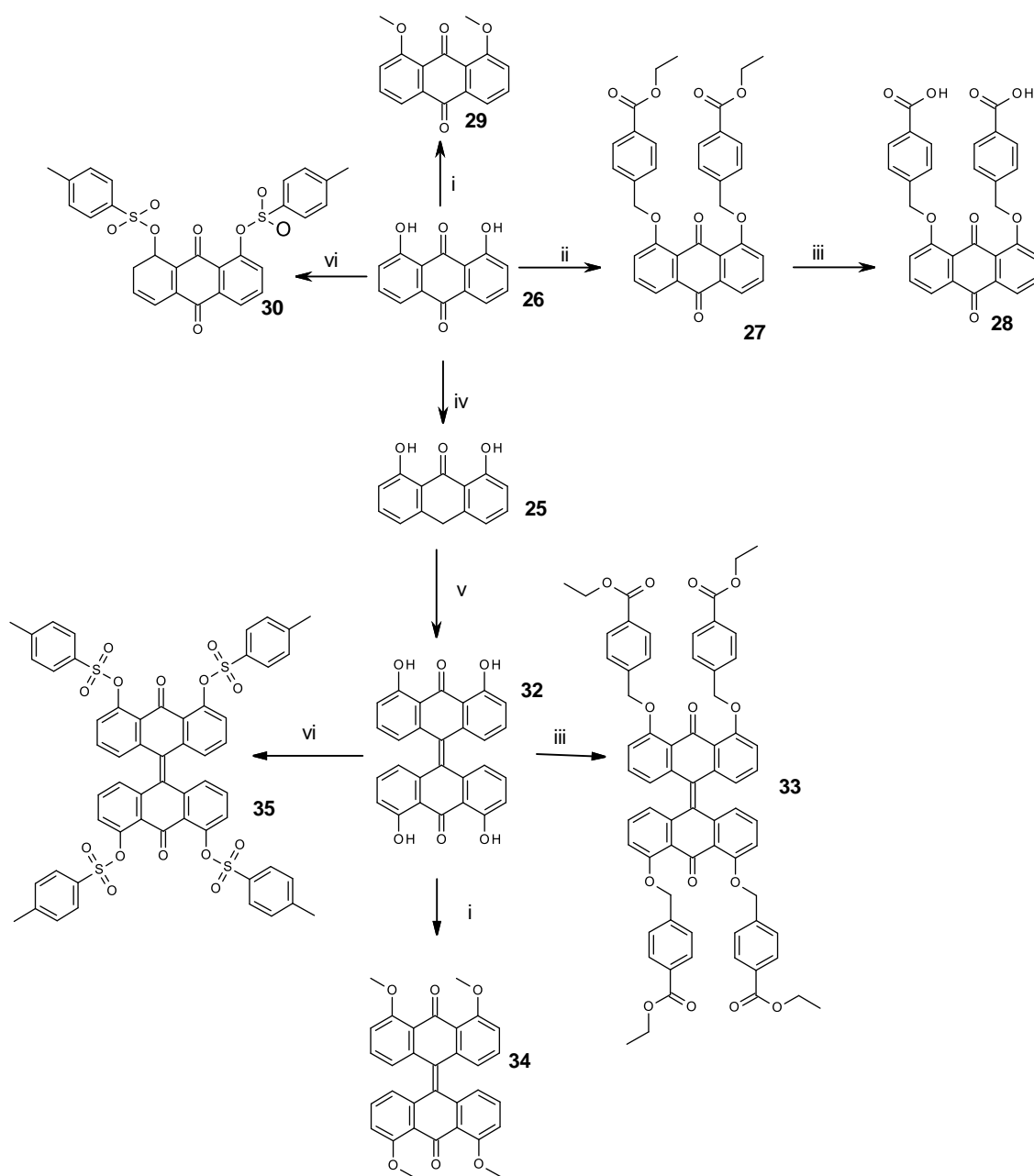
## 4.2 Synthesis

There are two methods in which anthraquinones can be synthesised (see scheme 4.2); Friedel-Crafts reaction of benzene and phthalic anhydride in the presence of  $\text{AlCl}_3$  or by oxidising anthracene<sup>[1]</sup>.



Scheme 4.2: Synthetic route showing the two possible synthesis routes **a**) oxidation of anthracene, **b**) Friedel-Crafts condensation reaction<sup>[2]</sup>

Scheme 4.3 shows the synthetic route for the synthesis of all the anthraquinone derivatives



i)  $K_2CO_3$ , MeI, MEK/DMSO, 15 hr,  $80^\circ C$ ; ii) Ethyl 4-(bromomethyl)benzoate,  $K_2CO_3$ , DMF,  $60^\circ C$ , 72 hr;  
 iii) KOH, EtOH, THF,  $80^\circ C$ , 5.5 hr; iv)  $SnCl_2$ , HCl, AcOH, reflux, 6 hrs; v) *t*-BuOK, DMF, reflux, 20 hrs;  
 vi) *p*-Ts-Cl, DCM,  $Et_3N$ , MeCN, reflux, 5 hr.

Scheme 4.3: Synthetic route for the synthesis of the anthraquinone derivatives

To expand the synthesis was accomplished by addition, reduction, and enolate reactions on 1,8-dihydroxyanthraquinone. 1,8-dihydroxyanthraquinone was reduced using tin(II)chloride to yield 1,8-dihydroxy-10H-anthracen-9-one, which was isolated at the pump. The  $^1\text{H}$  analysis of 1,8-dihydroxy-10H-anthracen-9-one is shown below in figure 4.5 and clearly confirms the structure of the reduced compound. The spectrum shows 10H in the expected regions and with the correct splitting and integrations. The 2H signal at 4.34 ppm can be attributed to the reduced  $\text{CH}_2$  in the centre fused ring. The aromatic region clearly shows 6 aromatic protons between 6.88-7.51 ppm. The mass spectrum of **32** can also show the reduction with a signal at 227.1  $[\text{M}^+]$  which can be seen in figure 4.6.

1,8-dihydroxyanthraquinone was reacted with **24** in the presence of potassium tert-butoxide and under nitrogen to yield 1,8-dihydroxybianthrone (**32**) in 7.24 % yield. Once again the  $^1\text{H}$  analysis, shown in figure 4.7, confirms the correct structure with an increase in the integration of aromatic protons, and the disappearance of the  $\text{CH}_2$  peak. There is also an increase in the OH protons from 2 to 4.

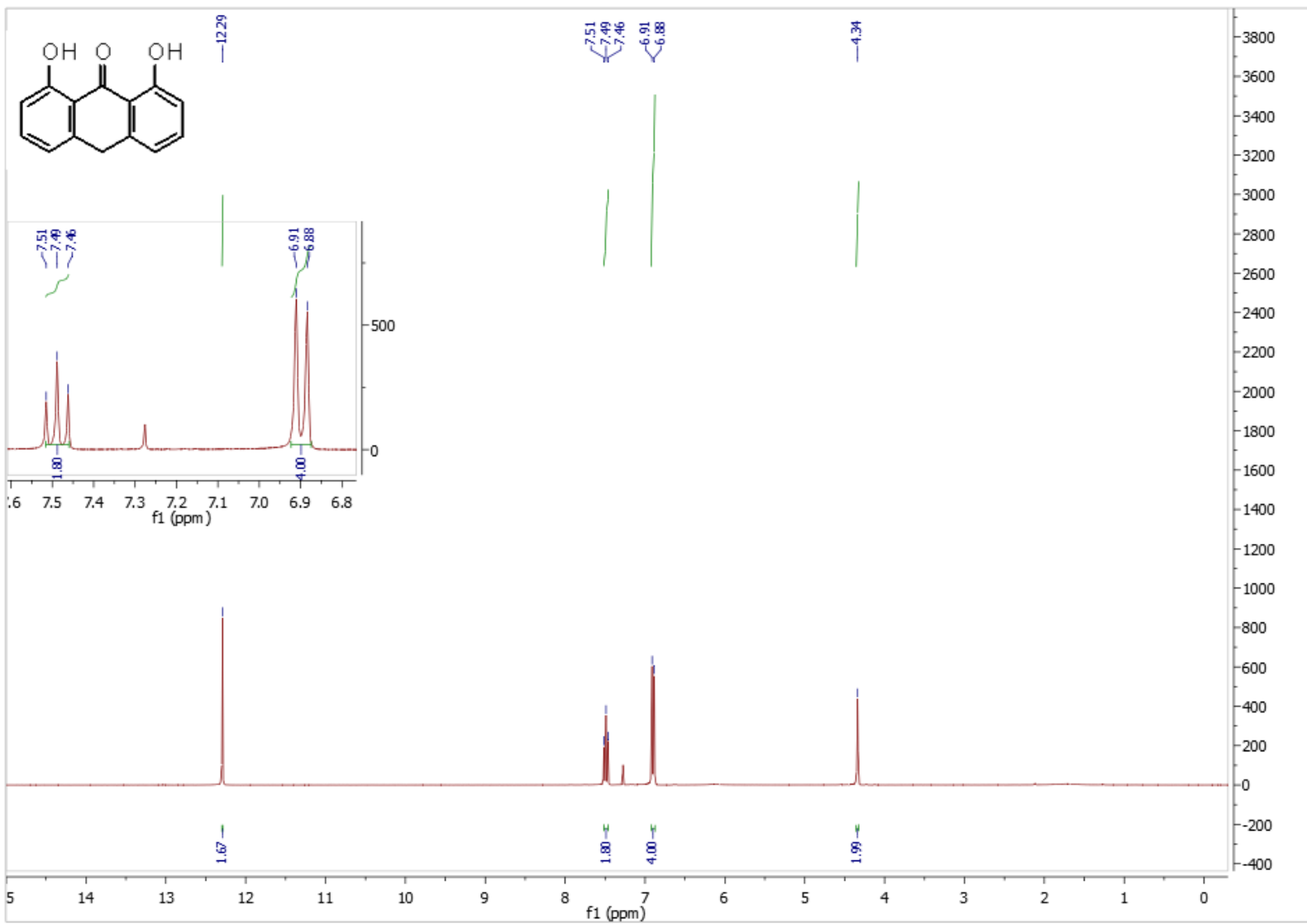


Figure 4.5: <sup>1</sup>H NMR of 26

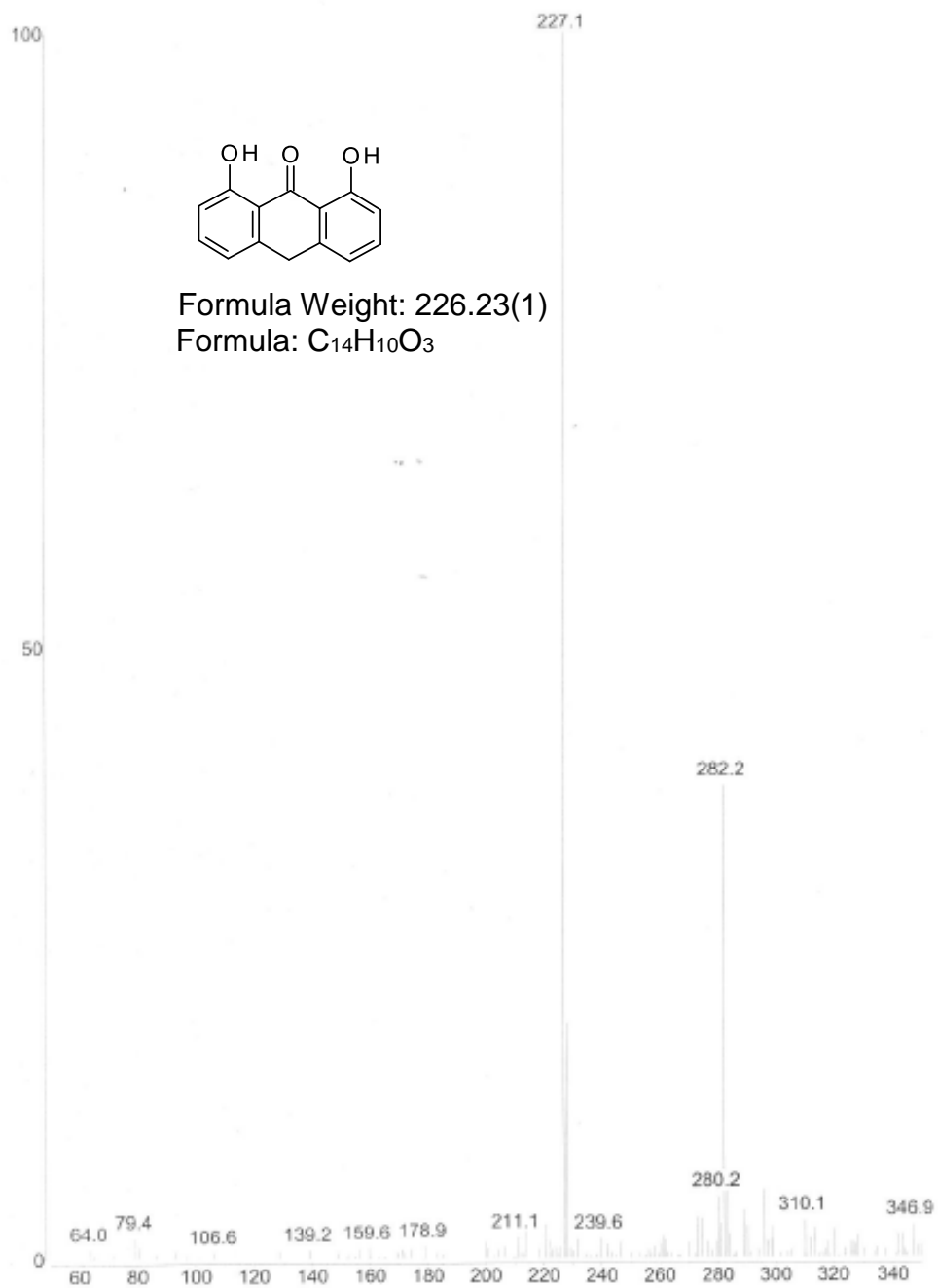


Figure 4.6: Mass spectrum of 26

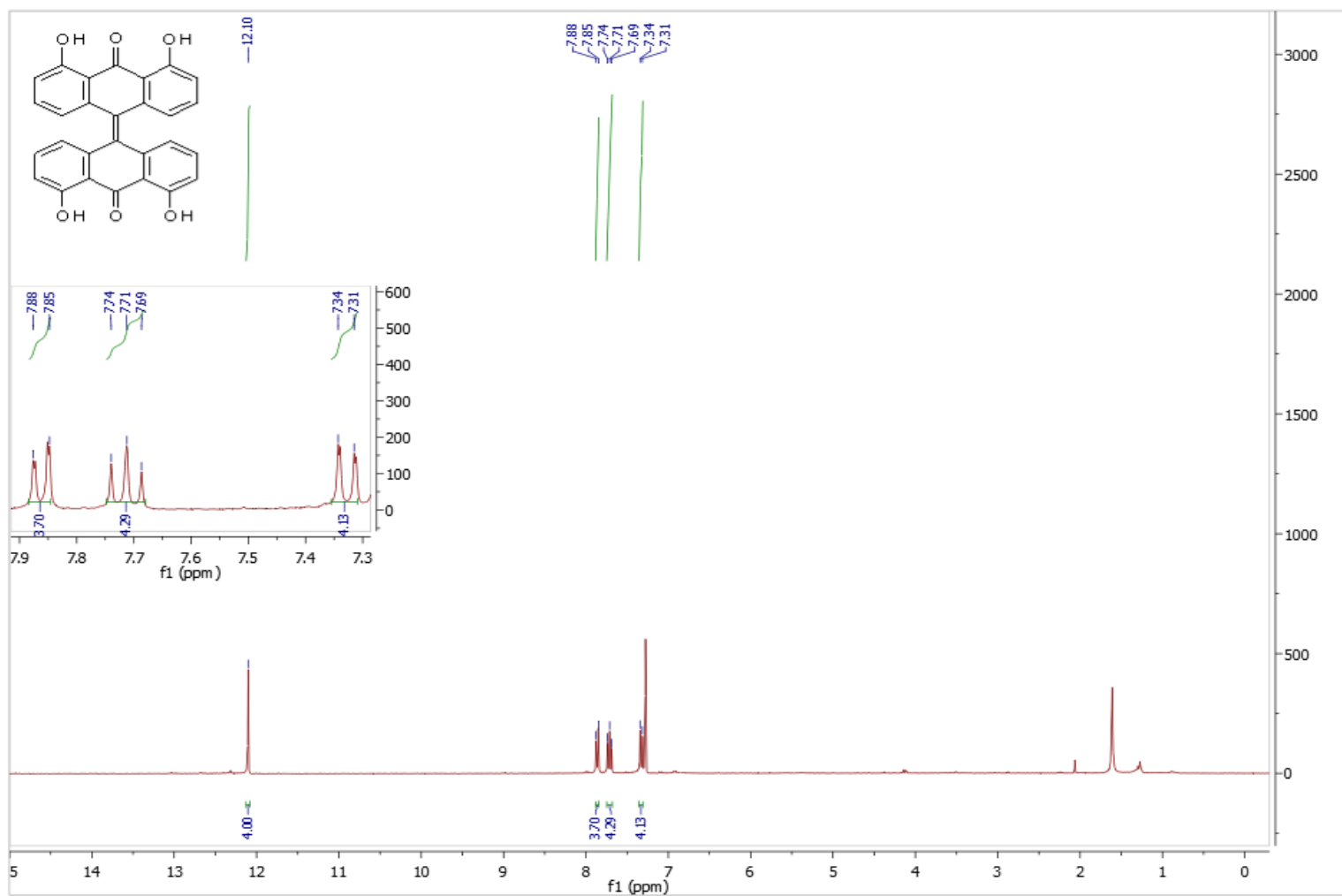


Figure 4.7 <sup>1</sup>H NMR of **32**

One substituted anthraquinone was done in a two-step synthesis (shown in scheme 4.3). 1,8-Dihydroxyanthraquinone was reacted with ethyl-(4-bromomethyl)benzoate in the presence of  $K_2CO_3$  to produce 1,8-bis(ethylbenzoate)-9,10-anthraquinone. This was then cleaved under basic conditions using KOH to produce 1,8-(diethyl benzoic acid)anthraquinone. Following  $^1H$  analysis, it is clear to see the cleavage of the ester to leave the COOH. The  $^1H$  NMR spectra of the two compounds (figures 4.8 and 4.9) clearly highlights the removal of the ester group.

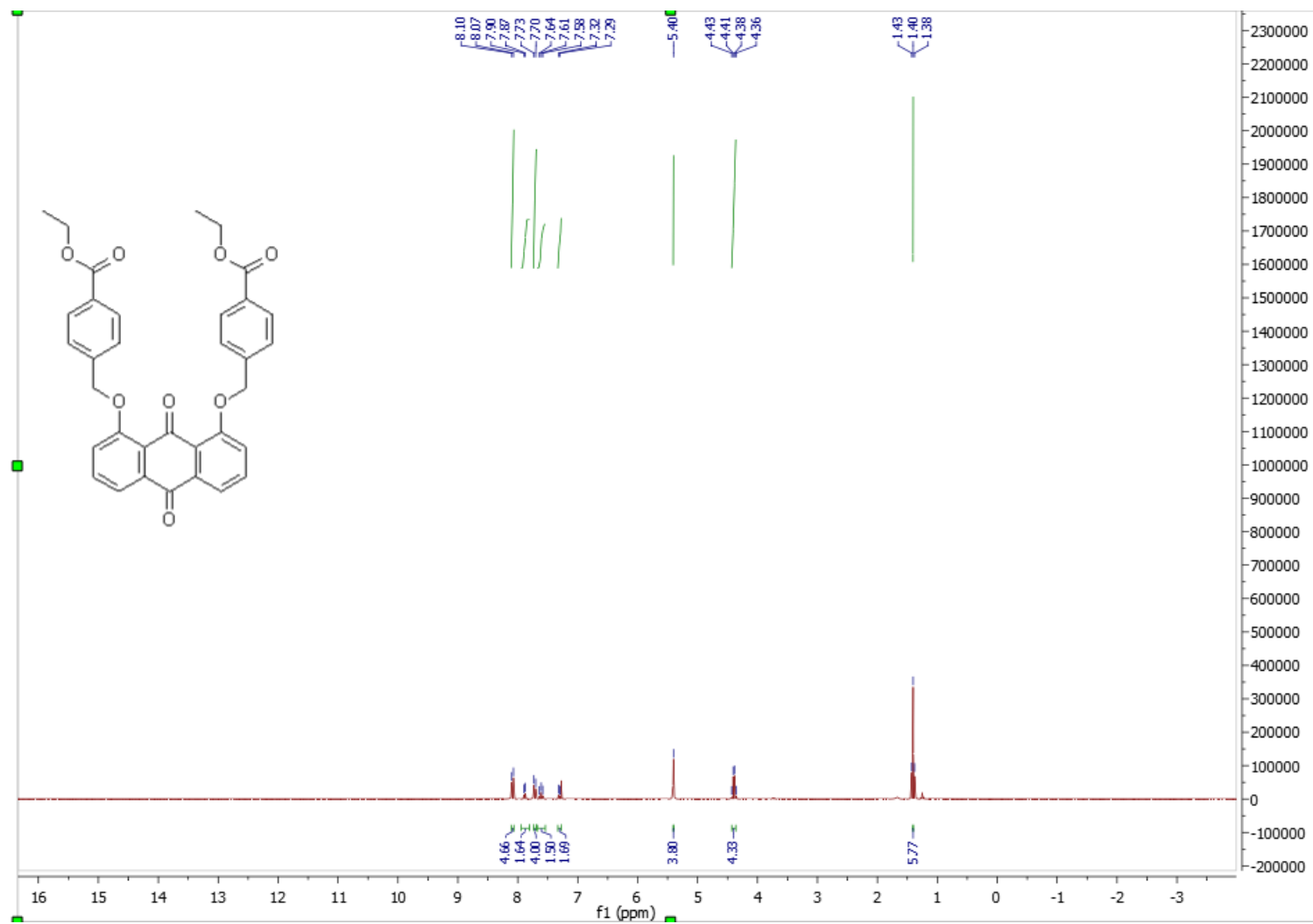


Figure 4.8 HNMR spectra for **27** ran in  $\text{CHCl}_3$



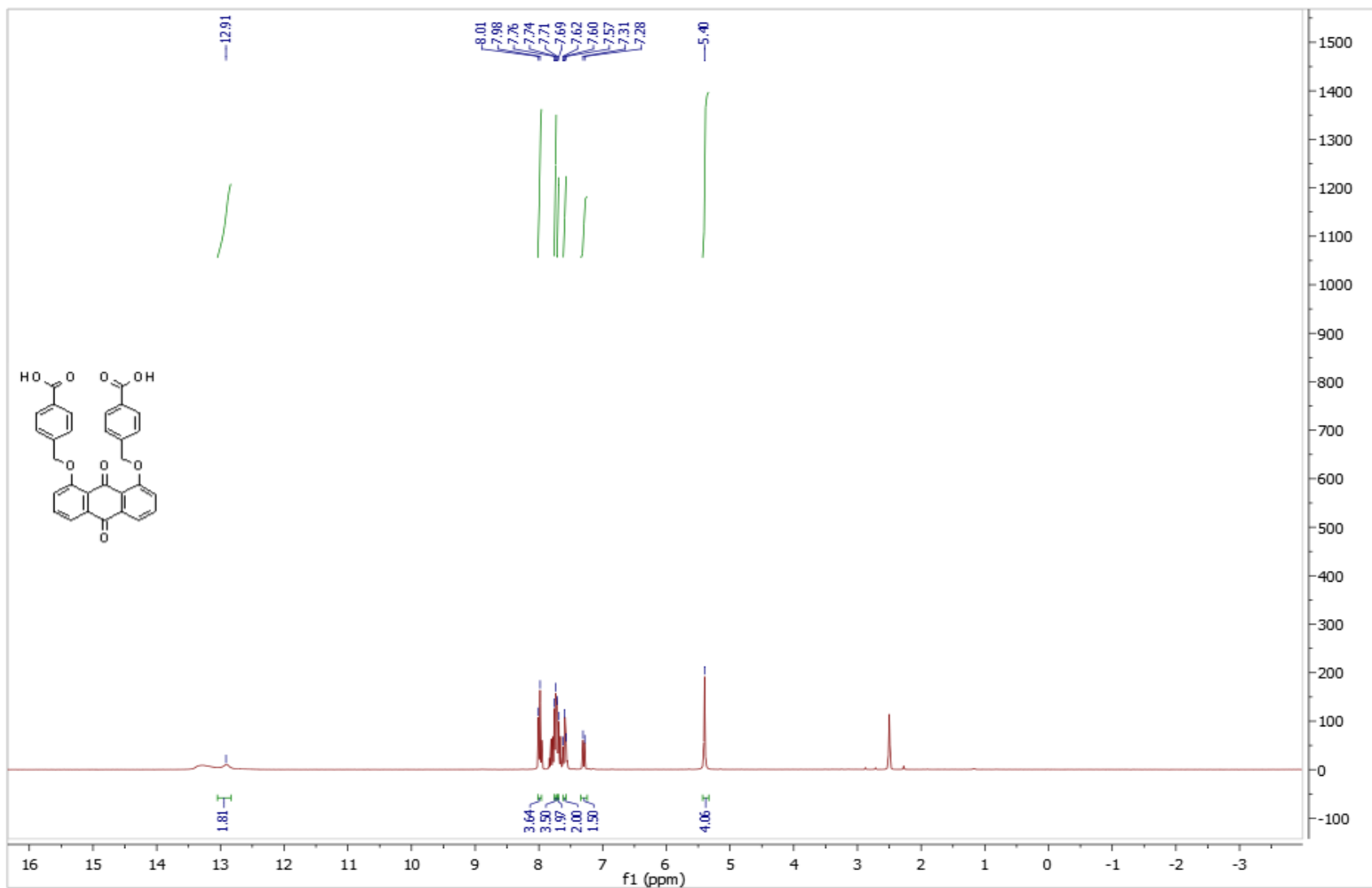


Figure 4.9 HNMR spectra for **28** ran in DMSO. Note the absence of the CH<sub>2</sub> and CH<sub>3</sub> due to cleavage.

### 4.3 Singlet Oxygen

The same methodology was used as on page 33. Anthrone, anthraquinone and bianthrone were the standards used dependent upon the structure of the derivative.

As it can be seen from table 4.1 below the hydroxy derivatives were the highest singlet oxygen produces when compared to their standards.

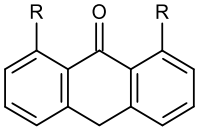
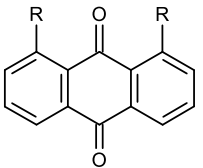
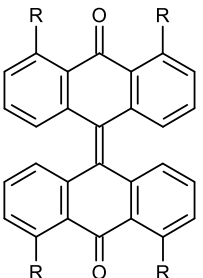
Compound	Structure	R group	cLog P	Absorption (nm)	Relative <sup>1</sup> O <sub>2</sub> Yield	Minimum inhibitory concentration (mg/mL)
23		H	3.49	265	1	*
24		OH	3.38	256	15.4	0.156
25		H	3.67	251	1	*
26		OH	3.13	253	20	0.039
28		OBnCO <sub>2</sub> H	6.70	256	1	*
29		OMe	3.69	254	1.33	*
30		OTs	6.40	251	0.73	*
31		H	7.69	228	1	*
32		OH	6.62	223	10	0.078
33		OBnCO <sub>2</sub> Et	10.23	256	2.22	*
34		OMe	7.72	254	2.67	*
35		OTs	9.82	235	4	*
Fluconazole	-	-	-	-	-	0.156

Table 4.1: Photophysical and growth inhibition for the anthraquinone derivatives. Minimum inhibition concentration shown for 20 minutes exposure to blue light. \* indicated growth was observed at the maximum concentration tested, 10 mg/mL. cLog P is a partition coefficient of compound between aqueous and lipophilic phases and was calculated using molinspiration.

## 4.4 Assay for Growth

The same methodology was used as on page 35.

### Results

**All anthraquinones, except the hydroxyl derivatives, had no effect on *C.albicans***

In order to see if the anthraquinone derivatives had an effect on growth of *C.albicans*, cells were exposed to a range of concentrations, 0.0195 mg/mL to 10 mg/mL, in the absence and presence of blue light. Visual inspection of the plates after 24 hr incubation at 34°C, table 4.1 and figure 4.10, showed compounds 23,25,28,29,30,31,33,34,35 have no effect on the growth of *C. albicans*, when compared to the control, at the concentrations tested. Compounds 24,26,32 did show an effect against the growth of *C.albicans*. In the presence of the antifungal agent fluconazole, an effect was observed with an MIC determined to be 0.156 mg/mL.

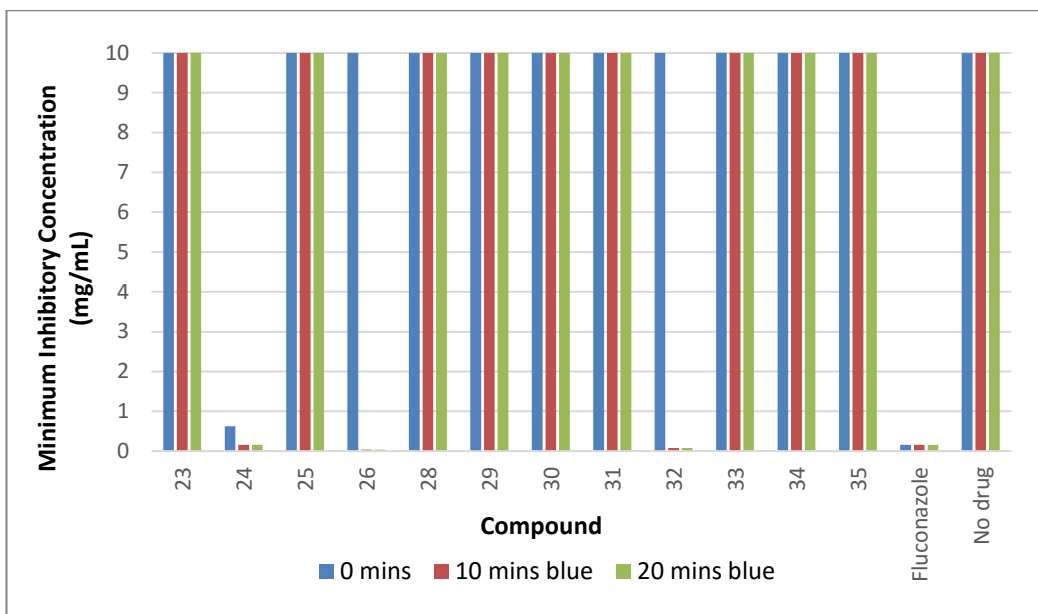


Figure 4.10: Comparison of compounds 23-35 with fluconazole on *C.albicans*. The MIC was obtained according to the EUCAST method in the absence and presence of blue light. The maximum concentration tested was 10 mg/mL.

## 4.5 Discussion

The synthesis of the anthraquinones was straightforward and required harsh or unusual methodologies as shown in scheme 4.3. Compound **24** was the result of the reduction of **26** with an excellent yield. Compound **32** was synthesised through an enolate reaction with compounds **24** and **26**. Compounds **27,29,30,33,34,35** were a result of substitution reactions with either tosyl chloride, methyl iodide or ethyl(4-bromomethyl)benzoate, onto the corresponding 1,8-dihydroxyanthraquinone or 1,8-dihydroxybianthrone.

The photophysical properties of the compounds **23-35** can be seen in table 4.1. It is clear to see all these compounds have an absorption spectra maxima in the UV region 223 – 265 nm. The reduction of one of the carbonyl groups causes an increase in the absorption spectra, in the case of compound **23** when compared to compound **25** there is an increase of 14 nm this could be a result of the reduction in the polarity of the molecule.

Due to the anthraquinones have three different structures, the singlet oxygen and growth assay results will be discussed separately below.

### Anthrone

The singlet oxygen yield of compound **24** showed a 15.4-fold increase in when compared to compound **23**. Indicating that the addition of the two hydroxy groups increases the singlet oxygen production. The growth inhibition data for the anthrone compounds showed activity for 1 compound, **24**. Compound **24** showed antimicrobial activity against *C.albicans* when used without illumination with blue light with an MIC of 0.652 mg/mL, suggesting this compound has an antifungal effect on it own. When compound **24** was tested in combination with blue light the MIC value showed a 4 fold decrease. When compared to

fluconazole, which had an MIC value of 0.156 mg/mL, compound **24** shows promising antimicrobial activity against *C.albicans*.

### Anthraquinone

The singlet yield of compound **26** shows a 20-fold increase when compared to compound **25**, indicating again that the addition of the hydroxy groups increasing the ability to produce singlet oxygen. Compound **29** also saw an increase in the singlet oxygen yield however a 1.33-fold increase was observed. Compound **28** saw singlet oxygen yield that was equal to compound **26**. Compound **30** saw a 0.733-fold decrease in the singlet oxygen yield when compare to compound **26**.

The growth inhibition data of the anthraquinones showed only one compound had an antimicrobial effect on *C.albicans*, compound **26**. When compound **26** was illuminated with blue light an MIC of 0.039 mg/mL was observed, this was a lower MIC value than fluconazole which had a value of 0.156 mg/mL. No other anthraquinone compound showed an microbicidal effect on *C.albicans*.

### Bianthrone

The singlet oxygen of compound **32** showed a 10-fold increase when compared to compound **31**, once again suggesting that the addition of the hydroxy groups increases the production of singlet oxygen. Compound **35** showed an 4-fold increase when compared to compound **31**. Compounds **33** and **34** showed a 2.22 and 2.67 fold increase respectively.

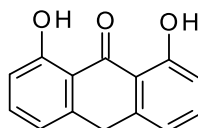
The growth inhibition data for the bianthrone showed only one compound had an antimicrobial effect on *C.albicans*, compound **32**. When compound **32** was illuminated with blue light an MIC value of 0.078 mg/mL was

observed, this was lower than fluconazole which had a value of 0.156 mg/mL.

No other bianthrone compounds showed a microbicidal effect.

## 4.6 Experimental

### 4.6.1 1,8-dihydroxy-10H-anthracen-9-one (24)



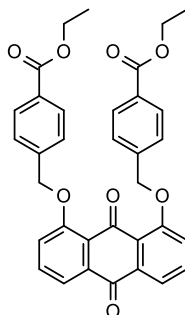
Tin (II) chloride dihydrate (20.14 g, 19.12 mmol) in concentrated hydrochloric acid (110 mL) was added to a solution of 1,8-Dihydroxyanthraquinone (2.4 g, 10mmol) in acetic acid (200 mL). The solution was heated at 120 °C for 8 hours. The reaction was then poured into ice water and left overnight. The precipitate was isolated and dried at the pump to yield **24** 1.2 g, as a pale yellow solid.

Yielding 1.2 g, 53 %.

$^1\text{H}$  NMR ( $\text{CDCl}_3$ , 300 MHz):  $\delta$  12.29 (s, 2H, OH), 7.49 (t,  $J=6\text{Hz}$ , 2H, Ar-H), 6.90 (d,  $J=9\text{ Hz}$ , 4H, Ar-H) 4.34 (s, 2H, CH<sub>2</sub>).  $^{13}\text{C}$  NMR (75 MHz,  $\text{CDCl}_3$ )  $\delta$  194.12, 162.95, 141.93, 136.20, 118.72, 115.83, 115.56, 32.82. IR ((ATR,  $\text{cm}^{-1}$ ): 2971.03, 1630.64, 1476.37, 1370.19, 1024.23, 871.69, 730.84. MS (ESI)  $m/z$ : 227.1 [ $\text{M}^+$ ].

Melting point = 175-177 °C

### 4.6.2 1,8-bis(ethylbenzoate)-9,10-anthraquinone (27)



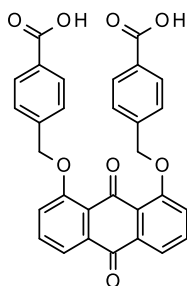


A round bottom flask was charged with 1,8-Dihydroxyanthraquinone (2.40 g, 10 mmol), *N,N*-dimethylformamide (60 mL), potassium carbonate (4.14 g, 30 mmol) and 4-bromoethylbenzoate (6.08 g, 25 mmol). The reaction mixture was heated at 60°C for 72 hours. Once cooled to room temperature, the reaction mixture was poured into cold water. The product was extracted into ethyl acetate (2 x 20mL), dried over sodium sulphate and the solvent was evaporated under pressure.

Purification via column chromatography with silica as adsorbent and 7:3 CHCl<sub>3</sub>:EtOAc as eluent to yield **27**, 2 g, 35% %.

<sup>1</sup>H NMR (CDCl<sub>3</sub>, 300 MHz): δ 8.08 (d, J= 9 Hz, 4H, Ar-H), 7.88 (d, J= 9Hz, 2H, ar-H). 7.22 (d, J= 9Hz, 4H, Ar-H), 7.61 (t, j= 9 Hz, 2H, Ar-H), 7.30 (d, J= 9 Hz,2H, Ar-H), 5.40 (s, 4H, CH<sub>2</sub>), 4.40 (q, J= 9 Hz, 4H, CH<sub>2</sub>), 1.40 (t, J= 9Hz, 6H, CH<sub>3</sub>)  
MS (ESI) m/z: 564 [M<sup>+</sup>].

#### 4.6.3 1,8-bis (ethyl benzoic acid)-9,10-anthracenedione (**28**)

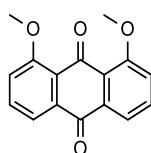


**27** (2 g, 4.4 mmol), ethanol (7.5 mL) and tetrahydrofuran (5 mL) was place into a two-necked 100 mL round bottom flask. The mixture was refluxed at 100°C. To the solution was gradually added powdered potassium hydroxide (0.53 g, 9 mmol). The mixture was then refluxed for 5.5 hours and left to cool. Once cooled to room temperature, the mixture was evaporated to dryness. The product was extracted with water and dichloromethane. Hydrochloric acid (8.5 mL) was added to the aqueous layer causing a precipitate to form which was isolated at the pump. The solid was the dissolved using ethyl acetate, dried over

sodium sulphate and the solvent was evaporated under pressure. Yielding 0.44 g, 39.2 %.

$^1\text{H}$  NMR (DMSO, 300 MHz):  $\delta$  12.91 (s, 1H, COOH), 8.00 (d, J= 9 Hz, 4H, Ar-H), 7.75 (d, J= 6 Hz, 4H, Ar-H), 7.70 (d, J= 6 Hz, 2H, Ar-H), 7.60 (t, J=9Hz, 2H, Ar-H), 7.29 (d, J=9 Hz, 4H, Ar-H), 5.40 (s, 4H, CH<sub>2</sub>).  $^{13}\text{C}$  NMR (75 MHz, DMSO)  $\delta$  188.40, 182.39, 107.58, 11.87, 159.52, 142.01, 136.61, 135.37, 132.71, 130.40, 129.93, 127.17, 117.15, MS (ESI) m/z: 509 [M<sup>+</sup>]. Melting point = 183-186°C.

#### 4.6.4 1,8-dimethoxy-9,10-anthracenedione (29)



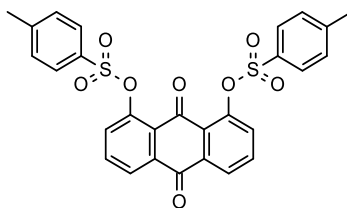
Potassium carbonate (4.32 g, 31.22 mmol) and Methyl iodide (5.9 g, 41.63 mmol) were added to a solution of 1,8-dihydroxyanthraquinone (2.5 g, 10.41 mmol) in 3:1 methyl ethyl ketone: DMSO (50 mL). The solution was refluxed for 15 hours. Once cooled to room temperature, 25 mL of 1 M HCl was added followed by 200 mL of water. The organic layer was extracted with toluene and washed with 3x 200 mL of water, followed by 2x200mL of NaHCO<sub>3</sub>. Finally washed with 200 mL of brine. Dried over sodium sulphate and solvent was evaporated.

The impure product was dissolved in toluene and washed with 5M NaOH. Solid was isolated at the pump. The toluene was separated from the water and dried over sodium sulphate and evaporated under pressure. Yielding 0.36 g, 4.30 %

$^1\text{H}$  NMR (CDCl<sub>3</sub>, 300 MHz):  $\delta$  7.85 (d, J= 9 Hz, 2H, Ar-H), 7.65 (t, J= 9 Hz, 2H, Ar-H), 7.31 (d, J= 9Hz, 2H, Ar-H), 4.02 (s, 6H, CH<sub>3</sub>).  $^{13}\text{C}$  NMR (75 MHz, CDCl<sub>3</sub>)  $\delta$  183.78, 178.16, 159.12, 134.76, 134.51, 123.95, 119.37, 118.56. IR (ATR, cm<sup>-1</sup>

<sup>1</sup>): 2840.63, 1659.62, 1465.60, 1314.00, 899.22. MS (ESI) m/z: 269 [M<sup>+</sup>]. Melting point = 195-197°C.

#### 4.6.5 1,8-bis(tosyloxy)-9,10-anthraquinone (30)

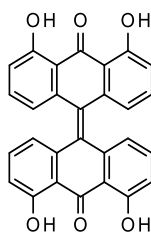


A round bottom flask was charged with 1,8-dihydroxyanthraquinone (1.21 g, 5 mmol), acetonitrile (50 mL), triethylamine (5mL) and Tosyl chloride (2.4g , 12.5 mmol). The mixture was refluxed for 5 hours. MeCN was removed via rotary evaporation and DCM was added. The mixture was washed with water and the organic layer was dried over sodium sulphate. The solvent was evaporated under pressure. The resulting solid was dissolved in hot DCM and petroleum ether was added and cooled in an ice bath. Yielding 1 g, 36 %

<sup>1</sup>H NMR (CDCl<sub>3</sub>, 300 MHz): δ 8.20 (d, J= 9 Hz, 2H, Ar-H), 7.94 (d, J= 9 Hz, 4H, Ar-H), 7.73 (t, J= 9Hz, 2H, Ar-H), 7.67 (d, J= 9 Hz, 4H, Ar-H), 2.44 (s, 6H, CH<sub>3</sub>).

<sup>13</sup>C NMR (75 MHz, CDCl<sub>3</sub>) δ 183.22, 179.02, 146.79, 146.44, 136.53, 134.89, 132.08, 130.68, 128.91, 127.62, 126.19. IR (ATR, cm<sup>-1</sup>): 3032.72, 1683.37, 1588.73, 1220.22, 847.54, 728.38. MS (ESI) m/z: 549 [M<sup>+</sup>]. Melting point = 184-186 °C.

#### 4.6.6 1,8-dihydroxybianthrone (32)

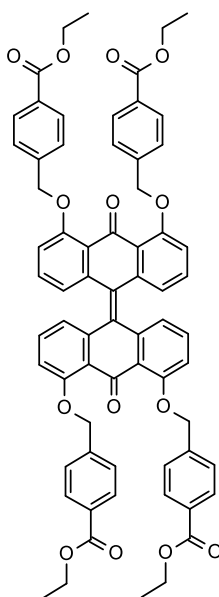


A 100 mL round bottom flask was charged with **24** (0.678 g, 3 mmol), 1,8-dihydroxyanthraquinone (0.72 g, 3 mmol) , DMF (6 mL) and potassium tert-

butoxide (0.056 g, 0.5 mmol). The mixture was refluxed under nitrogen for 20 hours. Ice water was added to quench the reaction. The pH was adjusted to 6 using dilute HCl, upon this, a green precipitate was produced. Ethyl acetate was added to dissolve the precipitate and the mixture was filtered at the pump. The ethyl acetate was washed with water, dried over sodium sulphate, and evaporated under pressure. The solid produced was washed with methanol until pure. Yielding 0.1 g, 7.42 %

$^1\text{H}$  NMR ( $\text{CDCl}_3$ , 300 MHz):  $\delta$  12.10 (s, 4H, OH), 7.86 (d,  $J=9$  Hz, 4H, Ar-H), 7.71 (t,  $J=9$  Hz), 7.33 (d,  $J=9$  Hz, 4H, Ar-H).  $^{13}\text{C}$  NMR (75 MHz,  $\text{CDCl}_3$ )  $\delta$  193.08, 181.75, 162.53, 137.30 133.57, 124.67, 120.08, 115.84. MS (ESI)  $m/z$ : 449 [ $\text{M}^+$ ].

#### 4.6.7 1,8-bis(ethylbenzoate)bianthrone (33)

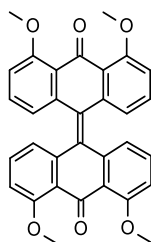


A round bottom flask was charged with **32** (1 g, 2.23 mmol), *N,N*-dimethylformamide (15 mL), potassium carbonate (1.658 g, 12 mmol) and 4-bromoethylbenzoate (2.43 g, 25 mmol). The reaction mixture was heated at 60 °C for 96 hours. Once cooled to room temperature, the reaction mixture was poured into cold water. The product was extracted into ethyl acetate (2 x 10

mL), dried over sodium sulphate and the solvent was evaporated under pressure. Yielding 0.2 g, 8.17 %

$^1\text{H}$  NMR ( $\text{CDCl}_3$ , 300 MHz):  $\delta$  8.09 (d,  $J = 9$  Hz, 8H, Ar-H), 7.87 (d,  $J = 9$  Hz, 4H, Ar-H), 7.72 (d,  $J = 9$  Hz, 8H, Ar-H), 7.61 (t,  $J = 9$  Hz, 4 H, Ar-H), 7.29, (d,  $J = 9$  Hz, 4H, Ar-H), 5.40 (s, 8H,  $\text{CH}_2$ ), 4.40 (q,  $J = 9$  Hz, 8H,  $\text{CH}_2$ ), 3.40 (t,  $J = 9$  Hz, 12H,  $\text{CH}_3$ ). MS (ESI)  $m/z$ : 1098 [ $\text{M}^+$ ].

#### 4.6.8 1,8-dimethoxy-bianthrone (34)



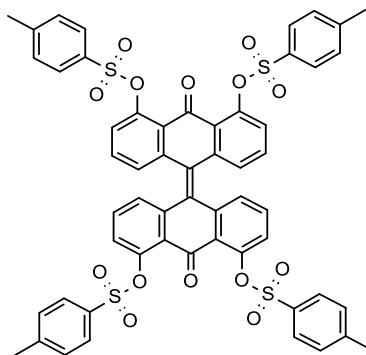
Potassium carbonate (0.12 g, 0.88 mmol) and Methyl iodide (0.156 g, 1.1 mmol) were added to a solution of **32** (1 g, 0.2 mmol) in 3:1 methyl ethyl ketone:

DMSO (25 mL). The solution was refluxed for 15 hours. Once cooled to room temperature, 10 mL of 1 M HCl was added followed by 100 mL of water.

Organic layer was extracted with toluene and washed with 3 x 100 mL of water, followed by 2 x 100 mL of  $\text{NaHCO}_3$ . Finally washed with 100 mL of brine. Dried over sodium sulphate and solvent was evaporated. Yielding 0.011 g, 2.48 %

$^1\text{H}$  NMR ( $\text{CDCl}_3$ , 300 MHz):  $\delta$  7.78 (d,  $J = 9$  Hz, 4H, Ar-H), 7.57 (t,  $J = 9$  Hz, 4H, Ar-H), 7.24 (d,  $J = 9$  Hz, 4H, Ar-H), 3.95 (s, 12H,  $\text{CH}_3$ ).  $^{13}\text{C}$  NMR (75 MHz,  $\text{CDCl}_3$ )  $\delta$  199.12, 135.22, 134.84, 134.51, 127.27, 123.94, 118.57, 104.89, 104.48. IR (ATR,  $\text{cm}^{-1}$ ): 2839.84, 1660.50, 1584.42, 1277.78, 840.70, 741.58. MS (ESI)  $m/z$ : 505 [ $\text{M}^+$ ].

#### 4.6.9 1,8-bis(tosyloxy)bianthrone (35)



A round bottom flask was charged with **32** (0.36 g, 0.8 mmol) acetonitrile (15 mL), triethylamine (1.5 mL) and Tosyl chloride (0.76 g, 3.98 mmol). The mixture was refluxed for 5 hours. MeCN was removed via rotary evaporation and DCM was added. Mixture was washed with water and DCM layer was dried over sodium sulphate. The solvent was evaporated under pressure. The resulting solid was dissolved in hot DCM and petroleum ether was added and cooled in an ice bath. Yielding 0.08 g, 9.38 %

$^1\text{H}$  NMR ( $\text{CDCl}_3$ , 300 MHz):  $\delta$  8.20 (d,  $J = 9$  Hz, 4H, Ar-H), 7.94 (d,  $J = 9$  Hz, 8H, Ar-H), 7.73 (t,  $J = 9$  Hz, 4H, Ar-H), 7.35 (d,  $J = 9$  Hz, 8H, Ar-H), 2.44 (s, 12H,  $\text{CH}_3$ ).  
 $^{13}\text{C}$  NMR (75 MHz,  $\text{CDCl}_3$ )  $\delta$  148.50, 146.80, 145.42, 135.52, 134.91, 132.09, 130.64, 129.76, 129.74, 128.90, 127.63, 126.17, 21.65. IR (ATR,  $\text{cm}^{-1}$ ): 2949.23, 1682.86, 1588.60, 121.62, 847.35, 727.76. MS (ESI)  $m/z$ : 1066 [ $\text{M}^+$ ]. Melting point =  $^\circ\text{C}$ .

## References

1. Langdon-Jones, E.E. and S.J.A. Pope, *The coordination chemistry of substituted anthraquinones: Developments and applications*. Coordination Chemistry Reviews, 2014. **269**(Supplement C): p. 32-53.
2. Baqi, Y., *Anthraquinones as a privileged scaffold in drug discovery targeting nucleotide-binding proteins*. Drug Discovery Today, 2016. **21**(10): p. 1571-1577.
3. Wainwright, M., *Photosensitisers in Biomedicine (1)*. 2009, Hoboken, GB: Wiley.
4. Gessler, N.N., A.S. Egorova, and T.A. Belozerskaya, *Fungal Anthraquinones*. Applied Biochemistry and Microbiology, 2013. **49**(2): p. 85-99.
5. Dave, H. and L. Ledwani, *A review on anthaquinones isolated from Cassia species and their applications*. Vol. 3. 2012. 291-319.
6. Malik, E.M.a.M., C. E., *Anthraquinones As Pharmacological Tools and Drugs*. Med. Res. Rev., 2016. **36**: p. 705-748.
7. Al-Otaibi, J.S. and T.M. El Gogary, *Synthesis of novel anthraquinones: Molecular structure, molecular chemical reactivity descriptors and interactions with DNA as antibiotic and anti-cancer drugs*. Journal of Molecular Structure, 2017. **1130**(Supplement C): p. 799-809.
8. Huang, Q., et al., *Anti-cancer properties of anthraquinones from rhubarb*. Medicinal Research Reviews, 2007. **27**: p. 609-630.
9. Wamer, W.G., P. Vath, and D.E. Falvey, *In vitro studies on the photobiological properties of aloe emodin and aloin A*. Free Radical Biology and Medicine, 2003. **34**(2): p. 233-242.
10. Singh, D.N., et al., *Antifungal anthraquinones from Saproisma fragrans*. Bioorganic & Medicinal Chemistry Letters, 2006. **16**(17): p. 4512-4514.
11. Uchimiya, M. and A.T. Stone, *Reversible redox chemistry of quinones: Impact on biogeochemical cycles*. Chemosphere, 2009. **77**(4): p. 451-458.
12. Gholivand, M.B., et al., *DNA-binding study of anthraquinone derivatives using Chemometrics methods*. European Journal of Medicinal Chemistry, 2011. **46**(7): p. 2630-2638.
13. Rajendran, M., R. Gandhidasan, and R. Murugesan, *Photosensitisation and photoinduced DNA cleavage by four naturally occurring anthraquinones*. Journal of Photochemistry and Photobiology A: Chemistry, 2004. **168**(1): p. 67-73.
14. Johnson Inbaraj, J., et al., *Cytotoxicity, redox cycling and photodynamic action of two naturally occurring quinones* <sup>1</sup>Part of this work was presented at the Second International Conference on Bioradicals and Fifth International Workshop on ESR (EPR) Imaging and in vivo ESR Spectroscopy, October 12–16, 1997, Yamagata, Japan.1. Biochimica et Biophysica Acta (BBA) - General Subjects, 1999. **1472**(3): p. 462-470.

## 5.0 Conclusion and future work

### 5.1 Conclusion

During this study, a total of 35 dye compounds were synthesised and structurally characterised, derivatives of either the flavin, porphyrin or anthraquinone families. The singlet oxygen relative yield was tested by monitoring the decolourisation of TPCPD. However due to the structural differences between these compounds, comparison between the singlet oxygen production can only be done with their half-lives and not the  $^1\text{O}_2$  yield. When comparing the half-lives of all 35 compounds it is seen that compounds **4, 5, 9, 16, 17, 18, 19, 20, 21, 26** reached their half-life within 1 minute. It can be seen when looking at these compounds that the porphyrin derivatives were the most efficient family of dye compounds when it came to the singlet oxygen production. It is also seen that the hydroxy anthraquinone and the halogen derivatives of the flavin compounds were just as efficient as the porphyrin compounds, this could be due to the heavy atom effect with the heavy atom effect with the flavin compounds.

The compounds were tested *in vitro* against *C.albicans*, with only 4 compounds showing microbicidal activity. The synthesised flavin derivatives showed no growth inhibition whilst, porphyrin compound **19** showed moderate inhibition, with an MIC of 2.5 mg/mL, when illuminated for 20 minutes when compared to fluconazole. The hydroxy derivatives (**24, 26, 32**) of the anthraquinones showed the most promising growth inhibition when compared to fluconazole, with compounds **26** and **32** having a lower MIC (0.039 mg/mL and



0.078 mg/mL respectively) when illuminated with blue light. Compound **24** had the same MIC (0.156 mg/mL) when illuminated with blue light as fluconazole.

## **5.2 Future work**

Further work on collecting growth inhibition data on another yeast, such as *Saccharomyces cerevisiae*, and bacteria should be performed to determine if the compounds which are biologically active are able to produce an microbicidal effect on other microorganisms. In the future, it would also be interesting to see if the addition of a bandage framework onto the compounds with the highest growth inhibition would change the ability of the compound, both in the production and in their ability to produce singlet oxygen.